The use of water as a refrigerant -- an exploratory investigation.

by

Dirk Van Orshoven

A thesis submitted in partial fulfillment

of the requirements for the degree of

MASTER OF SCIENCE

(Mechanical Engineering)

at the

UNIVERSITY OF WISCONSIN-MADISON

1991

Abstract.

This work presents an exploratory analysis of the different aspects related to the use of water as refrigerant. Thermodynamic analysis and literature study show the basic characteristics of water as a working fluid for refrigeration cycles. Water can be used as refrigerant down to its freezing point of 0 °C. Water excellently fulfills the basic refrigerant requirements of being chemically stable, non-toxic, non-flammable and ecologically benign. However, the operating pressures of a water-based refrigeration system are very low, resulting in very large volume flows. Also, the adiabatic head is higher than for other common refrigerants.

Thermodynamic analysis shows that the intrinsic thermodynamic properties of water make it a less efficient refrigerant in simple cycle configurations. For the case of water cooling or ice production, direct contact heat transfer can be applied in the evaporator. The heat transfer surface can also be eliminated in water cooled condensers. It is shown that these changes result in a potential for significant energy savings. In addition, the ice produced in a vacuum freeze evaporator is in the form of a readily pumpable slurry.

The high adiabatic head requires multistaging of centrifugal compressors. This offers the opportunity to modify the simple refrigeration cycle by applying multistage expansion and intercooling between successive stages. It is found that especially this last measure largely improves the efficiency. This can be attributed to the strong reduction of the otherwise high superheat temperatures.

The extreme flow and head requirements of the compressor pose a great technological challenge. Classical compressor technology does not offer an economic solution. The use of water as refrigerant therefore depends on the creative development of a radically new generation of efficient vacuum compressors.

Acknowledgements.

My stay here in the U.S. has been a very intensive and fascinating period. Both academically and culturally, it has been an unequalled opportunity to widen my background. Taking graduate courses has both deepened and broadened my education. Also, I have been able to work on an exciting research project that has captivated my own imagination and that of many of my fellow students. Finally, the total immersion into American society has given me an entirely new perspective. Although puzzling at moments, it is a thoroughly enriching experience. All this has only been possible with the help and support of innumerable people, to all of whom I am very grateful.

My thanks go first of all to Bill and Sandy for offering me a research assistantship in the lab and for letting me go ahead with this truly fascinating project, however inconceivable it may have appeared initially and at certain moments later on. Bill's ever critical questioning forced me to present my case accurately and soundly. Sandy's inexhaustible activity has been an inspiring but inimitable example. Thanks to John and Jack for the interest they have shown in my various questions. Also prof. C. Dorgan is acknowledged for the financial support he has provided through the Thermal Storage Applications Research Center (TSARC).

Next my thoughts go to my fellow students here in the lab and all those I have met elsewhere. They have made my time here in Madison really enjoyable. In my contacts with them I was surprised daily by the small, subtle differences that made things not quite the same as back in Belgium. These differences were revealing for the deeper-lying, yet almost intangible assumptions of and attitudes towards 'life'. Coming to grips with this latent confrontation has maybe been the most important aspect of my 'American experience'. Thanks to you guys for this unique experience! A special thanks also goes to those people in Madison who have given me hospitality upon my arrival and just before my departure.

My stay here in Madison was initially made possible by the International Student Exchange Program (ISEP). My thanks therefore go to all people who help organize this program: those at my home university of Leuven, those at the headquarters in Washington and those here in Madison. I am also very grateful to the professors at my home university who supported my application for the program with their letters of recommendation. Their full and unconditional support was a strong mental help during the application procedure.

Maybe a word of thanks should also go to the authors of the paper on the Danish vacuum ice maker. The succinctness of their article, combined with the speed with which I

read it the first time led me in the erroneous belief that it actually concerned an entirely water-based system. Months later, upon my arrival here in the lab, when I started fully realizing the importance of thermal storage, I became aware of the potentiality of the system, went back to the paper, ... and discovered -after careful reading- that the major temperature lift was still performed with a traditional refrigerant. Nevertheless, the idea for this project was born.

A deep feeling of gratitude goes to my parents and brother back in Belgium. They have provided me with all finances during the initial period and have supported me morally all the way along. Their frequent letters and press cuttings kept me in touch with the activities of different family members and the highlights of the Belgian political scene. Thank you very much for all of it!

Finally, I would like to thank those people and companies that have answered my multiple requests for information: A. Ophir, I.D.E., Raanana, Israel; S. Bettner and staff, 18th International Congress of Refrigeration, Montréal; R. Hill, Ingersoll-Rand, Elmhurst, IL; C. Tredo, Curtis, St. Louis, MO; Wenniger Compressor Co., Milwaukee, WI; Gas Research Institute, Chicago, IL; Atlas Copco, Holyoke, MA; Leybold, Export, PA; Thomas, Sheboygan, WI; Gast, Benton Harbor, MI; Perkin Elmer, Eden Prairie, MN; Thaxton, Mars, PA; Fuji, Lincoln Park, N.J.

Table of contents.

List of figures.

Chapter 1.

Chapter 2.

Chapter 3.

Chapter 4.

Appendix A

List of tables.

Nomenclature.

r	refrigeration capacity; after kJ or MW (kJr or MWr)
R	ideal gas constant (8.314 kJ/(K*kmol))
T	temperature
Tscd	condensation temperature (saturation temperature at condenser pressure)
Tco	temperature at the compressor outlet
Tev	evaporation temperature (saturation temperature at evaporator pressure)
P	pressure
Pev	evaporator pressure
Pcd	condenser pressure
v	specific volume
c_p	specific heat at constant pressure
c_v	specific heat at constant volume
k	ratio of the specific heat at constant pressure to the specific heat at constant volume
h	specific enthalpy
s	specific entropy
qev	latent heat at evaporation temperature
qdes	sensible heat rejected during desuperheating
sopt	entropy transfer if the heat of desuperheating were rejected at condensation temperature
sprod	produced entropy during desuperheating per unit mass
sgen	generated entropy during desuperheating per unit cooling capacity
wis	isentropic compression work
Had	adiabatic head
g	gravitational constant (9.81 m/s^2)

Appendix A. (Nomenclature continued)

index d	related to the discharge
index i	related to the inlet
η_{is}	isentropic efficiency
η_{vol}	volumetric efficiency
$\eta_{int\ is}$	internal isentropic efficiency
$\dot{V}_{real}$	net volume flow at inlet conditions
$\dot{V}_{theor}$	gross displaced volume reduced to inlet conditions
$\dot{V}_{leak}$	leakage volume flow
n	rotational speed
n_{leak}	'leakage speed'
$n_{leak,\ two}$	constant related to the leakage speed
G	geometrical constant
v	speed or specific volume
A_c	clearance area
w_{is}	isentropic compression work
w_l	minimum compression work of the lobe compressor

Chapter 1
Introduction.

1.1. Scope.

Water is an abundant and important constituent of the earth's atmosphere. It is a necessary condition for life. Regions where liquid water is scarce -be it because they are arid, or because all water is in the solid state as ice-, do not support plentiful ecosystems. As water is so crucial to any organic matter, it is an inherent aspect of any food processing operation: a decrease in water content e.g. often means lower product quality. However, the importance of water is by no means limited to biological matter. It penetrates every aspect of our society: most industrial processes use water in some way or another and water is a basic amenity in modern-day life. Given its omnipresence and its vital functions, it is no wonder that, in the view of medieval alchemists, water constituted one of the four basic elements, along with fire, wind and earth.

For the purpose of this work, three functions of water will now be described in some more detail.

Mixed with other substances, water often acts as a **process fluid**. A large number of techniques, based on a variety of physical principles, exists to separate mixtures into their different components. Phase change operations constitute the majority of separation processes in industrial practise. They are always very energy intensive. When a solid is dissolved in water, the separation operation is called concentration. If the solid maintains its structure, but is soaked with water, the word drying is used. Finally, if the water is mixed with another liquid, one speaks about distillation. Traditionally, the transition between the liquid and the vapor phase (vaporization) comprised the bulk af applications. For products that must not be heated in order to avoid thermal degradation, the solid-vapor transition (sublimation) has successfully been applied in a process known as freeze-drying. More recently, intensive development work has been going on to exploit the liquid-solid transition (freezing) in an operation called freeze-concentration. It has been claimed to reduce energy consumption (Heist (1979), EPRI reports (1987, 1989)).

Water often functions as a **heat transfer and heat storage fluid**.
Water has proven to be a practical substance for the transportation of thermal energy from one location to another. Examples include central heating systems in buildings (with radiators in each room), district heating and cooling systems and steam networks in chemical plants. In these instances, the sensible heat of the liquid phase or the latent heat of vaporization are the basis of the process. Less widespread so far is the use of the latent heat of freezing by means of an ice slush (e.g. fast cooling of freshly slaughtered meat or cooling of deep mines).

Thermal storage can also effectively be achieved by means of water. Stratified hot water tanks perform the crucial function of energy storage in solar water heating systems. The last decade has seen a growing interest in and application of cool storage as a means of electric load levelling and shifting. Thus far stratified cold water tanks and ice storage have constituted the majority of such installations.

A third way in which man has applied water is as a **working fluid** for cycles. The Rankine steam cycle has always been the core technology for the generation of electrical energy. It is a work producing cycle, taking up heat at high temperature and rejecting part of it at low temperature.

Reverse cycles that absorb thermal energy at low temperature and give up heat at a higher temperature, require an input of mechanical work. Installations achieving this unnatural heat flow are called heat pumps. Either the cooling effect at the low temperature or the heating effect at the high temperature may be the desired goal. In the former case one speaks about refrigeration. The working fluids for heat pumps often are halocarbons or ammonia. Since the second oil shock of '79, however, water is increasingly being applied in so-called open cycle heat pumps in the process industry. These cycles usually operate around 100 °C, the normal boiling point of water.

As an example, the operation of such a process is briefly described for the case of evaporation concentration. Fig. 1.1 depicts qualitatively a temperature versus concentration diagram for a given pressure. Water is the solvent; the solute may be any non-volatile substance (e.g. NaCl, NaOH, ...). The presence of the solute causes an elevation of the boiling temperature of the mixture, relative to pure water. When a solution of given composition is heated to its boiling point, evaporation will produce pure water vapor in a superheated state. Rather than venting this steam to the atmosphere or rejecting its energy in a condenser, one way of recuperating its latent heat is by means of mechanical vapor compression as shown in fig. 1.2.
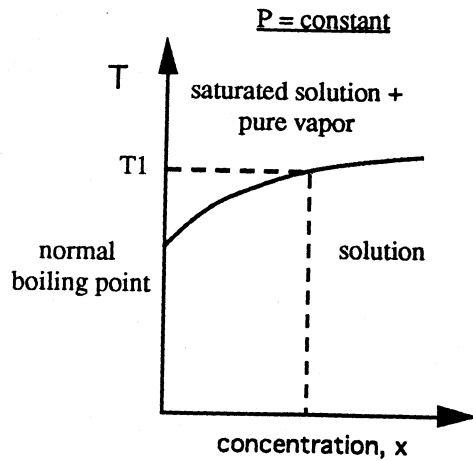
Fig. 1.1 Boiling point elevation
of a watery solution.
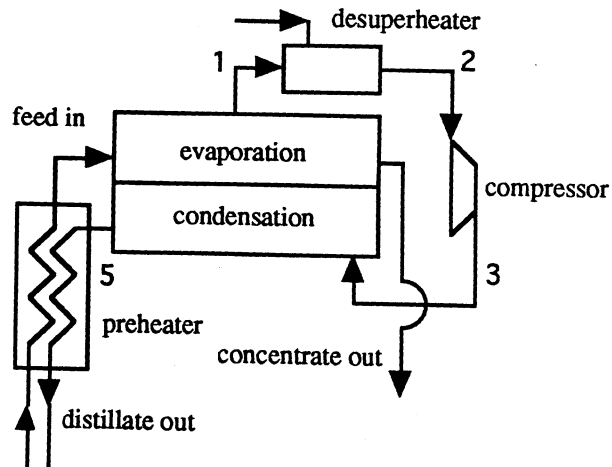
Fig. 1.2 Operation principle
of an open cycle heat pump.

Fig. 1.3 shows the different states on a (T,s)-diagram. Let the superheated vapor for instance be at state 1 (P = 101.325 kPa, T = 110 °C) First, the vapor is desuperheated at constant pressure by injecting liquid water, till it reaches the saturated state 2 (P = 101.325 kPa, T = 100 °C). Next the vapor is compressed adiabatically to a pressure corresponding
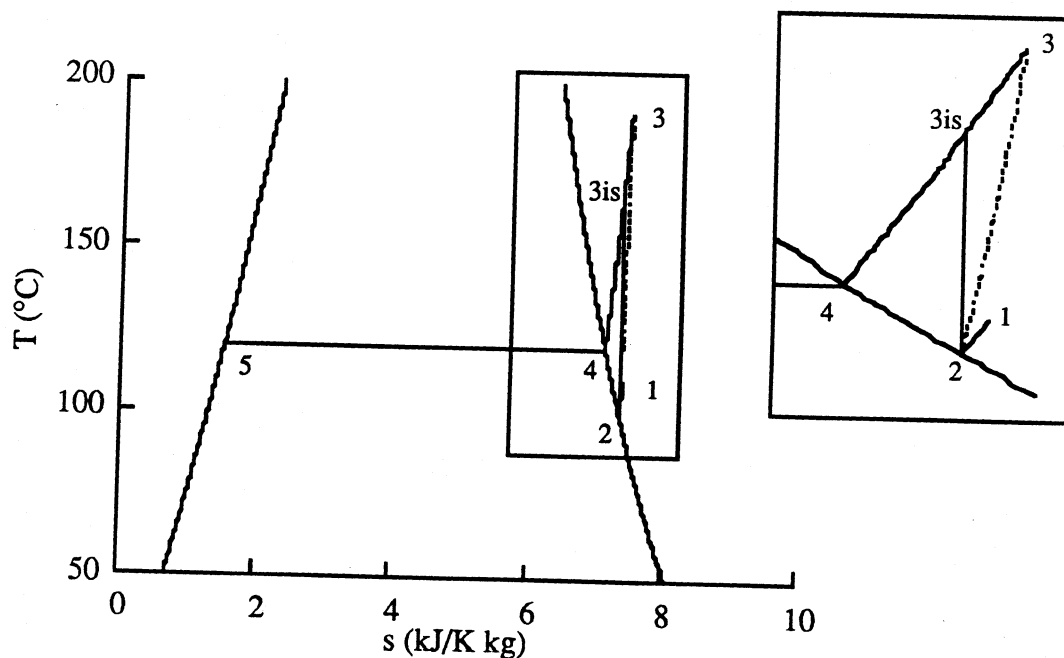
Fig. 1.3 Open cycle heat pump in T-s diagram.

to a saturation temperature higher than the boiling point of the solution (P = 198.7 kPa, Tsat = 120 °C). The condensing vapor can now furnish the necessary heat for further boiling of the solution. Finally, the saturated condensate (P = 198.7 kPa, T = 120 °C) is used to preheat the feed. The cold water is discarded, whence *open* cycle heat pump. Using the evaporating water itself as the working medium for the heat pump leads to a performance advantage compared to a separate, closed heat pump cycle with a secondary refrigerant because an extra heat transfer step is avoided. The research and development of this type of separation process has been extensively presented at 3 International Symposia on Heat Pumps (1982, 1984, 1987). Open cycle heat pumping is not limited to cases with water as process fluid but is in principle applicable to any solvent. A generalized study of mechanical vapor compression for heat pumping has been presented by Austmeyer et al. (1987).

The object of the research reported in this thesis can now very generally be described as follows:

to explore the different aspects related to the use of water as working fluid in heat pump cycles below or around ambient temperature.

It is thus an extension towards lower temperatures of the open heat pump just described. However, the analysis has been restricted to pure heat pumping rather than heat pumping integrated into separation processes. Also, the analysis has been done primarily with refrigeration in mind, as will be reflected in the formulation of this text. Nevertheless, the approach has been on such an elementary level that most conclusions also readily apply to systems where the high temperature energy release is the sought after goal. For this reason, most results are given for condenser temperatures up to 70 °C, which would be rather high in normal refrigeration applications. Furthermore, the basic problems associated with water vapor compression at these low temperatures also would occur in open cycle heat pumps if they were to operate at these low temperatures. Any specific compressor research will thus benefit such separation processes, too. Vice-versa, the experience accumulated with high temperature water vapor compression in the field of separation processes is a rich source of information for simple heat pumps.

1.2. Thermodynamic diagrams.

The usual operating range of substances in thermodynamic cycles is the gas phase, the liquid phase and the two phase region between them. The thermodynamic diagrams

presented in classical textbooks therefore emphasize this domain. When water is used as working fluid, however, the freezing point will be reached at 0 °C. As this feature is actively exploited in certain installations, it is appropriate to first introduce a few extended thermodynamic diagrams.
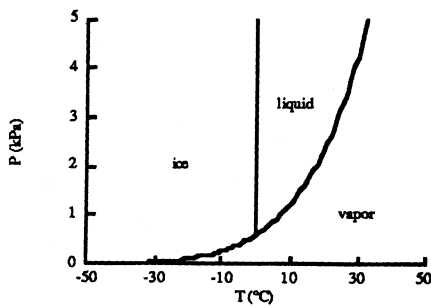
Fig. 1.4.a (P,T)-diagram for water.   **Fig. 1.4.b** (ln P,T)-diagram for water.
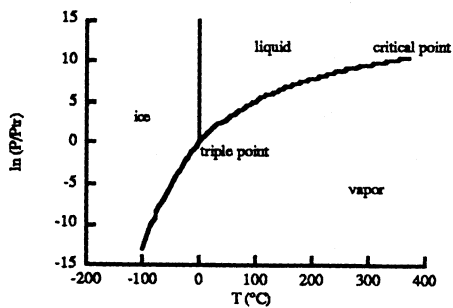
Fig. 1.4 delimits the different phase regions in the (P,T) and (ln(P/Ptr),T) diagrams. In the latter graph the pressure is first divided by the triple point pressure of water before the natural logarithm is taken. The normal (or atmospheric) boiling point of water occurs at 100 °C. For lower boiling temperatures the pressure is subatmospheric. The triple point, where the solid (ice), liquid and gas phase can coexist, corresponds to a pressure of 611 Pa and a temperature of 0.01 °C. This pressure is very low for industrial standards: less than 1 % of the atmospheric pressure (normal atmospheric pressure is 101.325 kPa). The freezing temperature is to a small extent dependent on pressure: at 1 atm it is exactly 0.00°C. The freezing line thus heels slightly to the left -a feature that makes water an extremely unusual substance. The effect is so small, however, that it is not perceivable on the scale of the graphs. At temperatures and pressures below the triple point the solid (ice) and gas phase can coexist along the sublimation line. The critical point is situated at 22.9 MPa and 374.14 °C.

Fig. 1.5 shows the extended (ln P,h)-diagram. At the right is the familiar vapor dome. The enthalpy of the liquid phase at the triple point (ordinate value of 0) is assigned the value 0 kJ. To its right is the saturated vapor at the triple point with an enthalpy of slightly more than 2500 kJ. This corresponds to the latent heat of vaporization between both points. To the left is the saturated solid phase, having an enthalpy of approximately - 333 kJ, the latent heat of fusion. At the triple point the latent heat of sublimation is equal to the sum of latent heats of vaporization and freezing. At lower pressures the liquid phase

does not exist and the difference between the saturated ice and vapor lines is the latent heat of sublimation. At higher pressures the liquid and solid phases can be in equilibrium with one another. The enthalpy at saturated conditions does not vary noticeably, as the effects of temperature decrease and pressure increase are very small and cancel each other in part.
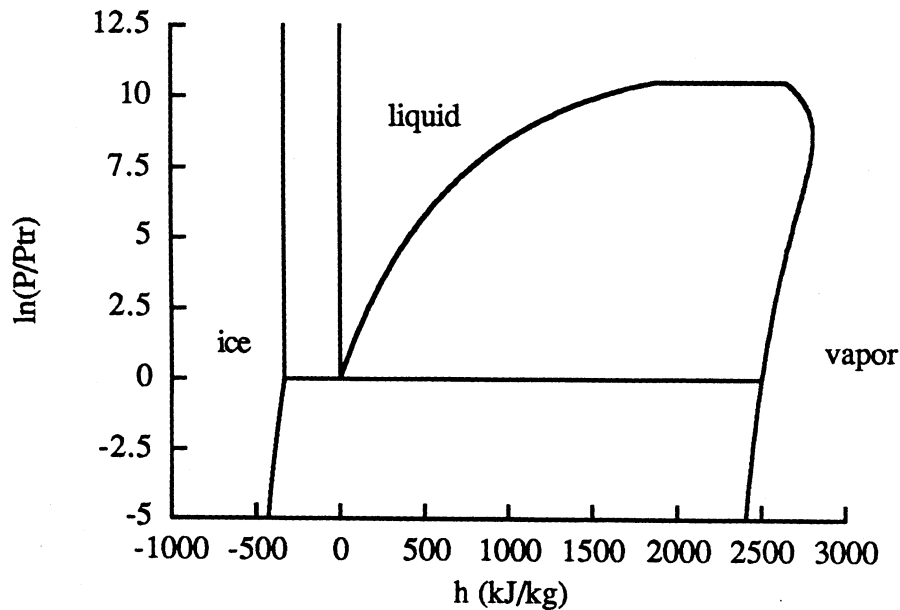
Fig. 1.5 (ln P,h)-diagram for water.

Fig. 1.6 is a temperature versus the entropy diagram. It is similar to the previous diagram, except for the freeze lines (bold). As mentioned earlier, the freezing temperature decreases with increasing pressure. This means that the saturated (with respect to freezing) liquid water line goes down, starting from the triple point. Similar for saturated ice. This implies that constant pressure lines for the liquid phase, which virtually collapse with the saturated liquid line (of the vapor dome), must cross this last line. This occurs at approximately 4 °C. Below this temperature they thus lie beneath the saturation line of the vapor dome, although still almost coinciding with it. All this is of no immediate importance for us here, however, and is not represented in the graph. The saturated liquid and ice lines do not sink unlimited: at a very high pressure of roughly 200 MPa the freezing point reaches approximately -20 °C. At this point another ice crystal structure forms and the freezing temperature will again increase with mounting pressure.
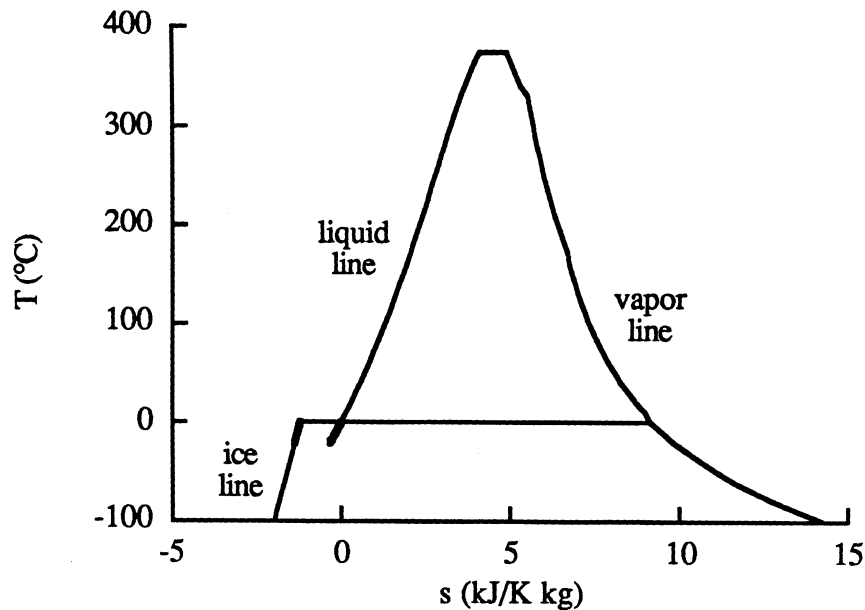
Fig. 1.6 (T,s)-diagram for water.

All calculations presented in this work were done by means of the Engineering Equation Solver program (Klein, 1990). The built-in thermodynamic property functions were used for all refrigerants, with exception of water. To obtain good accuracy, the equations of state given by Young (1988) were used for the gas phase. Although they were not developed to be used below 0 °C, it was found that they could serve very well down to at least -20 °C -a temperature much lower than needed for this work. The saturation properties for the liquid and gas phase were determined following Hyland and Wexler (1983). Their validity spans the range of -100 °C to 200 °C. This is more than sufficient for the saturated conditions, but is insufficient in the superheated region, whence the use of the Young relations. The properties of water were added to the program as an external function. A printout of the function is included in appendix B.3.

1.3. Previous applications of water as a working fluid.

A few instances were identified where water has been applied in whole or in part as working fluid for heat pump cycles around or below ambient temperature. Steam jet refrigeration has served as water chiller in chemical plants. Vacuum freeze evaporators

were first developed for desalination, but have more recently been used for pure heat pumping (for both heating and cooling purposes). Finally, open cycle heat pumping, too, has been used to produce fresh water from salty waters. These different installations will now briefly be presented.

a. Steam jet refrigeration.

Two references describe this type of system: an article by Spencer (1967) and a chapter totally devoted to this equipment in an old ASHRAE handbook (1969),where fig.1.7 and 1.8 are taken from. More recent handbooks no longer include this topic.

The water to be cooled is injected into a flash evaporator. The pressure in this tank is maintained at the saturation pressure corresponding to the desired cold water outlet temperature. Evaporation of part of the water removes thermal energy from the remaining liquid, thus effecting the desired cooling. The water flows over a cascade of flat trays so there is a very large interface between the liquid and the vapor phases, guaranteeing that equilibrium conditions are reached at the outlet.
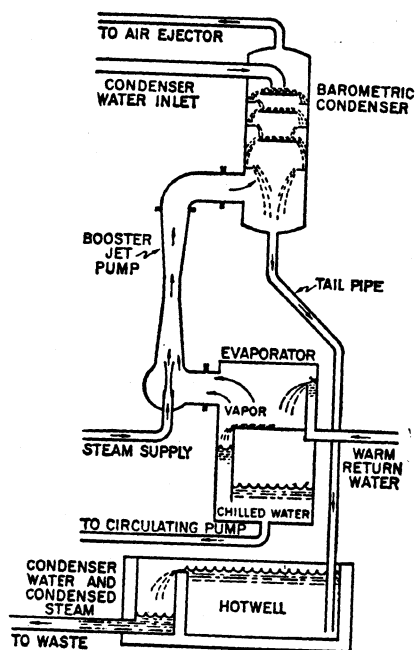
Fig. 1.7 Steam jet refrigeration system with barometric condenser (ASHRAE).
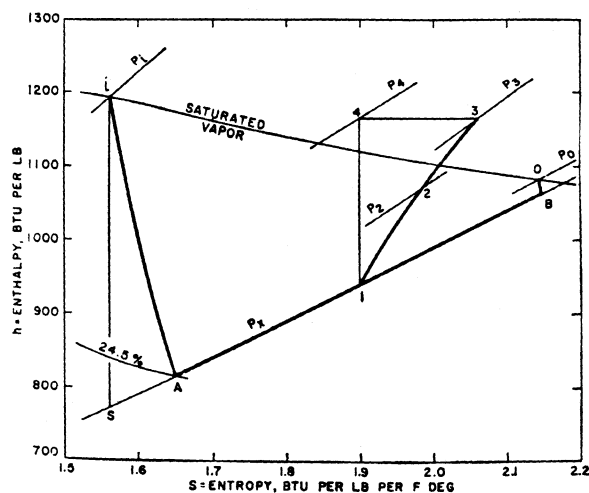
Fig. 1.8 Mollier diagram for typical steam ejector (from ASHRAE, 1969).

The removal of vapor and compression to the condenser pressure occurs by means of an ejector. Saturated, high pressure steam (state i in the Mollier diagram, fig. 1.8) is expanded in a converging-diverging nozzle to supersonic speed (state A). This jet entrains the low pressure, low speed vapor (state B) and imparts kinetic energy onto it. The resulting mixture (state 1) has in most designs a supersonic speed. It enters a converging-diverging pipe where the kinetic energy is converted into pressure energy, first through supersonic deceleration, then by means of a shock wave in the constant area throat (in the sonic region), and finally through further subsonic deceleration (state 3).

The mixture is finally condensed. There is usually no need to keep the steam separated from the cooling water with a heat transfer surface. Direct contact condensation (by means of either a spray or tray assembly) can therefore be applied, thus lowering the condensation temperature. Any non-condensables entering the system are usually removed with a small, two-stage ejector system.

The driving energy for this process is the thermal energy that generates the high pressure steam in a boiler. This is fundamentally different from most refrigeration cycles that use mechanical power (shaft power) as driving energy. The ejector method is therefore called thermal vapor compression (TVC).

Judging from the article of Spencer (1967), steam jet refrigeration has been used for water cooling in chemical plants where high pressure steam is readily available. In some applications the equipment performs simultaneously the desorption function of a sorption separation process (e.g. for the removal of trace contaminants in gases) (ASHRAE, 1969). The jet compressor is an intrinsically inefficient device, however. Basic physical laws (conservation of momentum and energy) applied to the mixing section, show that much of the energy of the motive steam is irrevocably lost. In the ASHRAE handbook (1969) speculation is made about improving the efficiency by using a two phase vapor-liquid mixture or even saturated liquid as motive fluid. The apparent disappearance of this device from the industrial scene indicates, however, that these developments have not occurred.

b. Vacuum freeze evaporators.

The production of ice poses a special problem. In almost all instances it is accomplished by removing heat from liquid water through a heat transfer surface (with an evaporating refrigerant or a colder heat transfer fluid on the other side). Once the freezing point has been reached, the water solidifies and deposits as ice on the surface. As the freezing proceeds, an increasingly thick ice layer forms. Since the conductivity of ice is

rather poor, this layer constitutes a significant thermal resistance. In order to keep the heat flux (and thus rate of ice formation) constant, a continuous decrease in cooling temperature is required, resulting in increased energy consumption. In addition, the process cannot continue indefinitely: after some period of time the ice must be removed. This can be through complete melting, by means of mechanical removal (scraper) or by melting the inner crust whereafter the remaining ice slides off the heat transfer surface (provided a suitable geometric design). When the latent heat of freezing is to be used as heat source for heating by heat pumping, only the last two solutions are possible.

Vacuum freeze evaporators (VFE) partially overcome these problems. Vacuum freeze evaporators operate at triple point conditions and produce ice in the form of a slurry of small crystals. When the pressure above a cold water bath is lowered down to the triple point, the water starts evaporating. If the process is executed adiabatically, the withdrawal of thermal energy from the bath through vaporization will cause the remaining water to start freezing: freezing is thus obtained by causing the water to boil! From the latent heats of freezing ($\pm$ 333 kJ/kg) and vaporization ($\pm$ 2500 kJ/kg), it can be concluded that the mass of ice will be 7.5 times the mass of vaporized water. To keep the process going, it is necessary to agitate the bath intensely and continuously. The resulting slurry of fine ice crystals is readily pumpable. Two different methods of vapor removal have been presented in the literature. They will now be described.

The first method was developed in the '60s in the field of desalination. Ice that crystalizes out from salt water, does not contain any solvents. The vacuum freeze evaporator offers a practical and continuous method of achieving such a process. As shown in fig. 1.9, a large centrifugal compressor in the upper part of the vacuum vessel is used to maintain a slightly sub triple point pressure above the water bath. The vapor is delivered to a condensing chamber at a pressure corresponding to a saturation temperature of typically 3.5 °C (Snyder, 1966). The vapor can now condense on the evaporator coil of a classical refrigeration cycle without danger of freezing. The temperature drop due to heat transfer is therefore lower as compared to common surface freezing equipment, resulting in improved performance. The water vapor compression ratio is 1.5 to 1.6 (Peled, 1965). The compressor is made of thin, flexible blades and can handle 90 m^3/s (Snyder, 1966). This corresponds to a refrigeration capacity of almost 1 MWr. The major part of the temperature lift is still achieved with a classical refrigeration cycle. The use of water as a

working fluid only resolves some technical problems (ice handling); it complements the traditional cycle but does not yet make it superfluous.
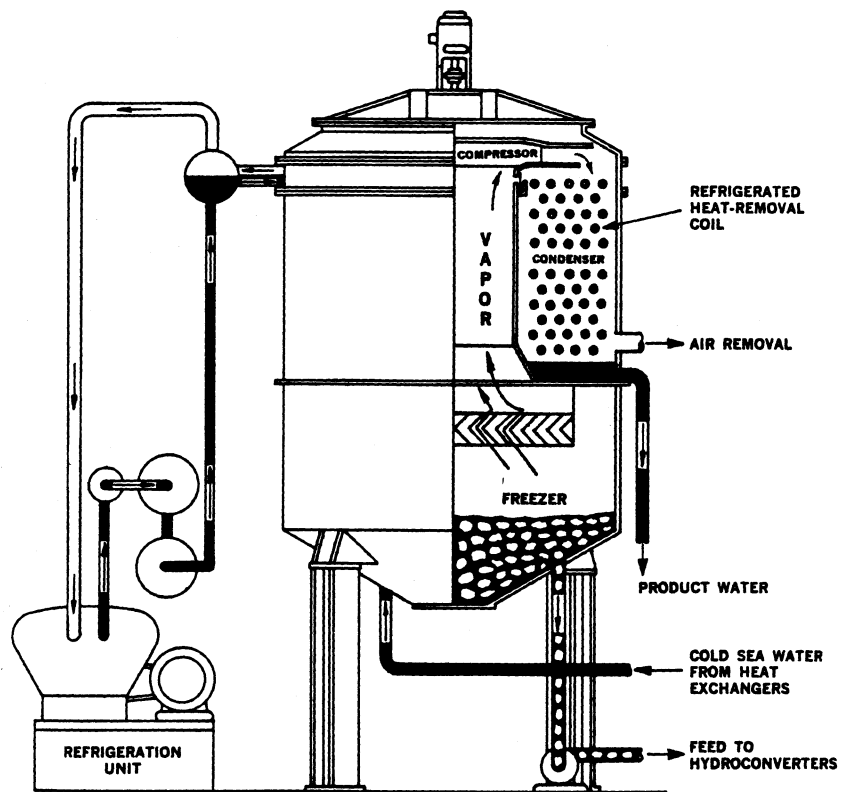
Fig. 1.9 Vacuum freeze evaporator with vapor compression for desalination (from Snyder, 1966).

The very same configuration and operation of a vacuum freeze evaporator has been utilized by a Danish company for heat pumping to a district heating system with the latent heat of freezing of seawater as heat source. Apparently, they also used it to produce an ice slurry to cool deep mines.

A second method was proposed in the Netherlands in the mid '80s (Collet et al., 1985, 1987, 1990). Although originally conceived for heat pumping from ice, its merits for thermal storage applications were also recognized. The same concept has more recently been suggested for desalination by Cheng et al. (1987). In this instance, a low pressure is maintained by directly desublimating the vapor onto a cooling coil in the upper part of the

vacuum vessel, thus simplifying the design (fig. 1.10). The mass of ice on the coil is only 1/7.5th of the amount produced water bath. Moreover, the ice layer is periodically melted off so that the temperature drop caused by heat transfer does not become too large. The evaporation temperature of the refrigerant is nevertheless reported to be around -6 °C. The energy consumption of this system must thus be situated somewhere between that of the previous configuration and that of traditional surface freeze installations.

Fig. 1.10 Vacuum freeze evaporator with vapor desublimation
for heating purposes (from Collet, 1987).

Removal of the ice layer from the evaporation coil is done by first emptying the vessel of the ice slurry, followed by the injection of hot water. The water flashes into the tank and creates a relatively warm steam atmosphere above triple point conditions. Under these circumstances, the vapor condenses on the ice and rapidly melts it off. Due to the short thawing time, there is no need for the heat pump cycle to be shut down during this time. The warm water required for the melting process is obtained by subcooling the refrigerant countercurrently between the condenser outlet and the expansion valve.

All vacuum freeze evaporators must be provided with a vacuum pump in order to pump down the vacuum vessel at start-up and to remove any non-condensables entering the system during operation.

c. Open cycle heat pumping at ambient temperature.

Apparently as a spin-off of the vacuum freeze evaporator desalination process, an associated Israeli company has applied the open cycle heat pump, as described under section 1.1, for desalination (Fisher 1977). The operating temperature is slightly above ambient (in the 30 to 50 °C range). The evaporator is of the falling film type over a bundle of tubes with the distillate condensing inside the pipes. The centrifugal compressor is again of the thin, flexible blade design (28 blades). The volumetric capacity and achieved pressure ratio are not given. Hoffman (1977) reports that by '77 more than 100 units had been sold and installed. As of today, Ophir and Paul (1991) mention the worldwide operation of over 200 such units.

By '85, a French company introduced a series of standardized, skid-mounted installations of this type on the market (Lucas et al., 1985). The larger units have multiple effect (2 to 6) evaporators operating in the 45 °C to 65 °C temperature range. A four stage demonstration unit was installed at a nuclear power plant to produce distilled water as boiler feed. In this case, the compressor achieved a pressure ratio of 1.85 and handled approximately 50 m^3/s. This corresponds to a thermal capacity of approximately 10.5 MWth.

1.4. Method and presentation of the present work.

The results presented in this work are entirely based on theoretical, thermodynamic calculations. No experimental work was performed. A literature search was done, though, to gather relevant information from such related areas as open cycle heat pumping, desalination, freeze concentration, etc. By comparison of cycles with conventional refrigerants and cycles based on water, it will be shown that water cycles have a potential for energy saving but that the development of radically new compressors will be required.

In chapter 2 an energetic comparison is made between water and traditional refrigerants for different configurations with single stage compression. Also, major other physical differences between water and conventional refrigerants are presented. In chapter 3 different options for vacuum steam compression are briefly explored. The next chapter presents a thorougher thermodynamic discussion of internal cycle irreversibilities, two phase and multistage compression, and the energetic impact of air infiltration. Conclusions are drawn in chapter 5.

Chapter 2
Thermodynamic analysis for different system configurations.

This chapter presents three possible ways to use water as refrigerant. For each system configuration the energy consumption of water is compared with that of conventional refrigerants. In the last section other basic physical features that pertain to the use of water as refrigerant are discussed.

2.1. Traditional vapor compression refrigeration cycle.

Fig. 2.1 depicts an example of a traditional vapor compression refrigeration cycle, with water the medium to be cooled. Water often acts as an intermediate heat transfer fluid between the refrigeration system and the actual load (e.g., in large HVAC installations or food handling plants).
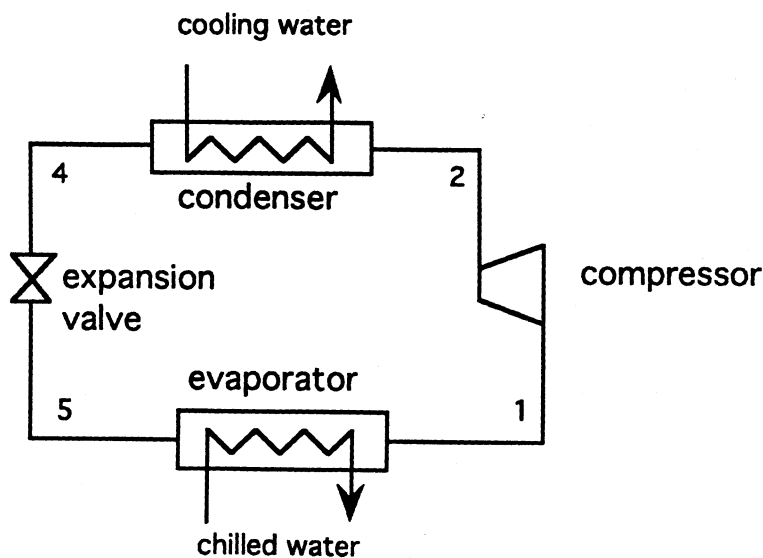
Fig. 2.1 Traditional vapor compression cycle.

The thermodynamic states of the refrigerant as it flows through the cycle are qualitatively represented in the (ln P,h) and (T,s) diagrams in fig. 2.2 and 2.3. Throughout this work, the following assumptions will be made (except for explicit mentioning to the contrary):

- the pressures in both the evaporator and condenser remain constant over their entire length; the pressure drop due to the flow is thus neglected

- the refrigerant leaves the condenser in the saturated liquid state; there is no sub-cooling

- the refrigerant enters the compressor in the saturated vapor state; it is not super-heated
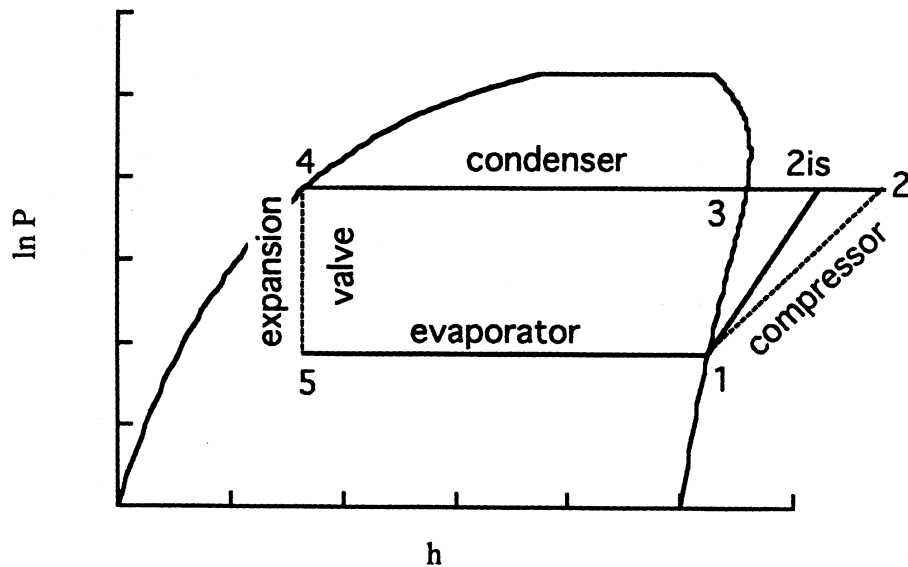
Fig. 2.2 Tradional vapor compression cycle
in (ln P,h)-diagram (qualitatively).
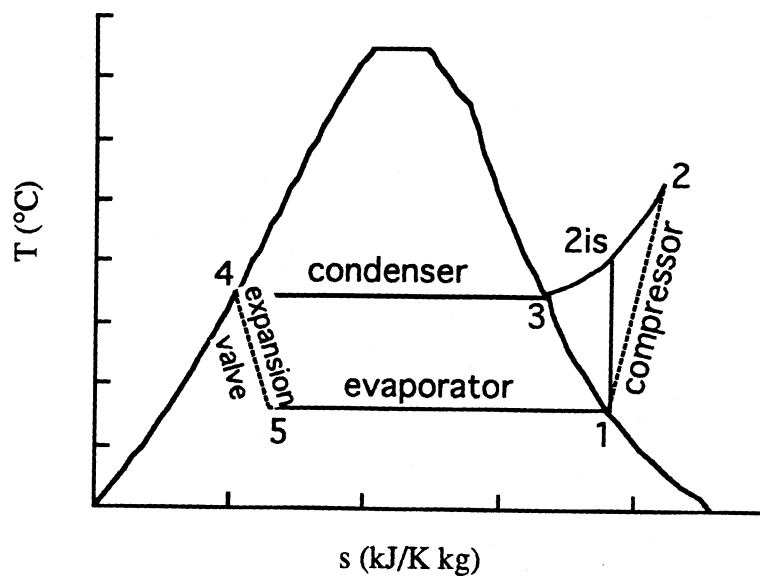
Fig. 2.3 Tradional vapor compression cycle
in (T,s)-diagram (qualitatively).

A classical vapor compression refrigeration system can not tolerate freezing: this could cause blockage of the evaporator pipes, thus rendering the whole installation inoperative. The lowest possible evaporation temperature for a water based system is therefore the triple point (0.01 °C).

The performance of different refrigerants will now be compared for an ideal cycle, i.e. with isentropic compression (A sample EES worksheet used for the calculation is given in App. B.1). Because the value of the COP varies widely with condensation temperature, merely plotting the COP does not give a clear graph since the differences between the refrigerants for a given condensation temperature are too small to show up on the overall scale. Many of the results in this work will therefore be presented as the ratio of the actual COP to the COP of a Carnot cycle between the same evaporation and condensation temperatures. The Carnot cycle has no internal cycle irreversibilities, but may or may not include a temperature drop to account for the heat transfer with the ambient, depending on the type of cycle under consideration. The ratio of the COP to the Carnot COP is also the second law efficiency: it gives the ratio of the actual cooling effect to the theoretically maximum obtainable cooling effect.
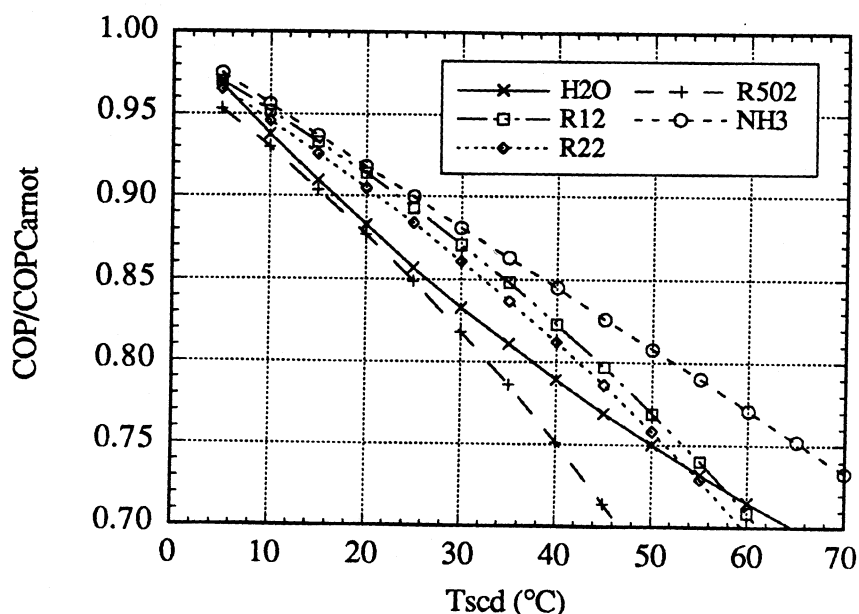
Fig. 2.4 COP as a function of condenser temperature for an ideal cycle (Tev = 0.01°C).

Fig. 2.4 shows the performance of different refrigerants for an ideal cycle. All refrigerants were assumed to evaporate at 0.01 °C and to condensate at the saturation temperature given in the abscissa. These were also the operating temperatures for the reference Carnot cycle. Since the heat transfer properties of different refrigerants are not identical, these assumptions mean that slightly different heat transfer areas may be necessary for the same external conditions (flow rates and temperatures of the cooling water and the chilled water).

From the plot, it can be concluded that ammonia outperforms the four other refrigerants over the entire temperature range. R502 systematically has a lower COP under these operating conditions. The R12 and R22 curves are almost identical, with R12 being slightly better. Water, finally, has a relatively low COP over most of the range. Only at about 60 °C does it match R12 and R22, but it is still far below ammonia. A 60 °C condensation temperature would be rather unusual for refrigeration applications anyway. (The temperature range was taken so large to make the results also relevant for heat pumping for heating purposes.)
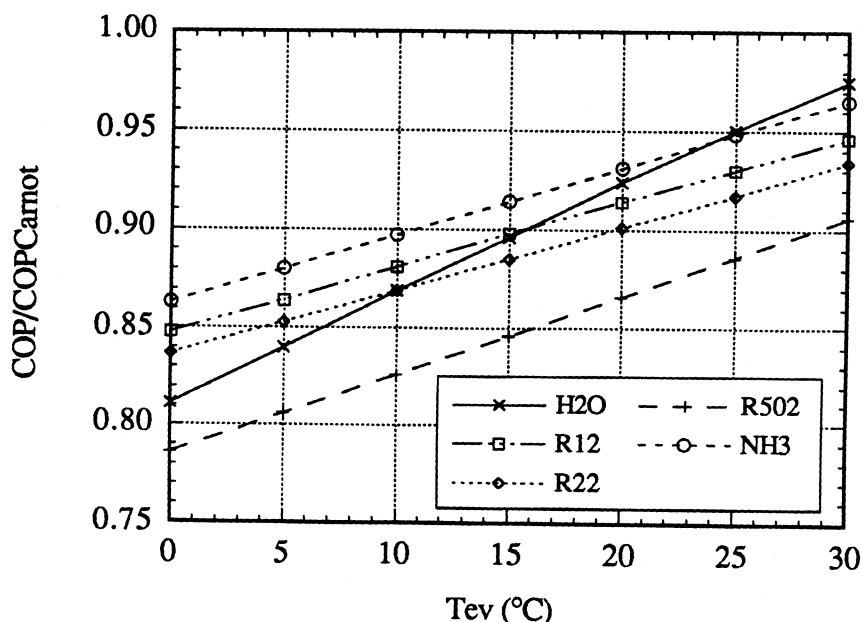
Fig. 2.5 COP as a function of evaporator temperature for an ideal cycle (Tscd = 35 °C).

In fig. 2.5, the condensation temperature is 35 °C and the evaporation temperature varied between 0.01 °C and 30 °C. (The utmost left points (at 0 °C) correspond to those of fig. 2.4 at Tscd = 35 °C.) The relative performance of the classical refrigerants remains unchanged. However, the COP of water increases more rapidly than those of the other refrigerants, and to such an extend that it surpasses all others at high temperature.

Combining the results of both figures leads to the conclusion that the intrinsic thermodynamic properties of water make it a less performant working fluid at temperatures close to its triple point, i.e. in the normal operating range of cooling cycles This disadvantage does not appear to persist at medium and higher temperatures, i.e. from about 30 °C onwards. (In figure 2.4 both effects seem to balance each other around 60 °C.) When a high temperature heat source is available, water appears to match other working fluids in heating cycles, at least as far as theoretical energy requirements are concerned. Some other important characteristics of the use of water as refrigerant will be presented in section 2.4. In section 4.1, a comparison of the irreversibilities of an ideal refrigeration cycle between the throttling and the desuperheating processes will shed some more light on the behavior of the different refrigerants.

The analysis above is of theoretical importance. The danger of freezing inside the evaporator excludes water from being used in traditional cycle configurations. However, as described in section 1.3, the use of a vacuum freeze evaporator or a flash evaporator deals effectively with the problem of freezing and actually results in an energetic advantage, as will be shown in the next two sections.

2.2. Vacuum Ice Making.

In section 1.3, the operation of a vacuum freeze evaporator with moderate water vapor compression was presented (fig. 1.8). Now, the case will be considered where the vapor is compressed to a much higher pressure so that it can condense at ambient temperature. The secondary refrigeration cycle is thereby eliminated and the water itself becomes the only refrigerant. With this modification the intermediate heat transfer step disappears, leading to a performance improvement.

The larger compressor that will be needed for the vacuum ice making cycle with ambient condensation temperature, will most likely no longer allow for the integrated design of fig. 1.8, where both evaporator and condenser are different compartments of one single vacuum vessel. Moreover, since the condensation temperature of the water will be
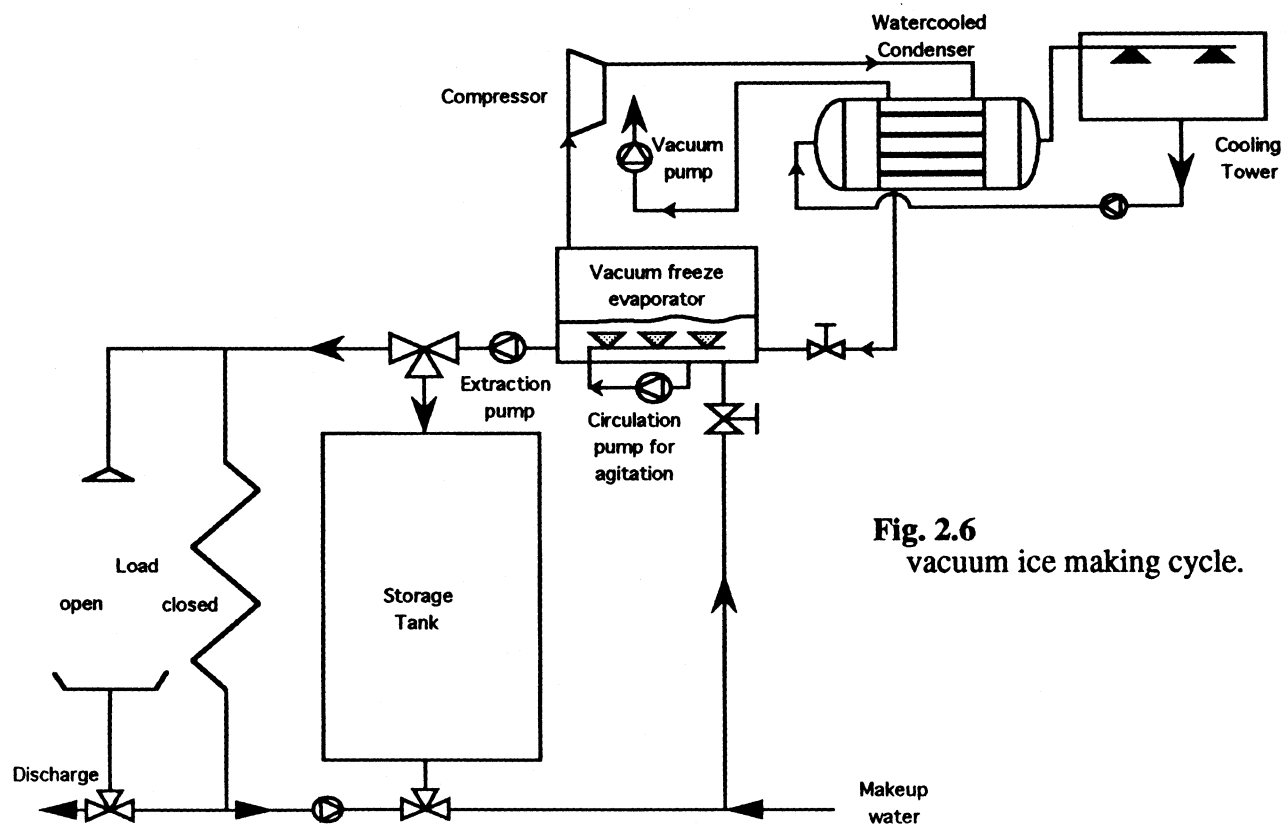
Fig. 2.6
vacuum ice making cycle.

approximately ambient temperature, an integrated design would result in a significant and undesirable heat flow from the condenser to the evaporator. Fig. 2.6 depicts a more likely configuration with each component as a separate entity. This is again very similar to a traditional vapor compression refrigeration cycle. The major differences are the vacuum freeze evaporator and the additional vacuum pump. In principle, the condenser can be any conventional type (air-cooled, water-cooled or evaporative) or with direct contact heat transfer (fig.1.6). Since the system operates at subatmospheric pressure, absolute tightness of the condenser (as well as all other components) is a necessity: any infiltration of air will increase the parasitic power of the vacuum pump. Airtightness appears more difficult to guarantee with air-cooled and evaporative condensers than with a compact water-cooled condenser of the shell and tube design. However, since a direct contact condenser also eliminates the temperature drop due to heat transfer on the heat rejection side, it may be the preferred choice. It will be shown later (section 4.4) that the air dissolved in the cooling water results in some extra vacuum pump power, but that this is more than offset by the energy savings in primary compressor power due to a lower discharge pressure. A shell and tube condenser may nevertheless be chosen in those applications where distilled water is a useful by-product. The results presented in this section assume that the saturated condensation temperature is the same for water as for
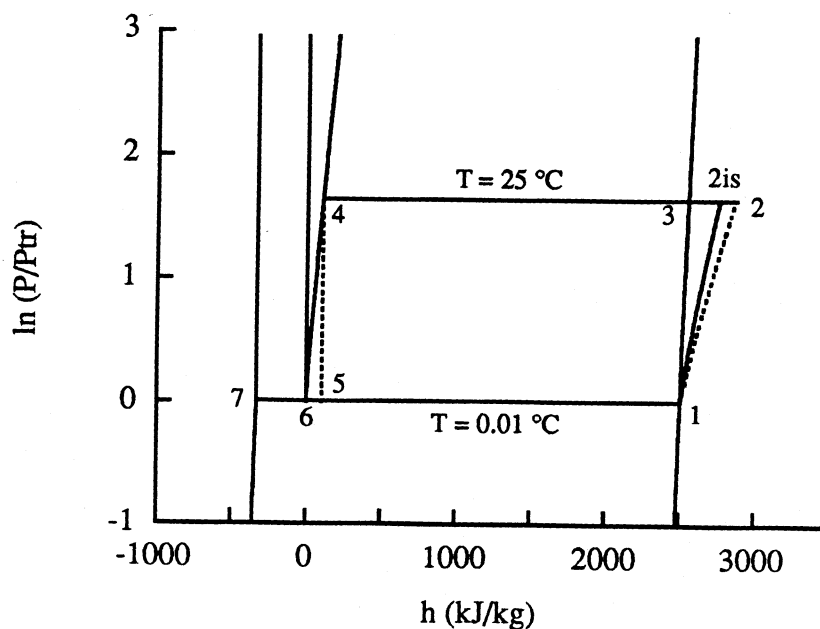
Fig. 2.7 Vacuum ice making cycle on a (ln P,h)-diagram.

other refrigerants. The energetic advantage of a barometric condenser is thus not included in the analysis here and all improvement solely results from the elimination of the freezing heat transfer step.

Fig. 2.7 and 2.8 represent the thermodynamic states of a vacuum ice making cycle (VIM-cycle) in the (ln P,h) and (T,s) diagrams, respectively (real scale). The cycle is similar to an ordinary refrigeration cycle, but the thermodynamic state in the evaporator corresponds to triple point conditions. Since the vacuum freeze evaporator is intended to operate in an adiabatic manner, evaporation of the water leads to freezing of a portion of the remaining water: from state point 6 (saturated liquid) to 7 (saturated ice).
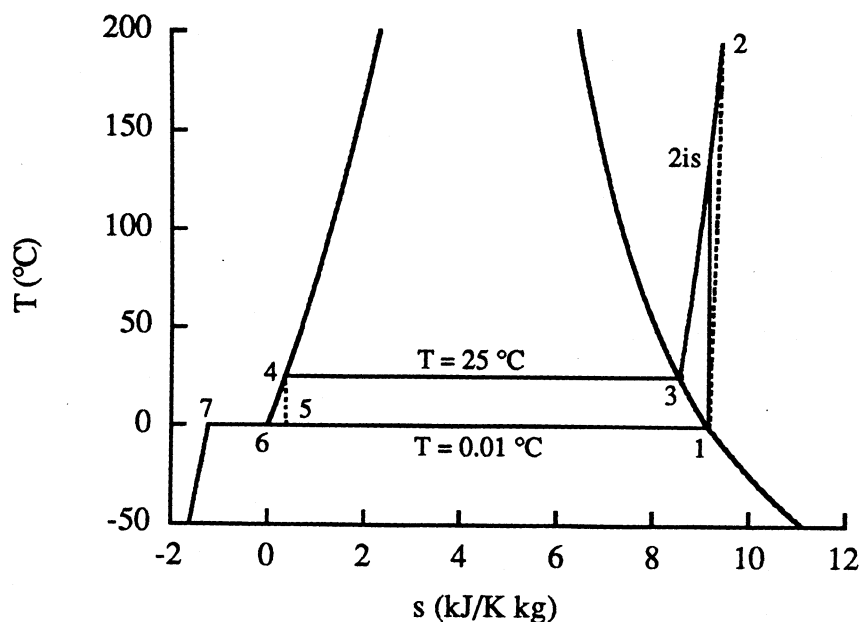
Fig. 2.8 Vacuum ice making cycle on a (T,s)-diagram.

The results of a thermodynamic cycle analysis are shown in fig. 2.9. The COP is again scaled to the Carnot COP, which was assumed to have a low temperature of 0.01°C and a high temperature equal to the condensing temperature given in abscissa.

For water the inlet compressor condition was assumed to be saturated vapor at -0.5 °C. This slightly lower temperature accounts for the small driving force needed to cause evaporation across the finite liquid-vapor interface. The value represents the high end of the range given by Peled (1965) for desalinators operating at about -3 °C: a pressure drop

of 0.1 to 0.2 mm Hg (13.33 to 26.67 Pa). At the triple point such a pressure drop corresponds to a temperature decrease of 0.27 to 0.55 °C.

Ice producing methods commonly in use all fall within the category of surface freezing techniques with ice forming on one side of a heat transfer surface and an evaporating refrigerant or a colder secondary coolant removing thermal energy on the other side. A more detailed description of these installations can be found elsewhere (e.g. Cummings (1989) or the ASHRAE handbooks). It appears that the most favorable evaporation temperature in this equipment is -6 °C. In many instances even lower average temperatures are used. As representative of a best possible case, the cycles with traditional refrigerants are here assumed to have a saturated compressor inlet state at -6 °C.

For both water and the other refrigerants the isentropic compressor efficiency is taken to be 0.7. The results are based on the primary compressor power only and do not include any parasitic energy consumption.
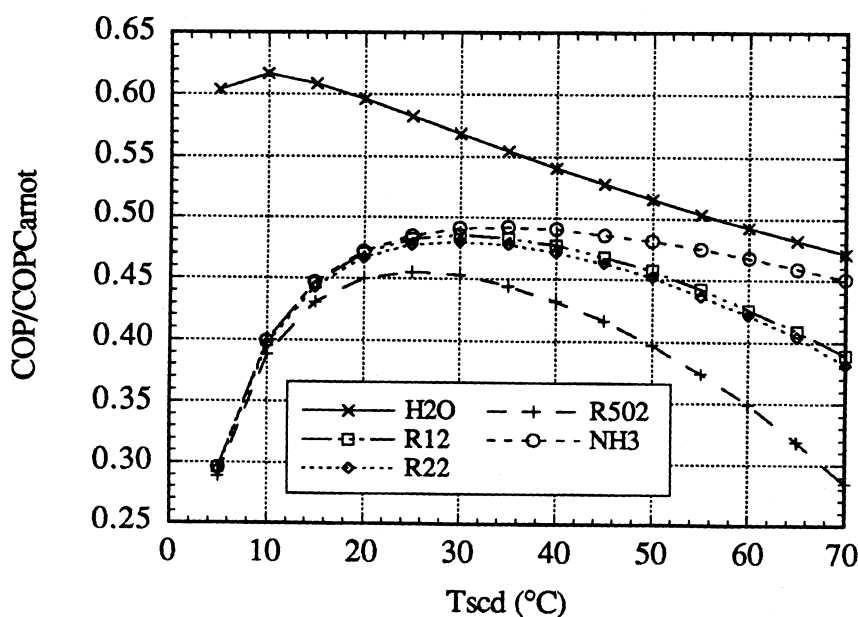
Fig. 2.9 COP of vacuum ice making vs. traditional methods.
(H2O: Tev = -0.5 °C (sat)   other: Tev = -6 °C)
(compressor efficiency = 0.7)

As can be seen from the graph, the elimination of the heat transfer step more than compensates for the slightly worse thermodynamic characteristics of water. The improve-

ment is especially large at low temperatures. The relative position of the different conventional refrigerants remains unaltered remains the same as for the ideal cycle (fig. 2.4 and 2.5).

The deviation from the Carnot cycle is due to two non-idealities: the internal cycle irreversibilities and the irreversible heat transfer at low temperature. As a first approximation, the former can be thought of as linearly increasing with the temperature difference between heat source and heat sink (cf. section 4.1). The latter, however, is linearly proportional to the absolute condensation temperature. Even at a low condensation temperature (5 °C) are the internal cycle irreversibilities thus important, but their value does further not increase very much over the temperature span considerd here. These two factors qualitatively explain the shape of the graph.

Since the contribution of the heat transfer irreversibility is very small in the water cycle (a 0.5 °C penalty), the deviation from the work of a Carnot cycle is almost entirely due to internal cycle irreversibilities. For the other refrigerants, the effect of the heat transfer is dominant at low condensing temperatures since the temperature difference, and thus internal cycle irreversibilities, are still small. The difference in performance between the two systems is therefore especially large at low temperature. At higher condensing temperatures, the fraction of the extra work due to heat transfer becomes increasingly small compared to the portion resulting from the internal cycle irreversibilities (because they grow at very different rates), and the difference between the water and the conventional system diminishes.

These two effects also explain the maximum in each of the curves. At low condensing temperatures the Carnot work is very small, and the relative effect of the heat transfer irreversibility thus very large. As the temperature increases, the Carnot work becomes rapidly larger (proportional to the temperature difference), whereas the heat transfer irreversibilities grow only slowly and the internal cycle irreversibilities have not yet reached a large value. The irreversible fraction of the total work becomes therefore smaller, or the COP over Carnot COP increases. At still higher condensing temperatures, the internal cycle irreversibilities overtake this effect (their real growth is actually more than linear), and the second law efficiency again drops, resulting in an overall maximum at medium temperatures. Since the heat transfer irreversibility is very small in water cycles, the maximum occurs at a much lower temperature.

Fig. 2.10 shows the relative energy savings of the water cycle vacuum ice maker over a conventional surface freezing system. The traditional refrigerant was taken to be ammonia, the most efficient alternative, and the evaluation was made for different

evaporation temperatures of the ammonia. As can be seen, the energy conservation is highly sensitive to the evaporation temperature of the traditional refrigerant; at a common condensation temperature of 40 °C, for instance, a temperature decrease from -6 to -10 °C makes the difference between 10 and 20 %, or a factor of 2.
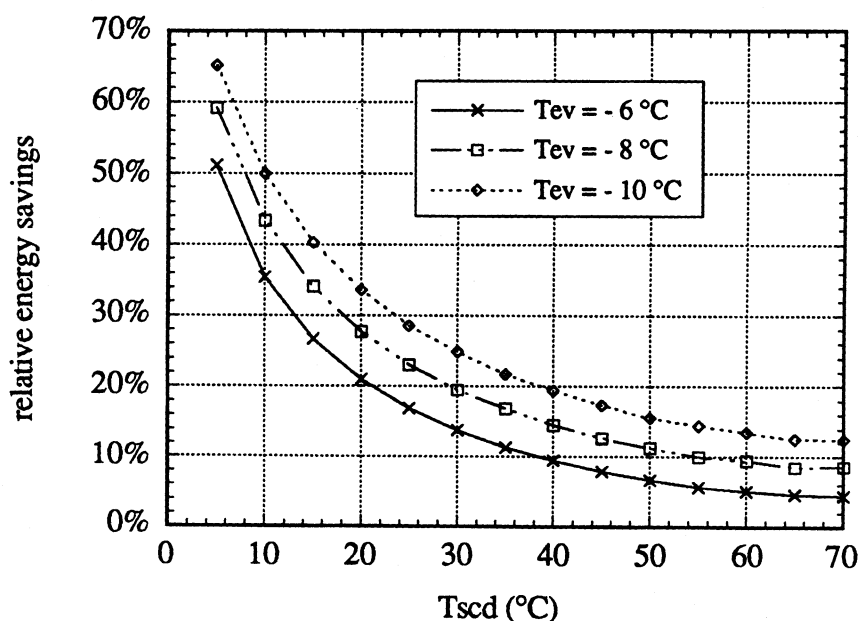
Fig. 2.10 Relative energy savings of vacuum ice making as compared to a traditional configuration with ammonia as refrigerant.
(H2O: Tev = -0.5 °C (sat)   compressor efficiency = 0.7)

2.3. Flash and batchwise water cooling.

The sensible cooling of liquid water (or for that matter any sensible load) by means of a vapor compression cycle with a pure refrigerant involves an important irreversibility. Fig. 2.11 depicts qualitatively the temperature of the water as it flows through a heat exchanger. The evaporation temperature of the refrigerant must be lower than the desired outlet temperature by an amount that still allows for reasonable heat transfer in the zone of small temperature difference (pinch point). This implies that in the entrance region the temperature differences will be much larger than what is economically necessary. Consequently, in the entrance region of the heat exchanger an unnecessary high rate of entropy generation will occur, and this in turn, leads to an extra work input.
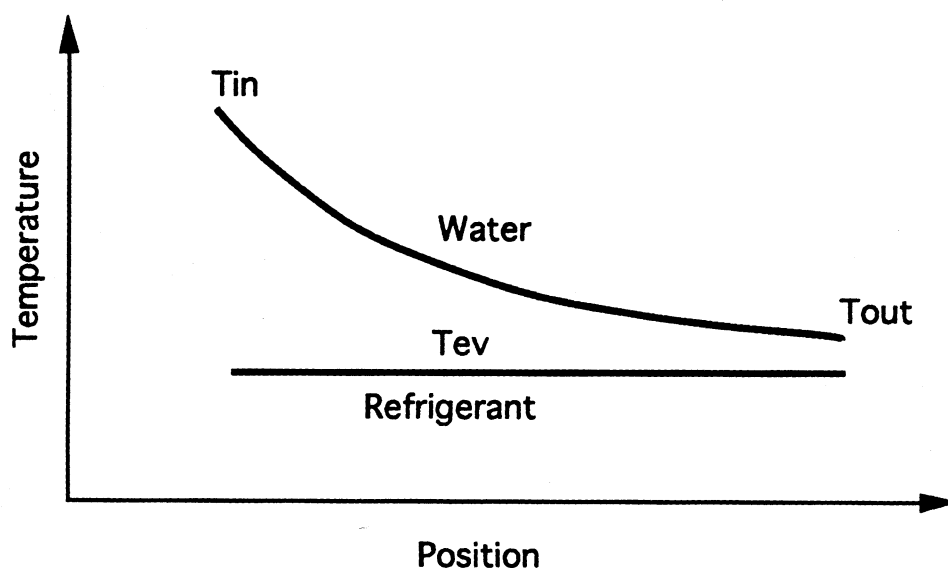
Fig. 2.11 Temperature profile in a water chiller.

A possible remedy to this problem is the use of non-azeotropic refrigerant mixtures in which the boiling point gradually increases with the altering composition during evaporation. In a countercurrent configuration, a better temperature match between the load and the working fluid is therefore obtained, resulting in a better COP. Although this technique has received much research attention over the last decade, it has as yet not been applied widely.

By using water as refrigerant at least a partial improvement over the traditional refrigeration heat exchanger can be made. Replacement of the vacuum freeze evaporator in fig. 2.6 by a flash evaporator (for instance the kind of fig. 1.6) virtually eliminates the temperature drop at the pinch point. As in the case of the vacuum freeze evaporator, in the calculations below it is assumed that a driving force of 0.5 °C is required, i.e. the pressure at the compressor inlet corresponds to a saturation temperature 0.5 °C lower than the desired outlet temperature.

In theory, it is possible to eliminate the irreversible flashing process too by operating in a batchwise mode. First, the evaporator tank is almost filled with the warm water that is to be chilled. Initially, the water is in liquid-vapor equilibrium at the (high) inlet temperature, corresponding to a relatively high saturation pressure. Under these conditions the throttling of the water occurs entirely in the liquid phase resulting in a very small entropy generation. Next, the compressor is activated and it begins withdrawing vapor from the top of the tank. This causes the water to start boiling, thus lowering its temperature (since the tank is well insulated). Ideally, the water vapor interface is very

large and the liquid water is perfectly mixed so that it maintains a homogeneous temperature. As the water temperature decreases from the inlet temperature to the desired outlet temperature, so does the vapor pressure: the system operates with a floating suction pressure. At any point in time, the compression ratio (which determines the work) is therefore not higher than is necessary, rendering the process in principle very efficient. Once the desired outlet temperature is reached, the chilled water is withdrawn from the tank and replaced with a new load of warm water.

Maintaining thermodynamic equilibrium between the entire liquid mass and the vapor phase during the whole course of the process, may prove relatively difficult to achieve. Either the water has to be circulated in the tank at a very high rate, so that fresh layers of warm water permanently appear at the interface (with the cooler water being efficiently directed to the bottom). Or, alternatively, all water must closely be exposed to the vapor, e.g. by having very thin water layers in a multitude of stacked trays. The water may either be stagnant in the trays or permanently be recirculated and cascading downwards. Means must be provided to completely empty all trays at the end of each cycle.

In the calculations below, the water temperature was assumed to be perfectly homogeneous and the driving force was, again, taken to be 0.5 °C all throughout the process. Since this may be somewhat irrealistic, the results of the batchwise cooling must rather be seen as a limiting case.

Batchwise operation will also require 2 extra buffer tanks of the same capacity as the evaporator: one to store the chilled water, another to receive the warm return water from the load. Another solution is to use one large, stratified storage tank. If dimensioned properly, such a tank allows for thermal storage, either levelling the electric load or completely shifting it to off-peak nighttime hours.

A final aspect of batchwise cooling is that the compressor must be able to continuously adapt to a changing pressure ratio while maintaining a good efficiency. It may not be necessary to stop and restart the compressor during the emptying/withdrawal process (provided it happens sufficiently fast), but a sudden rise in suction pressure must then be dealt with.

The calculation of the performance of the batchwise process was done by approximating the cycle as a succession of small throttling operations: the saturated warm water is flashed in a first throttling process and the resulting vapor is compressed to condensation pressure, whereafter the remaining liquid undergoes a second throttling, and so forth, until the desired outlet temperature is reached. It was found that the calculated performance did not change significantly once the temperature step between two stages was

taken as 0.01 °C or smaller. It is therefore believed that the 0.01°C temperature step, on which the presented results are based, yields a sufficiently accurate result, given the many other assumptions that are involved in the calculations (cf. App. B.4 for program printout).

The results also include the pump work (isentropic efficiency = 0.6) to extract the water charge from the tank and discharge it at atmospheric pressure. This work amounts to only a small fraction of the compressor work: always less than 5 %. It was also assumed that the condensate is not immediately returned to the evaporator, but stored on the bottom of the condenser (the total mass involved represents only a few percent of the amount in the evaporator tank). Only at the beginning of a new cycle, it is drained to the evaporator, together with the new warm charge. This also should contribute to a small performance improvement.

Some sample results are given in fig. 2.12. The saturated condenser temperature is set at 35 °C and the compressor efficiency at 0.7 (identical for all cases). The warm return water temperature, Tin, is varied and the chilled water temperature, Tout, is taken to be 4 °C. For the traditional chillers (R22, ammonia) the temperature drop at the pinch point is assumed to be 3 °C, i.e. the evaporation temperature is 1 °C.
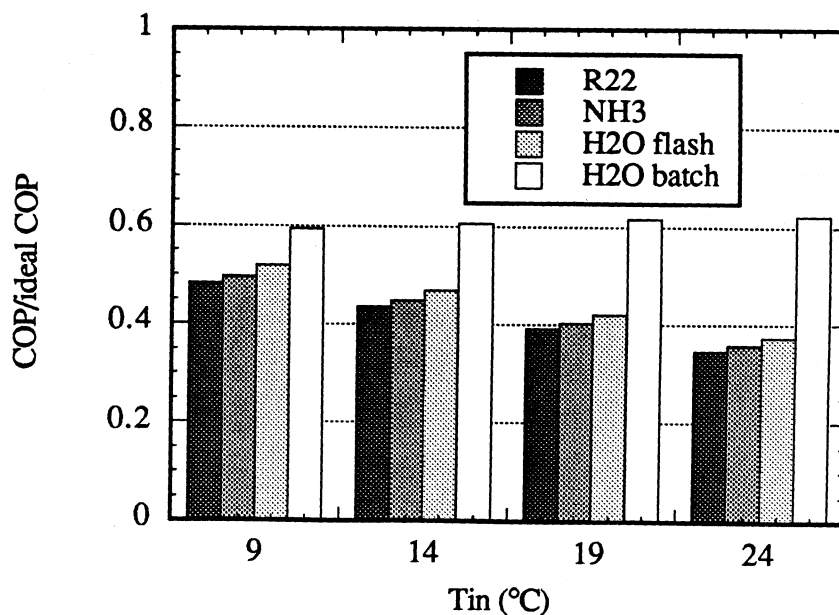
Fig. 2.12 COP of flash- and batchwise water cooling vs. traditional chiller (R22,NH3).
(Tout = 4 °C   Tscd = 35 °C   compressor efficiency = 0.7)
(H2O: batchwise: Tev = floating   flash: Tev = 3.5 °C)
(R22/NH3: Tev = fixed = 1 °C)

The results are scaled to the COP of a reversible cycle that produces no entropy. Between the inlet and outlet conditions of the chilled water, both the enthalpy and the entropy are reduced by a given amount. Rejection of the same quantity of entropy (reversible process) at the condensing temperature, requires a larger energy transfer. The difference between the energy rejected in the condenser and the energy removed from the water, is the minimal work requirement, from which the ideal COP can be determined.

The results confirm what is intuitively expected. Replacing the heat transfer by flashing leads to a small COP improvement on the same order as the difference between ammonia and R22. Further substituting the flashing by gradual cooling results in a much higher COP improvement, especially at high inlet temperatures. For batchwise cooling, the second law efficiency shows a slight improvement with increasing inlet temperature. For the other refrigerants it drops significantly with increasing inlet temperature, which is a logical consequence of the increased entropy generation. Once more, it can be seen that ammonia has a slightly better energy performance than R22.

As already indicated, the batchwise operation may not be very practical. An intermediate between gradual cooling and direct flashing may be two stage flashing (or more). As will be explained later, this may be well compatible with multistage centrifugal compressors. The efficiency of such a system is expected to lie between single flashing and batchwise cooling.

In principle, the batchwise operational mode can be applied to any refrigerant. Cold liquid refrigerant can cool a sensible load in a countercurrent manner. The warm liquid refrigerant thus obtained can then again be cooled in the same manner as described for water. Like in the case of water, the refrigerant now performs two functions: that of refrigerant and that of heat carrier. Given the need for a much larger refrigerant inventory and the difficulty of pumping and manipulating the refrigerant in an absolutely tight system, it appears unlikely that this option can easily be realized.

2.4. Other thermodynamic features of using water as refrigerant.

So far, the analysis has been limited to the energy requirements of the different configurations. It was shown that, in the case of water chilling and ice production, energy savings can be achieved through elimination of the heat transfer surface in the evaporator (and possibly condenser) and through batchwise operation. In this section, the large vapor volume flow and the high head are discussed. These features explain why water has not been used in vapor compression cycles in the past, despite its potential for energy savings.

It are the large volume flow and the high head. To eliminate the direct influence of the different molar masses of the different refrigerants, all properties are given on a molar basis. This facilitates the comparison.

For temperatures at or below ambient, the saturation pressure of water is far beneath atmospheric pressure (101.325 kPa): at the triple point it is 0.611 kPa and at 50 °C it is still only 12.35 kPa. As a consequence, the water vapor at these temperatures is very rare and has a large specific volume. Fig. 2.13 visualizes the striking difference with a common refrigerant, R22. At 0 °C, the specific volume of saturated water vapor is 3714 m^3/kmol, that of saturated R22 only 4.065 m^3/kmol: a difference of 3 orders of magnitude. On the same vertical scale, the 'right bar' for R22 does not raise up from the abscissa ! This discrepancy in specific volume is straightforward obvious when considering the ideal gas law $P*v = R*T$, with the universal gas constant $R = 8.314$ kJ/(K*kmol). The saturation pressure for R22 at 0 °C is 497 kPa, compared to 0.611 kPa for water (factor of approximately 800). Since the right-hand side is equal for both substances, the specific volume must be approximately 800 times larger. The actual ratio of both specific volumes is 913, due to the non-ideal behavior of especially R22.
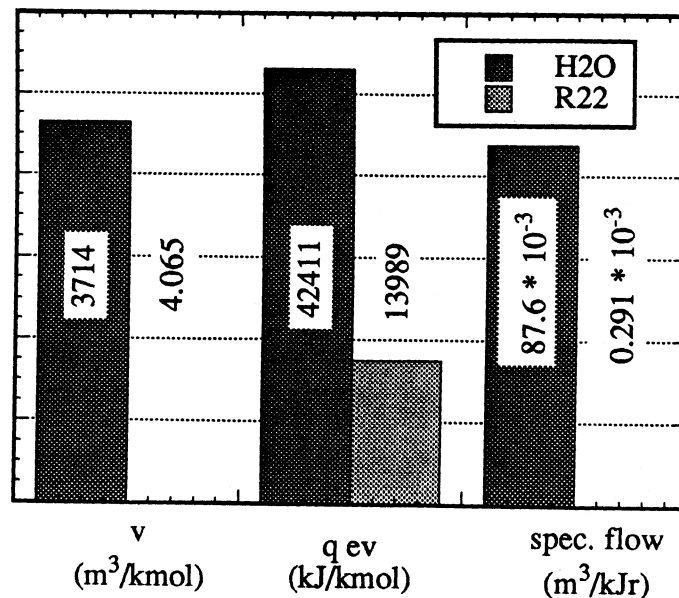
Fig. 2.13 Comparison of water and R22 at 0°C (Tscd = 35 °C).

To fully become aware of the immenseness of the specific volume, consider the following. In the liquid state, 1 kg of water (i.e., the contents of a medium sized bottle) has a volume of approximately 0.001 m³ (1 liter). In the saturated vapor state at the triple point, the same kg of water occupies approximately 206 m³ (3m * 7m * 10m): this is much larger than the volume of a typical office!

The amount of refrigerant needed to obtain a certain cooling effect is determined by the latent heat of vaporization, or, more precisely, by the enthalpy difference between the evaporator inlet and outlet. This last quantity is somewhat less than the total latent heat, because the refrigerant already enters the evaporator at a two-phased state. Assuming a saturated liquid state of 35 °C at the throttling valve inlet and a saturated vapor state at the evaporator outlet, the thermal energy absorbed during passage of the evaporator (qev) is 42411 kJ/kmol for water and 13989 kJ/kmol for R22, or, only one third as much water (on a molar basis) is needed for the same cooling effect. The high latent heat of water is a truly exceptional feature. In chemistry, Trouton's empirical rule states that the latent heat at the normal boiling point (i.e. at atmospheric pressure) divided by the corresponding boiling temperature is roughly constant for all substances. According to the ASHRAE fundamentals handbook (1989), traditional refrigerants cover the range from 73 kJ/(K*kmol) (CH4, methane) to 97 kJ/(K*kmol) (NH3, ammonia). Water has a value of 109 kJ/(K*kmol), which clearly is distinctively more.

The ratio of the specific volume to the heat absorbed in the evaporator (v/qev) determines a specific volume flow, i.e. the volume of vapor that must be compressed to obtain a unit cooling capacity. The 3 times larger latent heat of evaporation only very partially offsets the some 900 times larger specific volume, the net result being a 300 times larger volume flow (87.6 compared to 0.291*10⁻³ m³/kJr). Again, on an identical scale, the volume flow of R22 is not visible in comparison to that of water vapor (fig. 2.13). Obviously, a compressor with a very large volumetric capacity is necessary in order to achieve a reasonable cooling power.

Another characteristic of water is the high ratio of the condenser pressure (P_{cd}) to the evaporator pressure (P_{ev}). Both pressures, and thus the pressure ratio, are solely determined by the shape of the saturated vapor curve. For an evaporation temperature of 0 °C and a condensation temperature of 35 °C, the pressure ratio is 9.2 for water and 2.7 for R22, or a difference by a factor of 3.4 as illustrated in fig. 2.14. At higher condensation temperatures, this factor becomes even larger (e.g. 5 at Tscd = 50 °C).

This pressure ratio is of importance because it is directly related to the (isentropic) compression work (w_{is}). For an ideal gas the following expression holds:

$$w_{is} = R*T*\left(\left(\frac{P_{cd}}{P_{ev}}\right)^{\frac{k-1}{k}} - 1\right)$$

with R the universal gas constant and k the ratio of the specific heat at constant pressure over the specific heat at constant volume (c_p/c_v). For the same evaporation temperature T (K), a higher pressure ratio thus requires a larger molar work input. Under the conditions stated above, the isentropic compression work (real gas values) is for instance 6702 kJ/kmol for water, as compared to 2147 kJ/kmol for R22 (or a factor of 3.1). The difference in compression work is also apparent from the following consideration. The COP is the ratio of the heat taken up in the evaporator to the work input (COP = qev/w). The COP is only moderately different for the different refrigerants (cf. section 2.1). Above, it has been illustrated that the numerator (qev) is some 3 times larger for water. As a result, also the denominator, i.e. the compression work (w), must be times larger by roughly the same factor of 3. As will be explained in some more detail in the next chapter, the work (or equivalently head) is an important consideration with respect to centrifugal compressors.
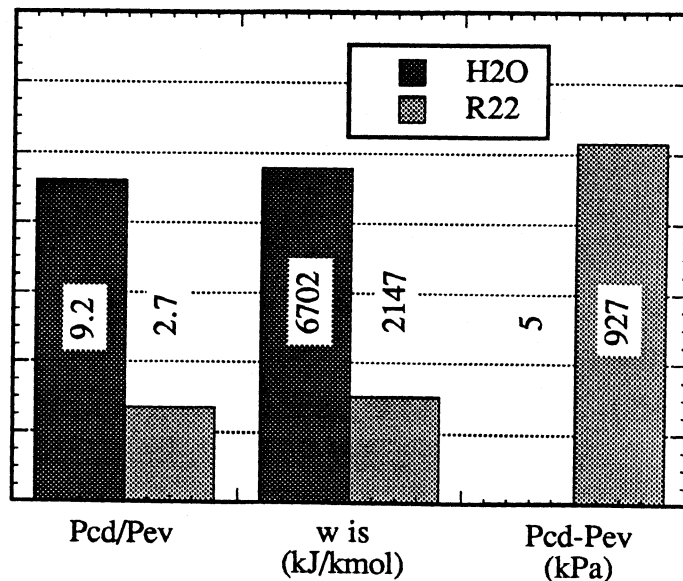
Fig. 2.14 Comparison of water and R22 (Tscd = 35 °C).

Another aspect related to the compression work is the degree of superheating. For water, the effect of the high molar work input is still amplified by its lower molar specific heat . This low specific heat is due to the simple molecular structure of water (consisting of only 3 atoms). At ambient temperature the vibrational mode of agitation is not yet activated, unlike in the case of other refrigerants -even though these are only slightly more complex (; R22: 5 atoms). The low specific heat is also related to the slope of the saturated vapor curve in the (T,s)-diagram (cf. fig. 2.8). Ideally, the curve would be perfectly vertical or even slightly tilted towards the right so that the adiabatic compression line would collapse with it . For this case no superheating would occur.
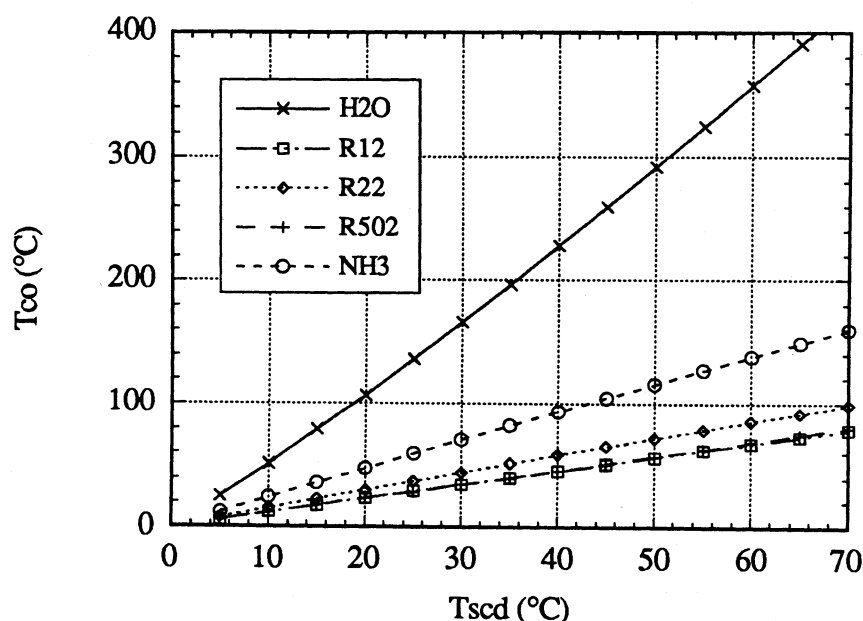
Fig. 2.15 Compressor outlet temperatures
as a function of the condensation temperature (Tev = 0.01 °C).

In fig. 2.15, the compressor outlet temperature (Tco) is plotted as a function of the saturation temperature in the condenser (Tscd) for the ideal cycle as described in section 2.1 (the evaporation temperature is 0.01 °C). As is obvious, the outlet temperature of water is substantially higher than that of conventional refrigerants. Even ammonia, a refrigerant known for its high superheat, has a far lower compressor outlet temperature. As a rule of the thumb, the outlet temperature for water (in °C) is some 5 times larger than the condensation temperature (also in °C). Not only may this high temperature lead to serious

technical problems, but it is also the cause of the lower efficiency of water in an ideal cycle (cf. section 2.1). This will be analyzed in more detail in section 4.1. Appropriate measures, such as intercooling and possibly two phase compression, can more or less mitigate this negative feature, however, and thus booster the COP. These measures will be analyzed later.

A final special characteristic of the use of water as refrigerant is the extremely small pressure difference between the condenser and evaporator. The absolute operating pressure is so low that, even with a 3 times higher pressure ratio, the pressure difference is still minimal. Under the above conditions, its value is only 5 kPa for water, in contrast to 927 kPa for R22. This time, it is thus water that remains invisible in the graph (fig. 2.14). In a careful compressor design, specifically for the purpose of compressing low temperature water vapor, this feature can be used to good advantage, as will be discussed in the next chapter.

Chapter 3
Compressor.

When water is used as refrigerant, the refrigeration cycle operates under vacuum conditions, resulting in a very large volume flow. In addition, the work per unit mass required to compress the vapor from the evaporator to the condenser pressure is larger than for other refrigerants. The combination of both demands is very extreme, to the extent that it has prevented the generalized use of water as refrigerant thus far.

Refrigeration cycles based on evaporation (as opposed to gas cycles) require the continuous removal of low pressure vapor and regeneration of this vapor to the liquid state. Four physical principles that allow to accomplish this goal are:

-mechanical vapor compression (MVC)
-ejectors
-liquid column entrainment
-sorption (absorption, adsorption and chemisorption)

In mechanical vapor compression systems the vapor is compressed to such a pressure that condensation can occur at ambient temperature. The power input is in the form of shaft work. In ejector systems a high pressure fluid (either vapor, liquid or two phase) is expanded in a nozzle. Next, it entrains the low pressure vapor and imparts kinetic energy onto it. The mixture of motive fluid and vapor then compresses to condenser pressure in a second nozzle assembly. The energy input in this instance is in the form of thermal energy (major part) and pumping power (minor fraction). A third way to increase the pressure of the vapor to its condensation value is by entrainment of the vapor into a vertical liquid column. As the vapor-liquid mixture flows down, its pressure becomes higher due to gravitational forces. Provided the downpipe is sufficiently long, the condensation pressure corresponding to ambient temperature will be reached. The work input is in the form of pumping power to circulate the entrainment fluid. In sorption systems the low pressure refrigerant vapor is not compressed but nevertheless condenses at ambient temperature due to the tendency of mixing between the refrigerant and the sorbent and/or an affinity between both substances. The saturated sorbent is regenerated by distillation, concentration evaporation or drying, with now pure refrigerant condensing a second time at ambient

temperature. The power input is primarily in the form of thermal energy and a minor part is as pumping energy.

Each of these four options will now be evaluated with respect to the use of water as refrigerant. Throughout the other chapters of this work only mechanical vapor compression is considered.

3.1. Mechanical vapor compression.

The requirements that the compressor must fulfill in a water-based system are straightforward:

-for the system to operate at all, the compressor must deliver a **high pressure ratio**. In order to achieve a reasonable cooling capacity, the compressor also has to process a **large volume flow**. Table 3.1 gives some sample values. (The values do not vary significantly with changing condensation temperature unlike for other refrigerants.)

-for the system to have low energy consumption, the compressor must be **efficient** over a large range of pressure ratios and flow rates: the condenser pressure varies with ambient conditions and the evaporator has a floating pressure in batchwise cooling (cf. section 2.3) or may change with the chilled water set point temperature. The volume flow depends both on the load and on the evaporator and condenser pressures. To minimize the energy consumption it is important to operate with the lowest possible pressure ratio at all times.

-finally, to be economically viable, the **capital cost** of the compressor must not be excessive.

Tev (°C)	specific flow (m³/kJr)
-0.5	$91.12*10^{-3}$
5	$62.21*10^{-3}$
10	$44.82*10^{-3}$
15	$32.71*10^{-3}$

Table 3.1 Inlet volume flow per unit cooling capacity for a condensation temperature of 35 °C.

Compressors that satisfy all three requirements are not readily available on the market. The flow capacity of the positive displacement compressors used in high temperature open cycle heat pumps is too low to achieve large cooling capacities. Series operation of 4 to 5 heavy centrifugal steam compressors is believed to be too expensive.

Consultation of the literature on vacuum technology (e.g. Pirani and Yarwood (1961) or Power (1966)) shows that the requirements in this field are very different from the above. Often significant flow only occurs at startup when vacuum conditions in the equipment are to be created. Maintaining the vacuum usually does not involve much gas removal. The time it takes to evacuate the system and the ultimate pressure that can be achieved are much more important considerations than the energetic efficiency of the process (since no large energy consumption is involved anyway). Ryans and Roper (1986) give isentropic efficiencies ranging between 0.2 and 0.5 for most vacuum pumps. Also, the operating pressures of vacuum installations are often still a few orders of magnitude smaller than in a water-based refrigeration cycle. Table 3.2 shows that the triple point of water (611 Pa) is still within the limits of so-called 'rough' vacuum.

type of vacuum	Pa
rough	133 - 101325
medium	0.133 - 133
high	< 0.133
ultrahigh	$< 0.133*10^{-4}$

Table 3.2 Vacuum classification (from Pirani and Yarwood (1961)).

Given the present unavailability of suitable compressors, implementation of vapor compression cycles with water as refrigerant thus depends on the successful development of adequate new designs. Some general considerations follow.

Although the requirements of both volume flow and pressure ratio are extreme, the vacuum operating conditions also have a positive consequence: the pressure difference between condenser and evaporator is very low (at a condensation temperature of 50 °C still less than 12 kPa). This pressure difference limits the maximum force difference (due to flow forces) that the internal compressor parts see, allowing for light construction

materials. Also, axial thrust as a result of the pressure difference will be minimal, eliminating the need for large axial bearing provisions.

In some compressor types (e.g. screw compressors) extensive oil circulation through the compressor provides sealing between the different components, thus reducing the vapor leakage flow and enhancing the volumetric efficiency. In section 4.1 it will be shown that the throttling of water does not involve a large irreversibility. Oil flooding can therefore easily be substituted by liquid refrigerant (i.e. water) flooding. This may have the beneficial side effect of somewhat alleviating the superheat temperatures, thereby augmenting the COP. Water sealing is being used in high temperature steam compression and has been applied for a long time in for instance lobe air compressors.

The forces occurring in a compressor can roughly be categorized into three groups: aerodynamic forces from the vapor flow, inertial forces associated with the trajectory of moving parts and friction forces between different components. Due to the low density of water vapor, the mass of refrigerant compressed per unit swept volume, and thus the work performed, is very low. In order to achieve a good compressor efficiency, it is therefore necessary to keep the friction forces as low as possible. For this reason, compressor geometries that inherently require contact between moving parts (e.g. reciprocating or rolling piston compressors) do not seem very promising. Careful selection of for example bearings to minimize friction appears a necessity for all compressor types.

Handling large volume flows requires large, high speed compressors, resulting in large inertial forces. As explained above, aerodynamic forces are expected to be rather small. So as to avoid that inertial forces become disproportionately large compared to the aerodynamic load and entirely dominate the strength dimensioning of the compressor, materials with a high strength-to-density ratio are called for. Indeed, such a material as titanium is increasingly being used in high speed impellers. The aeronautic industry, where a similar imperative for high-strength, lightweight materials exists, has seen a growing use of synthetics in recent years. Fiber reinforced, composite materials, which form the flexible blades of many modern windmills, may possibly also be suitable for vacuum compressors. Resistance to high temperatures is an additional consideration in steam compressors.

Different types of compressors will now be analyzed in more detail with respect to the compression of low pressure water vapor. Table 3.3 lists most types of mechanical compressors and gives some sample maximum flow rates.

	(1)	(2)	(3)
Positive displacement compressors (volumetric compressors)			
- reciprocating compressors (cylinder-piston)		5	
(membrane/diaphragm)			
- rotating compressors			
- screw			
- mono			
- twin	2.8	8 / 17	
- eccentric compressors			
- (rotating or sliding) vane	1.7	1	2.8
- rolling piston (fixed vane)			0.4
- liquid ring (liquid piston)			8.5
- scroll			
- trochoidal (Wankel)			
- lobe compressors (Roots)	22.6	17	14
- regenerative compressor (drag compressor)			
Dynamic compressors (continuous flow)			
- radial (centrifugal)			
- mixed (partial emission)			
- axial			

Table 3.3 Compressor types and some sample flow rates (m^3/s).

(1): ASHRAE Handbook "Equipment" (1988)

(2): Berghmans (1988)

(3): Ryans and Roper (1986)

Compressors can be subdivided in positive displacement and dynamic compressors. The former create a volume that fills up with vapor from the low pressure plenum, then close the volume off and reduce it to a more or lesser extent thereby compressing the gas, and finally annihilate the remaining volume while discharging the fluid into the high pressure plenum. The cycle then repeats from the beginning. Dynamic compressors, on the contrary, process a continuous flow. The pressure increase is achieved through the creation of a centrifugal force field and/or the imparting of kinetic energy onto the fluid which is consequently converted into a pressure rise in a special flow channel. In general, positive displacement compressors can reach high pressure ratios but have limited flow capacity. Dynamic compressors can process much larger flows but have more difficulty achieving high pressure ratios. As can be seen in table 3.3, the maximum achievable flow rates vary widely depending on the source, reflecting an evolving technology. No values are given for dynamic compressors for which the limits are even more scattered.

The flow handling capacity of **positive displacement compressors** is small compared to the needs of vacuum steam compression (15 m^3/s corresponds to some 165 kWr at triple point conditions). In addition, mechanical friction is an inherent feature of many of them. The cyclic motion of *reciprocating compressors* results in large accelerations and decelerations which restrict the maximum allowable speed and thus the volumetric throughput. Furthermore, relative motion and friction between the piston and cylinder is unavoidable. Reciprocating compressors appear therefore not suitable for low pressure vapor compression. Both mono and twin *screw compressors* have successfully been applied for high temperature steam compression (Degueurce (1980 and 1984), Tabb (1982) and Severson (1987)). Geometrically, it appears possible to scale up this type of compressors to larger dimensions. However, the strength limitations of the rotor material and the difficulty of maintaining machining tolerances seem to prevent this possibility. *Rolling piston compressors* have a very small capacity and involve unavoidable friction. It is also believed that the viscous friction of the sealing fluid in *liquid ring compressors* bars them from compressing efficiently low pressure water vapor (Hakin Faragallah, 1988), although they have been proposed for high temperature steam compression (Gromoll, 1987). *Rotating vane compressors* appear more promising with respect to a scaleup: the pressure difference between both sides of the vanes is very small so that large vanes can be used without danger of breakage. Care must be taken to minimize friction between the vanes and casing. Heaton and Benstead (1984) found that it is important for the

performance to compress the gas precisely to the discharge pressure (i.e. no under- or overcompression). This can be accomplished by means of a sliding valve in the sidecasing. *Scroll and trochoidal compressors* have not widely been used in the past. Tabb (1982) reports on development work of trochoidal compressors for high temperature steam compression, funded by the Gas Research Institute. From the GRI-reports by Roche, Hoffmann, Wurm, Stewart et al., it can be concluded that some technical problems remained to be solved. The present status of these developments is unknown to the author. Scroll compressors normally have a fixed volume ratio. Only if they are equipped with an additional discharge valve, can they maybe operate efficiently in refrigeration cycles. The positive displacement compressor with the largest flow is the *lobe compressor*, which is commonly described as suitable for low pressure rises. A more detailed analysis of its performance is given in appendix A. It is shown that its efficiency rapidly deteriorates with increasing ratio of the discharge pressure to the inlet pressure. Since water-based refrigeration cycles feature a high pressure ratio, this type of compressor is inappropriate for this application.

In conclusion, it can be said that both the volume flow and low-pressure efficiency of present positive displacement compressors is insufficient for vacuum water vapor compression. Although some types maybe can be modified to accommodate the specific requirements, their application will at all times be restricted to small capacity installations.

Centrifugal forces and vibrational and bearing problems limit both the rotational speed and the diameter of **dynamic compressors**, in turn restricting the work that can be performed onto the fluid per stage. The total work per unit mass required to compress a fluid from one pressure to another is therefore an important characteristic with respect to dynamic compressors. This work is given by (for isentropic compression):

$$wis = h2is - h1$$

with h1 the enthalpy at the compressor inlet and h2is the enthalpy at the outlet after isentropic compression (cf. fig. 2.7). An equivalent quantity that is commonly used is the adiabatic head, defined as

$$Had = \frac{wis}{g}$$

with g the gravitational constant. Table 3.4 gives the numerical values of these quantities as a function of the condensation temperature for simple isentropic compression of water vapor.

Tscd (°C)	P_d / P_i	wis (kJ/kg)	Had (m)
5	1.488	53	5352
10	2.094	102	10398
15	2.908	154	15664
20	3.988	207	21143
25	5.404	263	26828
30	7.240	321	32710
35	9.596	380	38779
40	12.590	442	45027
45	16.358	505	51441
50	21.058	569	58013
55	26.873	635	64732
60	34.007	702	71586
65	42.695	771	78566
70	53.197	840	85659

Table 3.4 Pressure ratio, isentropic compression work and adiabatic head
for water as a function of the condensation temperature
for a compressor inlet temperature of -0.5 °C.

The values given for the adiabatic head that can be achieved per stage by centrifugal compressors varies widely among different sources. In an article on the selection of compressors, Neerken (1979) puts forth a value of 60 kJ/kg. Commercial information from compressor manufacturers indicates that a value of 90 kJ/kg is standard in modern compressors. Occasionally, values up to 150 kJ/kg are found. Tuzson (1984) and Severson (1987) report on a development whereby the first stage of the centrifugal compressor of a gas turbine was slightly modified so as to be used for steam compression. These developments are extensively documented in 4 GRI reports by Iles et al.. The

titanium impeller achieves a pressure ratio of 3 which, under the operating conditions of the application corresponds to an isentropic work input of 192 kJ/kg. The flow is 18.8 m^3/s. Table 3.5 gives the number of stages that are required to achieve a condensation temperature of 50 °C for different adiabatic heads per stage. Real adiabatic compression requires slightly more stages, but intercooling reduces the number, as will be explained in section 4.3.

wis (kJ/kg)	Had (m)	# of stages
60	6116	10
90	9174	7
150	15291	4
190	19368	3

Table 3.5 Number of stages for a compressor inlet temperature of -0.5 °C and a condensation temperature of 50 °C as a function of the work input per stage.

The most promising compressor development, specifically for the purpose of water-based refrigeration cycles, was recently reported by Ophir and Paul (1991). It concerns an extended design of the compressors used in desalination applications (cf. section 1.3). The centrifugal compressor has a diameter of 2.5 m and flexible, titanium alloy steel blades (thickness: 1.5 mm). The flow rate reaches 300 m^3/s and the pressure ratio is between 2 and 3. At triple point inlet conditions a value of 3 corresponds to a work input of approximately 160 kJ/kg. Ophir and Paul propose a vacuum ice maker with two such compressors (driven by separate electric motors) in series, with direct contact condensation and with intercooling by means of a water spray. For this configuration the maximum condensation temperature is estimated to be some 33 °C. The authors claim that the light compressor construction makes the design economically viable. This system appears to be the first ever to achieve a mechanical vapor compression cycle with only water as refrigerant.

In order to obtain good efficiency over a wide range of operating conditions (variable pressure ratio / variable capacity), the use of inlet guide vanes and/or variable

speed drives is desirable. Many configurations are possible with multistaging. All stages can be assembled onto one single shaft. In three-stage or four-stage plant air compressors, each stage has a separate, small shaft with a pinion gear which are all linked to a common, large bull gear. This configuration allows each stage to operate at its own optimal specific speed. If all stages are driven by independent electric motors, a wide range of control strategies becomes possible.

Although axial flow compressors are well suited for large volume flows, they are not so appropriate for high and variable pressure ratios. Mixed flow compressors are usually characterized as medium flow, medium head machines. If the ratio of both quantities is important, rather than each of them separately, then this type of machine can in principle be applied to low pressure steam compression. Theoretically, mixed flow compressors can achieve higher efficiencies than either centrifugal or axial compressors.

It can be concluded that the extreme requirements of volume flow and pressure ratio necessitate the development of an entirely new type of vacuum compressor. Only if full advantage is taken of the low operating pressures in order to hold capital cost down, only then can a new design make water competitive with traditional refrigerants.

3.2. Ejectors.

A description of a steam jet refrigeration system was given in section 1.3. The mixing of the high and low speed vapor is an inherently inefficient process, rendering the whole system very energy intensive. In addition, the nozzles are designed to operate under one particular set of conditions (e.g. capacity, condensation temperature, ...), further reducing the efficiency at off-design conditions. Even in evaporators, where the thermal energy of the motive steam is still used to good advantage, appears thermal vapor compression to be abandoned in favor of mechanical vapor compression (cf. the part of section 1.1 on open cycle heat pumps). If ejectors were to be used for ice production, it would be necessary to superheat the motive steam so that it does not end in the two phase region after expansion, since this might involve the formation of ice particles in the high speed jet. Superheating further deteriorates the efficiency of the system. The use of a secondary substance with low latent heat of vaporization as motive fluid offers in principle the possibility to improve the efficiency. However, problems with the separation of both fluids have prevented the use of this option (ASHRAE, 1969).

3.3. Liquid column entrainment.

Rice (1981) explains the operation principle of an hydraulic refrigeration system, as illustrated in fig. 3.1. A pump circulates water in a loop over a considerable height difference. At the top, the pressure in the circuit equals the evaporation pressure of the refrigerant. At the connecting tube with the evaporator, the water flow entrains the refrigerant vapor. The water is at ambient temperature, the vapor at evaporation temperature. Heat transfer therefore occurs from the water to the colder refrigerant in the entrainment zone till a temperature equilibrium between both is established (point 2). Next, the mixture flows downward with the vapor bubbles having an upward drift velocity. At point 3 the condensation pressure is reached and the refrigerant starts condensing, giving off its latent heat to the water. At point 4 the condensation is completed. The mixture separates through gravitation in the separation chamber, whereafter the water is recirculated and the liquid refrigerant pumped back to the evaporator. During return both fluids cool sensibly through heat rejection to the ambient. For refrigerant R114 the vertical height of the system is about 25 m.
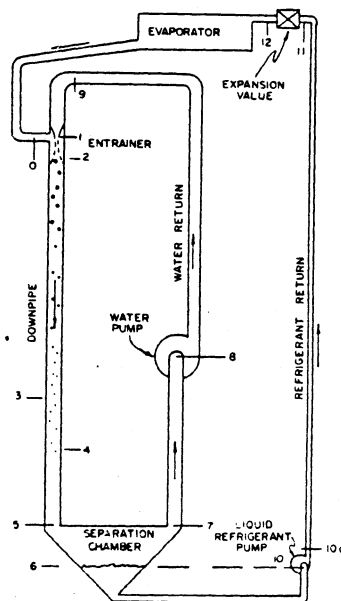
Fig. 3.1 Schematic diagram of a hydraulic refrigeration system (from Rice, 1981).

Theoretical calculations indicated that the COP could be higher than that of a traditional cooling cycle. Initial experiments failed to confirm this, due to inadequate

performance of the separation chamber. It was believed that a centrifugal separator would be required.

If this system would be used for the compression of low temperature water vapor, the downpipe could be much shorter: a few meters would suffice since the difference between evaporation and condensation pressure is very small. On the other hand, in order to process the huge volume flow, the circulation rate of the entrainment liquid can be expected to be many times larger, requiring large diameter pipes. If the entrainment liquid is kept to be water, two phase expansion will occur in the expansion nozzle, giving the flow a high kinetic energy. Appropriate measures must be taken to reconvert this energy into a pressure buildup. It will not be possible to produce ice since the entrainment water would freeze upon expansion. The two phase expansion may also cause cavitation problems in the expansion nozzle. In order to avoid these problems, another substance - immiscible with water- must be chosen as entrainment fluid. Care must be taken that its boiling point is high enough at the triple point pressure of water so that it does not expand into the vapor dome itself.

3.4. Sorption.

Sorption systems have historically been the first to achieve refrigeration. They require thermal energy for the regeneration of the sorbent; the electricity consumed to drive for example pumps only amounts to a small fraction of the total energy usage. They thus constitute an effective means to reduce the electric peak load due to summer air conditioning. Since the temperature requirements of the heat source are moderate (typically around 100 °C), they appear well suited to operate in combination with electricity producing topping cycles. In large scale applications (e.g. industrial cooling or district cooling) gas turbines or internal combustion engines can perform this function. In commercial and residential applications highly efficient fuel cells may be more appropriate since they involve no moving parts. Using to good advantage the waste heat of such electricity generating devices during both the heating and cooling season may considerably enhance the economic feasibility of these combined heat-power schemes.

Water is used as sorbent for ammonia. In combination with lithium-bromide, it functions as the actual refrigerant. This working pair cannot be used for the production of ice, however, due to crystallization problems with rich solutions at low temperatures. Lazare (1984) reviews the literature on different working pairs for absorption cycles. The

water-ethylene glycol pair has been selected for the production of ice in experiments presently in progress at Clarkson University, NY (personal communication by Lazare). The temperature lift of this working pair is sufficiently high to allow for a single stage configuration. Due to the presence of ethylene glycol in the vacuum freeze evaporators (at a concentration of about 1 %), needle-like ice crystals of some 5 mm form without the need for stirring of the water bath. The resulting ice slurry is expected to be pumpable up to a concentration of 50 %. Finally, Zhu et al. (1990) report on the experimental development of a water-zeolite adsorption refrigeration cycle for the cooling of aquatic products on a fishing boat. The heat source is the exhaust gas of the diesel engine. From their measurements can be derived that freezing temperatures can be obtained with condensation temperatures as high as 60 °C.

Chapter 4
Further thermodynamic analysis and miscellanea.

A basic analysis of simple refrigeration cycles was made in chapter 2. In this chapter a more detailed thermodynamic analysis is presented. First a breakup of the irreversibilities between those due to throttling and those caused by superheat sheds more light on the particular behavior of different refrigerants. Next, the theoretical potential of two phase compression as a means of eliminating the superheat peak of water is evaluated. This is followed by a closer look of multistaging and the different options for cycle modifications it offers. Then, a crude estimate of the parasitic power of the vacuum pump is given. Finally, a brief performance comparison is made between thermal storage by means of ice and hydrocarbons (but still with water as refrigerant).

4.1. Irreversibilities.

In section 2.1 the second law efficiency of different refrigerants was given for an ideal refrigeration cycle. Since the reference Carnot cycle was considered to operate between the evaporation and condensation temperature of the real refrigerants, the deviation from ideality did not result from heat transfer with the environment, but was solely due to internal cycle irreversibilities, i.e. the throttling and the desuperheating processes (the compression was modeled isentropically). The contribution of each of these two processes is now quantified separately. This breakup will elucidate the results of the next two sections.

Ideally, saturated liquid refrigerant leaving the condenser would expand isentropically to the evaporator pressure. The enthalpy difference between the corresponding inlet and outlet states would be converted into external work that could comprise part of the compression work. However, it is technically difficult to recover the work from the two phase expansion process; in addition, the amount of work concerned is usually relatively small. In all real refrigeration equipment the expansion is therefore achieved by an isenthalpic throttling process. (A recent, noteworthy study by Kornhauser (1990) proposes an ejector configuration to recuperate the energy of expansion, and accomplish partial compression of the vapor leaving the evaporator. In this instance the two phase conditions also prove to be a serious problem.)

The isenthalpic throttling process is not isentropic. This entropy generation (sgen) unavoidably leads to a higher work input as can be understood as follows. Since the extra entropy must be rejected to the environment, an additional heat flow will occur in the condenser. The supplementary energy dumped is at least equal to Tscd*sgen (with Tscd the saturation temperature in the condenser) and must entirely originate from an additional work input since any extra heat flow in the evaporator would by accompanied by an other (even larger) entropy input.

The entropy generated in the throttling process can very easily be calculated. It depends on the condenser and evaporator pressures and on the thermodynamic properties of the particular refrigerant. Since the latent heat of different refrigerants varies widely, the entropy produced per unit mass was divided by the heat absorbed per unit mass during passage of the evaporator (qev = h1-h5; cf. fig. 2.7 and 2.8). In fig. 4.1, the generated entropy has therefore the units of (mJ/K)/kJr, with r standing for refrigeration effect. This allows a sound comparison.
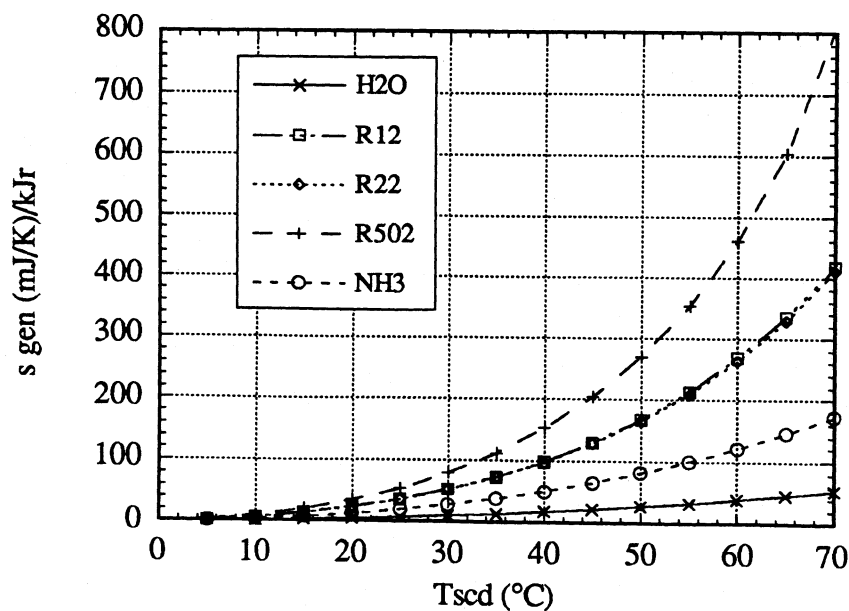
Fig. 4.1 Entropy generation during the throttling process.

As is obvious from the plot, water generates much less entropy during the throttling process than ammonia, which in turn is still better than R12 and R22. R502 is the worst of the five. The good performance of water in this respect can also be seen on fig. 2.8: the

line 4-5, representing the throttling process, is almost vertical. The generated entropy for different refrigerants follows the same order as their respective vapor fractions (i.e. quality) at the throttling valve outlet: the higher the vapor fraction, the higher the produced entropy. The vapor fraction is determined by the latent heat of evaporation and the specific heat of the liquid. The relation between the vapor fraction and the irreversibility is logical since the throttling of a liquid between two pressure levels constitutes a much smaller irreversibility than executing the same process in the gas phase.

The second irreversibility in an ideal refrigeration cycle is the desuperheating process. Ideally, the compression would initially occur adiabatically -until the compressed gas reaches the ambient temperature-, followed by an isothermal part -up to the condensation pressure. In reality the entire compression is much closer to an adiabatic process and the gas leaves the compressor in a more or less superheated state (cf. section 2.4 for superheat temperatures). The cooling of this gas down to its condensation temperature constitutes an irreversibility since the temperature difference with the ambient is much larger than what is considered economically optimal (which should be the condensation temperature).

The irreversibility due to desuperheating can be calculated as follows. The heat evolved during desuperheating (qdes) is

$$qdes = h2 - h3$$

with states 2 and 3 as defined in fig. 2.7 and 2.8. Since the condensation temperature (Tscd) is considered optimal for transferring heat to the environment, the entropy rejection associated with qdes would optimally be

$$sopt = \frac{qdes}{Tscd}$$

The real decrease in entropy (s2-s3) is lower. The difference between both is the needlessly produced entropy, thus:

$$sprod = sopt - (s2-s3)$$

In order to account for the different amounts of heat absorbed in the evaporator

(qev = h1-h5), the produced entropy is each time divided by this quantity, and labeled sgen in fig. 4.2.
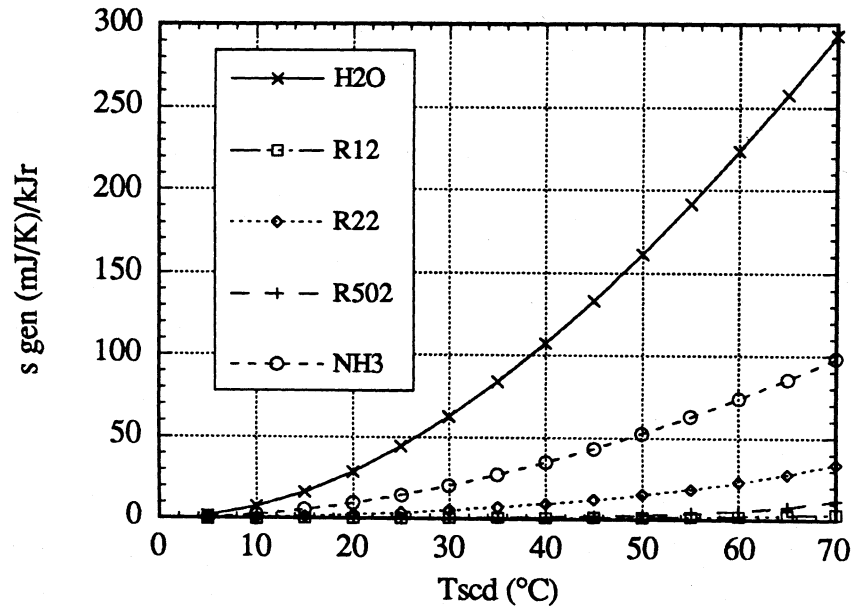
Fig. 4.2 Entropy generation due to desuperheating.

This time, the order of the different refrigerants is inverted, with the exception of R502. Also, R12 and R22 no longer coincide. The most salient feature, however, are the high values for ammonia and, especially, water. This is totally in line with the high superheat temperatures presented in section 2.4.

The total irreversibility in an ideal cycle, i.e. the sum of the throttling and desuperheating irreversibilities, is plotted in fig. 4.3. Overall, ammonia turns out to have the least intrinsic irreversibilities, followed by R12 and R22. Water is next and R502 is worst. Only around 60 °C does water become slightly better than R12 and R22. All these conclusions are perfectly parallel to those drawn concerning the COP of ideal cycles in section 2.1 (cf. fig. 2.4). Indeed, when the generated entropy is multiplied with the saturated condenser temperature (Tscd*sgen) and added to the Carnot work needed to achieve 1 kJ of refrigeration (i.e. inverse of Carnot COP), the total work of an ideal cycle is obtained (for 1 kJr). The inverse of this sum then gives the COP of the ideal cycle. This

relation between the generated entropy and the COP constituted a verification of the irreversibility calculations of this section.
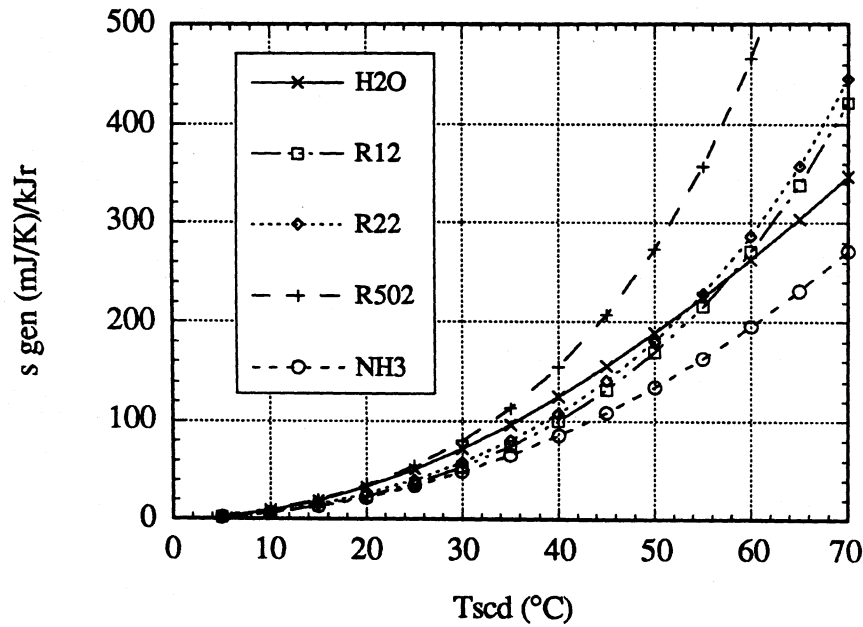
Fig. 4.3 Total entropy generation for an ideal cycle.

The main difference between the ideal cycle considered here and a simple real cycle is the non-isentropic compression. Since the definition of the isentropic efficiency relates to the total work, i.e. both the Carnot work and the added work due to irreversibilities, it directly affects the whole COP to the same measure, thus amplifying the differences between the refrigerants.

In general, it can be concluded that those refrigerants that do not produce much entropy during the throttling process, do so during the desuperheating stage, and vice versa. Modifications to the simple cycle that target the throttling irreversibility, will not affect the performance of water very much. Those, on the contrary, that remedy the superheating problem can be expected to have a significant impact. This will be illustrated in the next two sections.

4.2. Two phase compression.

One way to avoid the high desuperheating irreversibility, theoretically at least, is to start the compression in the two phase region and end exactly at the saturated vapor point, as illustrated in fig. 4.4. Two phase compression poses serious technical problems, though. Small liquid droplets in a vapor flow tend to impact with tubing or compressor parts whenever the direction of the flow changes. These collisions can lead to serious erosion. To avoid this danger, the vapor leaving the evaporator is therefore, in some installations, superheated by subcooling the condensate at the condenser outlet. As a rule, textbooks usually state -sometimes in an almost dogmatic manner- that two phase conditions at the compressor inlet must be avoided at any price. However, since two phase compression can lead to a significant reduction of the work input (as will be shown hereunder), it is important to carefully reevaluate this imposed limitation, and, if possible, make the necessary modifications to safely accommodate two phase flow.
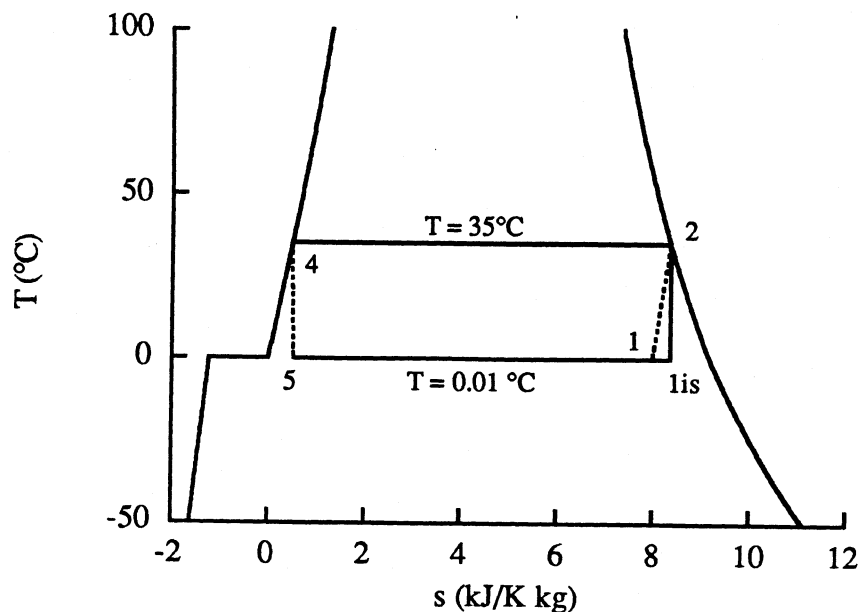
Fig. 4.4 Two phase compression with saturated vapor outlet in (T,s)-diagram.

In the literature some examples can be found that indicate that the limitation on two phase compression does not need to be so absolute. An anonym studied, among other things, the influence of an oil spray travelling with the refrigerant through a screw

compressor. The purpose was to reduce the superheat of ammonia (due to the fact that the oil droplets absorb part of the energy input when heating up), and thus improve COP. A small performance increase was indeed measured, and, moreover, no mentioning at all was made of any physical damage to the compressor! There is no obvious reason to believe that a cloud of refrigerant droplets would behave differently from a cloud of oil droplets with respect to collisions with compressor parts. A more recent paper by Severson (1987) describes the use of a screw compressor with stainless steel rotors for the compression of contaminated vapor in a meat rendering process. The paper explicitly points out that the compressor is able to accept wet steam and that this does indeed reduce the shaft work. A final example that two phase flow maybe is not as detrimental as usually stated, comes from tests reported by Banquet and Merigoux (1987). In a high speed, two stage centrifugal compressor with titanium impellers, liquid water was injected in the interstage conduit to intercool the vapor. Due to the high velocity of the flow, and thus short residence time, only 25 % of the spray vaporized before reaching the second stage inlet. Nevertheless, no erosion of the leading edge of the impeller could be observed, although the rotational speed was more than 48000 rpm!

Those few examples illustrate that the prohibition on two phase conditions does not need to be as absolute as often contended. Whatever the practicality of two phase compression, a theoretical analysis is a worthwhile exercise by itself because it gives some insight into the tradeoff between throttling and desuperheating irreversibilities.

Fig. 4.5 shows the relative energy savings that theoretically can be achieved by means of two phase compression as compared to the ideal cycle analyzed in section 2.1. For both cycles, the evaporation temperature was taken to be 0.01 °C and the compression was assumed to occur isentropically (i.e., following the vertical line 1is-2 in fig. 4.4. for the two phase case). As is obvious from the plot, only for water and ammonia are there energy savings. The other refrigerants do (almost) not benefit, and at high condensation temperatures there even would be a penalty. Since in all cases the irreversibility due to superheating (cf. sections 2.4 and 4.1) is eliminated, these results may appear puzzling at first. However, because this modification of the base cycle reduces the heat absorbed in the evaporator per unit mass (the enthalpy of state 1 is less than that of saturated vapor), a larger mass flow is required to maintain the same cooling power. This implies that the throttling process will generate more entropy. Indeed, for those substances that intrinsically have a low superheat temperature -and thus a low desuperheating irreversibility- and that have large throttling irreversibilities (i.e. R12, R22 and R502), for

these substances the gain from eliminating the superheating is more than offset by the extra loss in the throttling process. On the contrary, ammonia and especially water, which throttle fairly reversibly but have high desuperheating irreversibilities, benefit from the change in inlet state. At a typical condensation temperature of 35 °C, the theoretical energy savings attain approximately 5 % for ammonia and approximately 15 % for water.
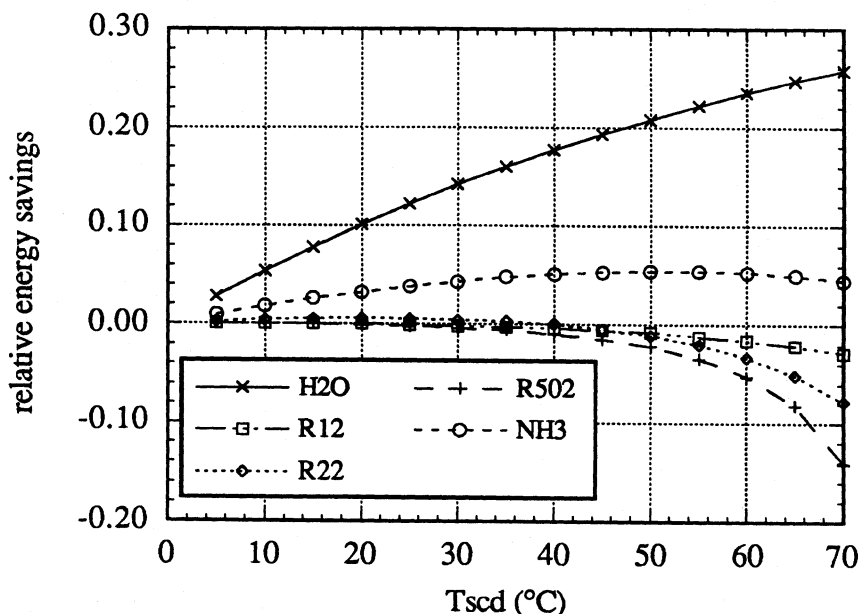
Fig. 4.5 Relative energy savings of two phase compression.

Although two phase compression involves a larger mass flow, the volume flow through the compressor does not increase to the same extend because a major fraction of the additional mass flow is in liquid form. As an example, the mass flow for water increases by some 10 %, but the growth of the volume flow remains limited to roughly 1.7 % (for a condensation temperature of 35 °C). In reality the compression will indeed be non-isentropic. To still have a saturated vapor state at the outlet of the compressor, it is necessary to start out with a larger liquid fraction at the inlet , i.e. a shift from point 1is to point 1 in fig. 4.4. In a conventional cycle with saturated vapor at the compressor inlet, the non-isentropic behavior of the compressor only affects the work term (i.e. the denominator) of the COP, and not the numerator (qev). For a two phase compression, however, both the work term and the evaporator heat term change, increasing and decreasing respectively. The really achievable savings will therefore always be less than

those calculated in fig. 4.5. Moreover, the dynamics of heat transfer in the two phase flow make it unlikely that the same isentropic compressor efficiency can be attained as in the case of dry compression. (To stay close to equilibrium during the entire compression, it will be beneficial to have a homogeneous cloud of very fine dispersed droplets that are in relative motion in the vapor.)

For all these reasons two phase compression is not an obvious method to successfully address the problem of the desuperheating irreversibility. In the next section, a more likely solution is presented.

4.3 Multistaging.

In section 3.1 it was shown that the compression work for water is too large to be performed in a single stage of a centrifugal compressor. The number of stages needed to achieve the necessary work input is highly variable and depends on the maximum desired condensation temperature and the head per stage. Although the need for multistaging may appear a nuisance at first, it permits some modifications to the simple cycle that will now be shown to lead to a significant performance improvement. Except when stated otherwise, the compression will be considered to occur in 7 consecutive stages. This number was chosen so that the condensation temperature of 50 °C can be reached for a modest work input of 90 kJ/kg per stage (i.e., an adiabatic head of roughly 9150 m per stage). The intermediate pressures were chosen such that for isentropic compression each state contributed an equal amount to the overall work (per unit mass), i.e. all stages delivered the same head. All calculations in the preceding parts assumed that the overall compression occurred with an isentropic efficiency of 0.7. In this section, every single stage will be modeled as having an efficiency of 0.7.

The different modifications to a simple cycle are illustrated in fig. 4.6 and 4.7. For the purposes of clarity, the processes are drawn for 3 stages only. Simple adiabatic multistaging corresponds to a process along states I-II-III-IV in fig. 4.6.

A simple modification consists of replacing of the single throttling process by a number of small expansion steps, as depicted in fig. 4.7. The intermediate pressures correspond to the pressures between two compressor stages. After each flashing, the generated vapor is separated off and led to the corresponding interstage compressor duct, where it mixes with the bulk vapor flow. The saturated liquid undergoes another expansion process, and so forth. In this way the needless expansion of all the vapor to the
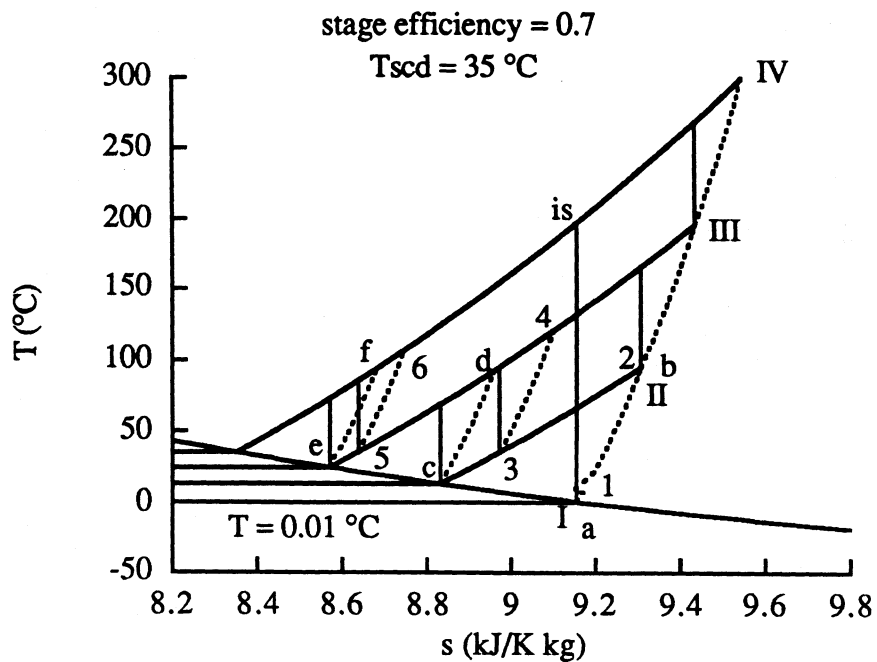
Fig. 4.6 Three stage compression without intercooling, with external intercooling and with refrigerant intercooling.
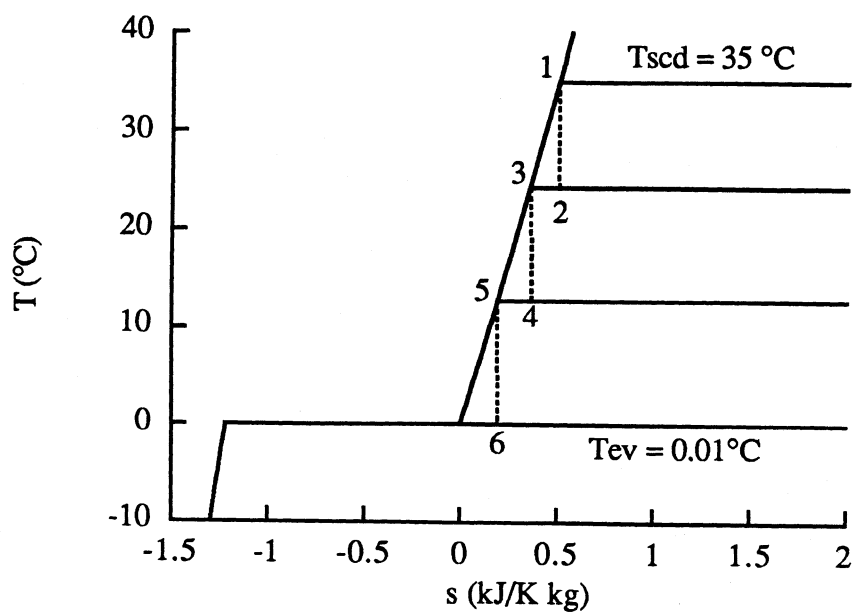
Fig. 4.7 Three stage throttling process.

evaporator pressure is eliminated and the flow through the lowest compressor stages reduced. This mode of operation is called the economizer principle.

A further modification is the cooling of the superheated vapor between two stages. This intercooling can be done in two different ways: by injecting liquid water or by rejecting heat to cooling water in a heat exchanger. In the first case, the vapor can be cooled down to its saturation temperature by carefully dosing the amount of injected water. As the liquid vaporizes, it absorbs sensible heat from the superheated vapor. In fig. 4.6, the vapor leaves the evaporator at state a and is non-isentropically compressed to point b in the first stage. The liquid spray cools the vapor down to the saturated state c. This is followed by a second compression to state d, another intercooling to state e, and a final compression to state f, at which point the steam enters the condenser. By adding the spray water, the mass flow increases in each stage. If the impeller is susceptible to erosion damage from two phase flow (cf. section 4.2), specific precautions must be taken to avoid droplets from entering each stage (e.g. louvers or demisters). In the case of intercooling with a heat exchanger, the superheated vapor cannot be cooled below the ambient temperature (or inlet temperature of the cooling water). In the calculations below, it was assumed that the vapor could be desuperheated to a temperature equal to the condensation temperature. Since the heat transfer coefficient for gas is much lower than for condensation and since a large interstage heat exchanger may result in a significant pressure drop, this assumption may be too optimistic. In fig. 4.6 the process with external intercooling goes through states 1-2-3-4-5-6. The temperature of points 3 and 5 is 35 °C, as is the condensation temperature. For the case of 7 stage compression, the exit temperature after the first stage does not -or barely- attain the condensation temperature. External intercooling was therefore modeled with intercooling starting after the second stage only.

Fig. 4.8 shows the performance of the different configurations. As a reference, the ice making cycle with ammonia of fig. 2.9 is repeated here (compressor inlet is saturated vapor at -6 °C). For all water cycles, the compressor inlet state is saturated vapor at -0.5 °C. The non-isentropic compression with an overall efficiency of 0.7 (labeled 'single stage') also corresponds to the same case in fig. 2.9. This cycle will be considered the base case for further comparison. (A sample EES worksheet is given in App. B.3.)

Applying 7 stage compression, each stage having an isentropic efficiency of 0.7 (labeled 'multistage'), severely affects the COP. This is due to the fact that the stage inlet temperatures are higher than for the base case, as can be seen fig. 4.6. Since the isobars in a (T,s)-diagram diverge towards the right (i.e. with increasing entropy), a larger

temperature difference, and thus enthalpy difference or work input, exists between the same two pressures. At a condensation temperature of 35 °C e.g., the isentropic efficiency of the overall compression process is thereby reduced to 0.63. The higher work input per stage also implies that the design head (90 kJ/kg) will not suffice to reach a condensation temperature of 50 °C. Multistaging in a further unmodified cycle thus not only destroys much of the gain of eliminating the heat transfer in the evaporator, but, in addition, aggravates the already extreme compressor requirements.
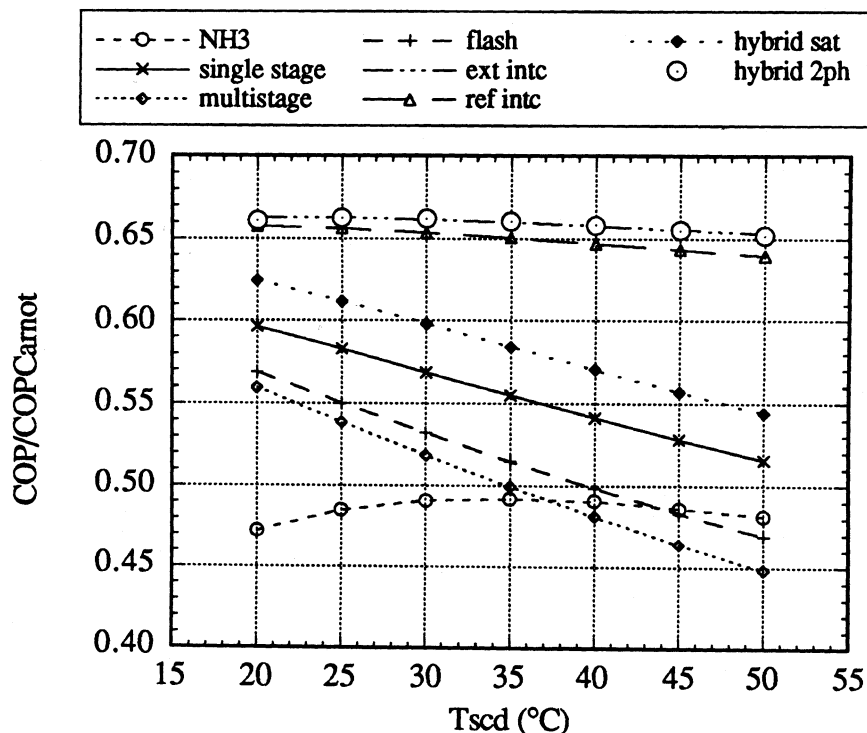
Fig. 4.8 Second law efficiency for different multistage configurations.

The simple cycle modification to multistage flashing (labeled 'flash') only partially compensates for the loss in performance of multistage compression. The small improvement is primarily due to a reduction of the flow through the lower stages of the compressor (for the first stage e.g., on the average 5 % less). Also, the interstage mixing of the saturated flash vapor with the superheated vapor somewhat reduces the inlet temperature of the next stage. In fig. 4.6 this would correspond to a slight shift of points II and III to the left. However, since the amount of flash vapor is relatively small, this cooling effect is limited: under most conditions it is barely a few degrees Celsius. In order not to confuse the graph, these changes are not represented in fig. 4.6. It is not unexpected

that multistage flashing results in an only moderate performance improvement. In section 4.1 it was shown that for water the throttling irreversibilities are only a small fraction of the desuperheating irreversibilities, and those are virtually not affected by the multistage throttling.

As is obvious from fig. 4.8, interstage desuperheating (in addition to multistage flashing) has a much bigger impact. Under the assumptions made (see above), intercooling by means of a heat exchanger (labeled 'ext intc') turns out to be slightly better than intercooling through injection of liquid refrigerant (labeled as 'ref intc'). Noteworthy is the fact that the second law efficiency does almost not diminish with increasing condensation temperature, unlike in the other instances. Since, for the case of external intercooling, the mass flows through the different stages remain unchanged as compared to simple flashing, the improvement is solely due to the much lower stage inlet temperatures (taken equal to the condensation temperature). As explained above, the pressure lines converge towards the left in the (T,s)-diagram, corresponding to a lower compression work per unit mass. As a consequence, not only improves the COP, but also is it possible -for a given head per stage- to reach a higher condensation temperature, or, alternatively, lower heads per stage suffice for an equal condensation temperature. Maximum superheat temperatures are on the order of 50 °C above the condensation temperature. As can be seen in fig. 4.6, the high superheat spike is replaced by a seesaw of much smaller triangles, thus effectively reducing the irreversibility and more closely approaching the ideal isothermal compression. In the case of liquid intercooling, the extra -but small- irreversibility of throttling an additional amount of liquid water clearly is more than outweighed by the strong reduction of the desuperheating irreversibility. The superheat temperature remains limited to maximally 30 °C (in contrast to the hundreds of degrees Celsius for the simple adiabatic compression; cf. fig. 2.15). From the improved COP, one also can conclude that the increasingly larger mass flow through the higher stages (on the average some 15 % extra in the last stage) is more than compensated for by a lower work per unit mass. This lower work is due to the lower inlet temperature. The head between two pressures has now -i.e.under saturated inlet conditions- reached its lowest value (for compression entirely in the gas phase). For a given head per stage the configuration with spray intercooling therefore requires the lowest number of stages to reach a given condensation temperature. Table 4.1 gives the condensation temperatures that can be achieved under these optimal conditions. Comparison with table 3.5 (purely adiabatic case) shows that the number of stages to reach a given condensation temperature is reduced by roughly one fourth.

w (isentropic) (kJ/kg)	adiabatic head (m)	3 stages (°C)	5 stages (°C)	7 stages (°C)
60	6116	19.0	33.2	48.3
90	9174	28.9	51.0	75.5
120	12232	38.9	69.7	105.2
190	19368	62.5	117.2	187.3

Table 4.1 Condensation temperature for various heads and number of stages.

So far, no attention has been paid to the effect of the different modifications on the volume flow. Fig. 4.9 shows the inlet volume flows per unit refrigeration capacity of the different stages for 4 different configurations. The most important feature is the significant reduction of the specific flow at higher stages. After 2 stages the flow has already been reduced by at least one third. The flow requirements of the higher stages are thus somewhat less extreme than those of the initial stages. Nevertheless, the specific flow of the last stage is still between 40 and 75 times that of a traditional refrigerant. Multistage
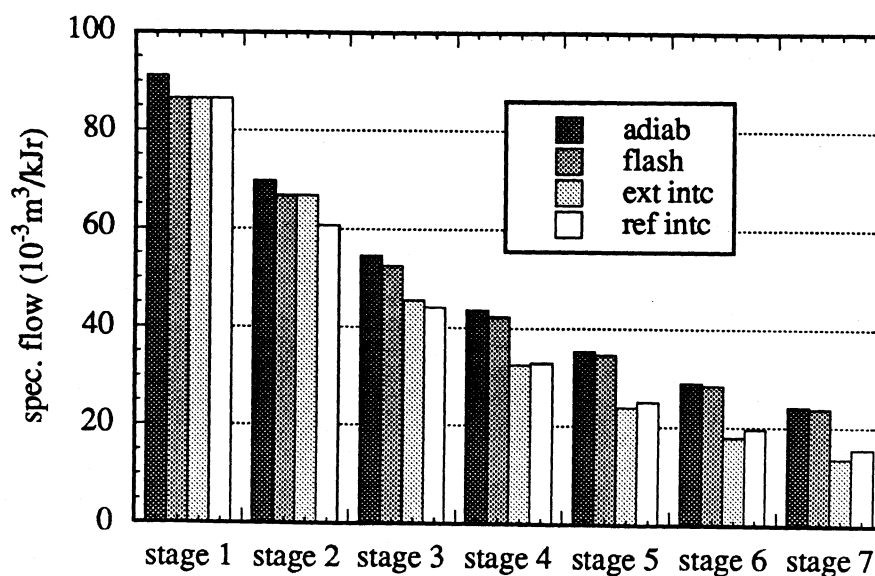
Fig. 4.9 Specific volume flows at the stage inlets for different configurations.

flashing slightly reduces the mass flow, and thus volume flow through the lower stages. As can be seen, this effect is small: about 5 % for the lowest stage. With increasing stage the difference with the simple adiabatic base case becomes progressively smaller. The mass flow through the last stage is identical for both cases. However, the temperature, and thus specific volume, at the last stage inlet is a bit lower for flashing, whence the tiny difference in volume flow.

Intercooling (both external and with refrigerant injection) leads to larger reductions, especially for the higher stages. External intercooling can only be applied after the second stage. Consequently, the inlet flow of the second stage is not affected. In the case of spray intercooling, the inlet conditions of each stage have been assumed to be at the saturated vapor state. The specific volume thus corresponds to its lowest possible value for the given pressure. This is at the expense, however, of an increasingly higher mass flow through the successive stages. As a result, the volume flow through the 4 highest stages is somewhat larger than in the case of external intercooling, although the stage inlet temperatures in the latter instance are always higher. The relative differences are small, however, and of greater importance is the fact that both methods of intercooling produce approximately half the volume flow by the last stage, as compared to the adiabatic and flash cases.

In fig. 4.8 two more configurations, labeled as 'hybrid sat' and 'hybrid 2ph', are represented that have not been elucidated yet. It concerns a two stage combination. The first stage performs a modest compression from a saturated inlet state at -0.5 °C to a pressure of 0.872 kPa, the equivalent saturation temperature of which is 5 °C. This compression corresponds to a low adiabatic head of 52.5 kJ/kg ($\approx$ 5350 m), which can easily be realized with a centrifugal compressor. Since the exhaust pressure is constant, the compressor is not subjected to variations in head, which should simplify both control and design. The second stage performs the remaining compression up to the condensation pressure. This function would be performed by an hypothetical positive displacement compressor with very large flow handling capacity. Since, due to the first compression, the inlet temperature is no longer at freezing point, it is possible to apply both water sealing (to improve the volumetric efficiency) and/or two phase compression (to improve the COP). In a first case (labeled as 'hybrid sat') the steam leaving the first stage is considered to be desuperheated to exactly the saturated state by injection of liquid water before undergoing further compression. In the second case (labeled 'hybrid 2ph') a larger amount of water is injected so that a two phase inlet state is obtained with a composition such that

the second compression results in saturated conditions. In both instances the throttling process is taken to happen in two steps, and all compressions occur with an isentropic efficiency of 0.7. Apart from eliminating all freezing problems in the second compressor, the first centrifugal stage has the additional benefit of reducing the inlet flow of the second compressor by about one fourth under common condenser conditions. As can be seen from the plot, simple two staging constitutes a first improvement over the purely adiabatic case. Coincidentally, the performance of the two phase compression case (represented by large circles with center points) is virtually identical to the performance of external intercooling (represented by the intermittent line with 3 dashes). Two phase compression thus constitutes a further important performance improvement over dry compression, and, moreover, the result is again nearly independent of the condensation temperature. This once more illustrates the potential benefits of two phase compression technology when water is applied as refrigerant.
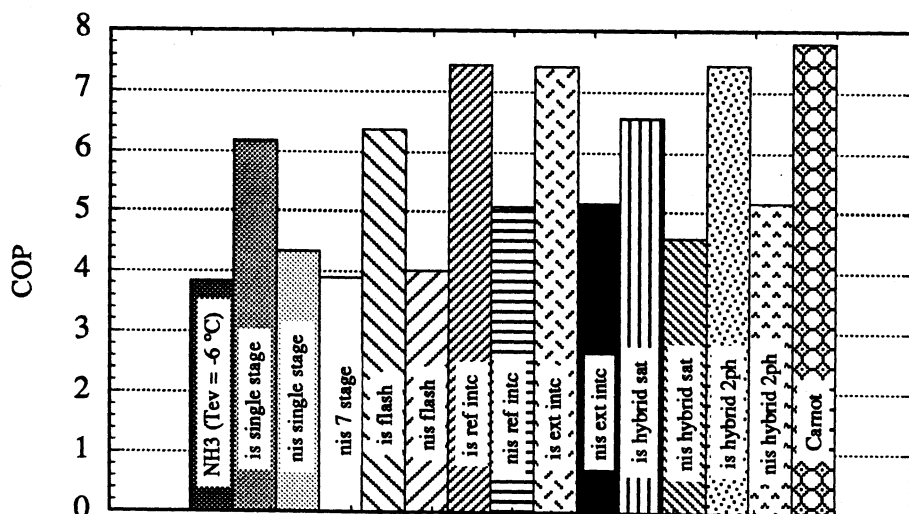
Fig. 4.10 COP for different multistage configurations for a condensation temperature of 35 °C and a compressor inlet state of -0.5 °C (saturated).

Fig. 4.10 replots many of the previous results for a condensation temperature of 35 °C. In addition, the performance of the different configurations is included for the case that all compression processes occur isentropically (labeled with the prefix 'is' as opposed to

'nis'; the labels further follow the notation of fig. 4.8). It is clear that both cases of intercooling as well as the case of two phase compression almost reach the Carnot COP. This indicates that these modifications effectively remedy the problem of internal cycle irreversibilities, which are inherent to the thermodynamic properties of water. Major further performance improvements can therefore only result from a better isentropic efficiency or a condensation temperature closer to the ambient.

The number of stages in the previous analysis (7) was fairly high. For reasons of practicability, preference will more likely be given to a smaller number of stages with a higher adiabatic head each. The corresponding performance will presumably not be quite as good as for 7 stages. The already significant COP increase of the two stage case of fig. 4.8 suggests, though, that the major improvement comes about with the breaking up into the first few stages, and that any further breakup in a higher number of stages has a diminishing benefit. No explicit calculations to support this hypothesis were performed. Neither was any analysis made of the combination of external intercooling followed by refrigerant injection cooling. Although this most likely will result in a further performance increase, it is not expected that this improvement will be very large, at least not for the 7 stage case: with saturated vapor inlet conditions, the stage outlet temperatures do not exceed the condensation temperature by very much, especially for the lowest stages, and the external heat removal thus necessarily is very limited. The situation may be different for a small number of stages.

In summary, one can conclude that multistaging -however inconvenient it may be in se- offers the opportunity to make beneficial modifications to the basic refrigeration cycle. Multistage flashing and, especially, intercooling largely cure the inherently less favorable thermodynamic properties of water, resulting in a better COP. Furthermore, intercooling mitigates both the adiabatic head and the volume flow requirements, allowing for less and compacter stages.

4.4. Parasitic power of air removal.

A refrigeration cycle with water as refrigerant operates at strongly subatmospheric pressures. As a result, air will tend to leak into the system. Careful design and construction can, if not eliminate, at least minimize this infiltration of air. Air leakage along the compressor shaft can for instance be avoided by means of a buffer space between two seals, filled with pressurized liquid water. Air can also enter the system dissolved in the

chilled water and/or cooling water. The refrigeration system must therefore be provided with special air removal equipment that continuously discharges air to the ambient. This equipment must also be able to create vacuum conditions at startup. Because the air leakage into the system due to incomplete tightness cannot be predicted, the following analysis only takes into account the air entering the system dissolved into the water.
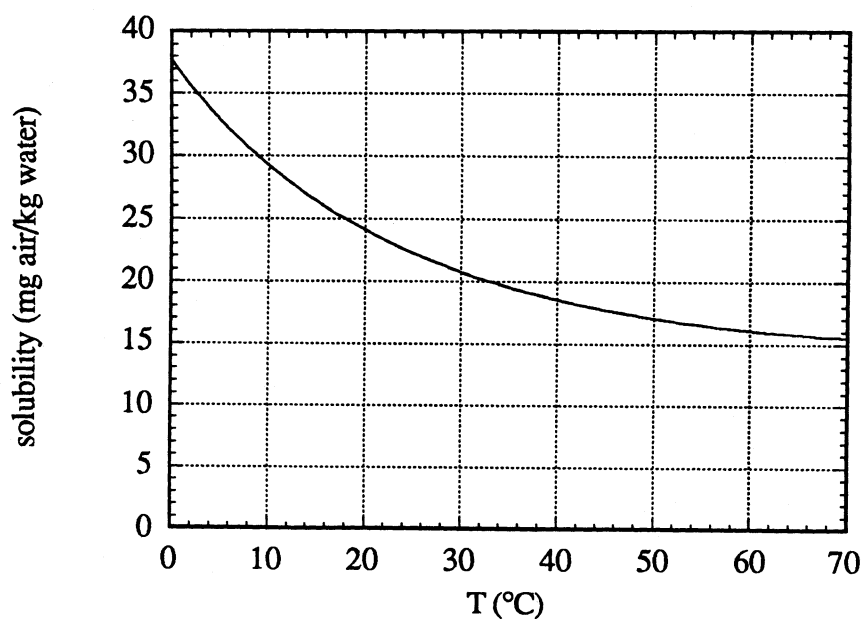
Fig. 4.11 Solubility of air in water at atmospheric pressure (101.325 kPa).

The quantity of air dissolved in a given amount of water at equilibrium conditions depends both on temperature and pressure. Fig. 4.11 shows the solubility of air into water as a function of temperature at atmospheric pressure, as calculated according to Hyland and Wexler (1983). The solubility is much larger at lower temperatures; nevertheless, it remains fairly limited in absolute terms. It is assumed that in applications with an open load the water becomes fully saturated with air before returning to the vacuum freeze evaporator. In a closed system, i.e. with a heat exchanger coil, this source of air infiltration will indeed be minimal.

Fig. 2.6 depicted a vacuum ice making cycle with surface condenser and simple vacuum pump. It is possible to cool the flow entering the vacuum pump by evaporating an additional amount of water at low pressure in a separate heat exchanger, as illustrated in
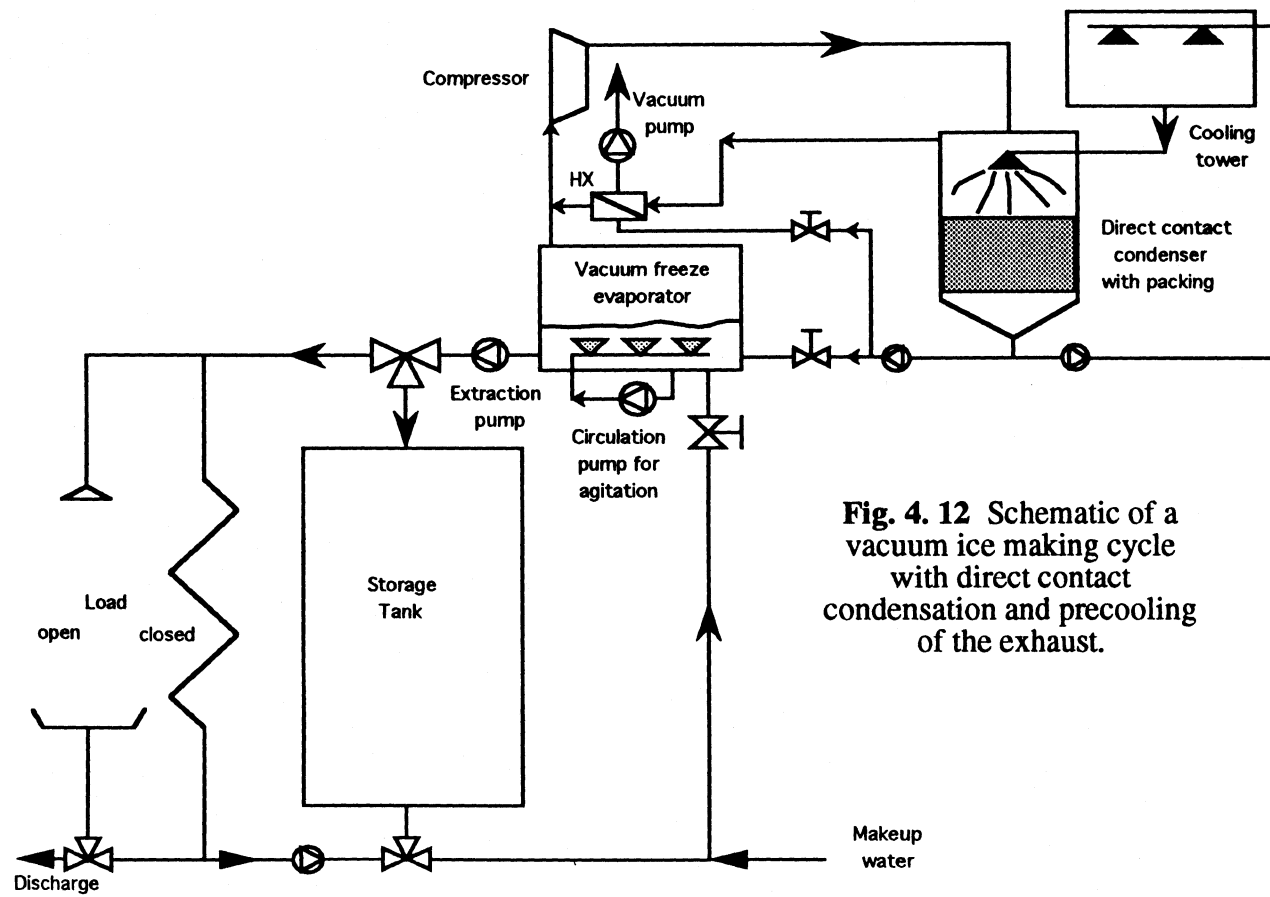
Fig. 4. 12 Schematic of a vacuum ice making cycle with direct contact condensation and precooling of the exhaust.

fig. 4.12. During the process a large fraction of the water vapor in the mixture condenses, reducing the mass flow through, and thus work of, the vacuum pump. On the other hand, the flow through the primary compressor increases. This figure also shows a spray type, direct contact condenser instead of a surface condenser (A variant would be the falling film type, direct contact condenser of fig. 1.7). By eliminating the heat transfer through the tubes, the condenser pressure can be lower as compared to surface condensers, at the expense, however, of an additional air load. Each of the possible combinations (surface / direct contact condenser, with / without cooling) is now evaluated with respect to total power consumption.

Several assumptions are made in the calculations. To insure pumpability, the ice fraction of the slurry withdrawn from the tank is taken to be 0.2. Five times more water thus passes through the vacuum freeze evaporator than the amount of ice produced. The water enters the vacuum freeze evaporator saturated with air at 0 °C. The pinch point temperature drop in a surface condenser is assumed to be 3 °C so that the condensation temperature of a direct contact condenser is taken lower by the same 3 °C for identical cooling water outlet temperatures. The mass flow of the cooling water is such that the temperature rise between inlet and outlet is 8 °C. The amount of air freed in the vacuum freeze evaporator is so small compared to the vapor flow through the primary compressor (less than 1/10th of a percent by mole) that its contribution to the increase of primary compressor power is believed negligible. The biggest assumption concerns the condenser, which is approximated by a point model. Physically, this means that the state variables (temperature, pressure, air fraction) are homogeneous throughout the entire plenum of the condenser (perfect mixing), which may be substantially different from the real conditions. The molar fraction of air in the condenser then follows from a simple mass balance (the amount entering equals the amount withdrawn by the vacuum pump). The partial pressure of the water vapor is taken equal to the pressure for the case without air, i.e. the saturated pressure corresponding to the condensation temperature given in abscissa of the graphs. The total pressure is higher by the partial pressure of the air. This higher discharge pressure increases the primary compressor work. The vacuum pump is responsible for the other part of the extra work, which is calculated by considering the air-water mixture an ideal gas with constant specific heats. Its isentropic efficiency is set to be 0.4. For the cases with cooling it is assumed that the air-water mixture enters the vacuum pump at 5 °C in the saturated state. For the case of direct contact condensation the pump work to extract the cooling water from the condenser is included (isentropic efficiency of 0.6). The point

model of the condenser is believed to be crude. The following results must therefore considered with the necessary reserve.
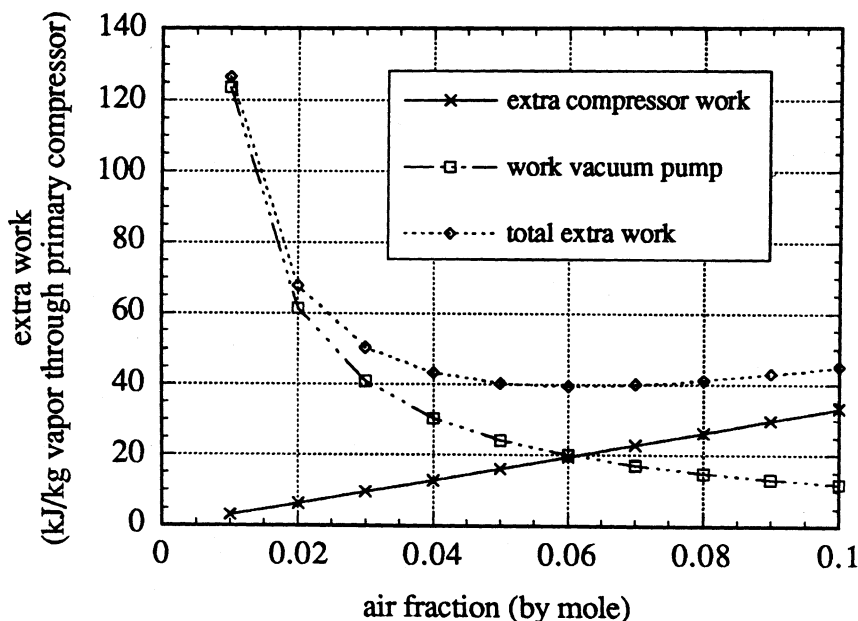
Fig. 4.13 Extra work due to air entering the system.
(through evaporator only; Tscd = 35 °C)

Fig. 4.13 illustrates the dependance of the work of the vacuum pump and the increase of the work of the primary compressor as a function of the molar fraction of air in the condenser for the case of a surface condenser (air only entering the system dissolved in the evaporator water). With increasing air fraction the total pressure in the condenser goes up, increasing the extra work of the primary compressor. The mass flow through -and thus work of- the vacuum pump, however, decreases since for a given amount of air less water vapor accompanies it. As a result, the total additional work reaches a minimum for a certain composition, which depends on condensation temperature, the amount of air entering the system and whether or not the air-water mixture is cooled before entering the vacuum pump.

Fig. 4.14 shows the optimum air fraction for the different instances. This optimum concentration can be obtained by controlling the rotational speed of the vacuum pump. When no cooling is applied, the optimal air fraction decreases with increasing condensation temperature and is larger when more air enters the system (i.e., both in the condenser and

evaporator as opposed to in the evaporator only). As the condensation temperature increases, the power of the primary compressor increases, but the power of the vacuum pump decreases since its suction pressure becomes higher. At low condensation temperatures a high air fraction is therefore favorable: the penalty for the primary compressor is limited and the vacuum pump processes relatively low quantities of water vapor. Vice-versa for higher condensation temperatures. Precooling causes an extra flow through the primary compressor. At low temperatures this does not involve very much work and it is advantageous to have a low air fraction in the condenser, i.e. much water condensation in the heat exchanger. At higher temperatures the penalty for a larger primary compressor flow becomes larger and the optimum air fraction shifts to a slightly higher value. For more air leakage the optimum concentration is again higher.
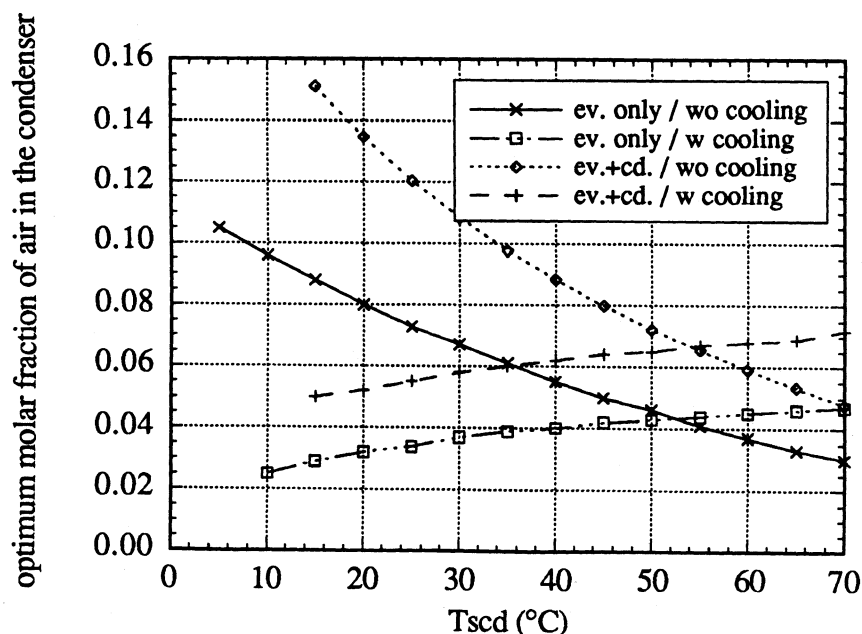
Fig. 4.14 Optimum air fraction in condenser (point model).

Fig. 4.15 gives the influence of the parasitic power on the COP for the different instances. The reference COP is for a surface condenser and no air infiltration (the only case considered throughout the rest of this work). The relative penalty of air leakage is highest at low condensation temperatures when the primary power consumption is lowest. In both instances (air entering through the evaporator only or through both the evaporator and the condenser) cooling of the mixture before it enters the vacuum pump is

advantageous till about 55 °C, at which temperature the cooling should ideally be disabled. In fig. 4.14 it is seen that the optimum air fractions for both instances cross at about the same temperature. For the case of a surface condenser, the COP decreases with roughly 5 % over most of the temperature range. When a direct contact condenser is used, the lower condensation temperature approximately offsets the parasitic power for condensation temperatures from 15 °C upwards.
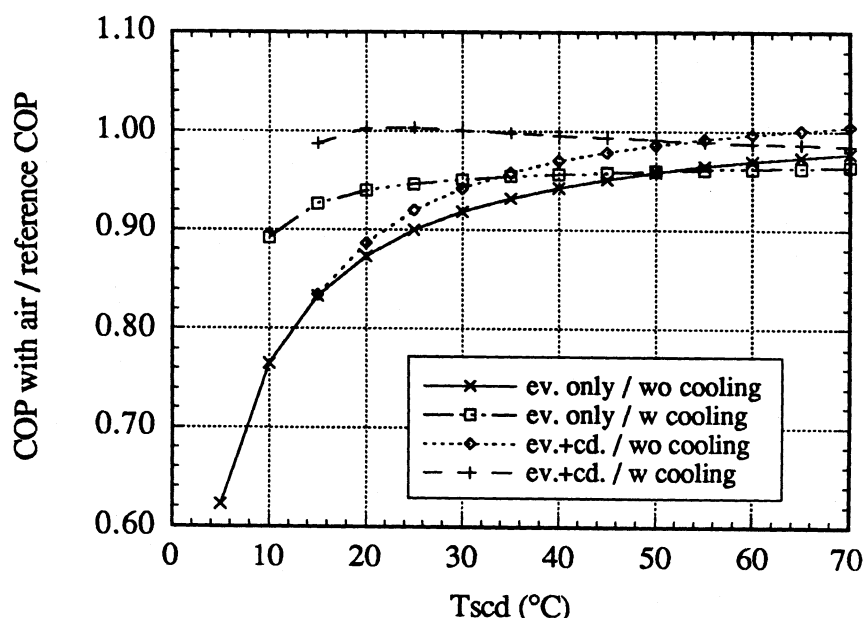
Fig. 4.15 Influence of air entering the system on overall COP (point model).

It is the author's belief that the point model of the condenser overpredicts the actual parasitic energy consumption. In real condensers the air concentration strongly varies throughout the condenser. At the vapor inlet the air fraction is extremely low. As the vapor flows through the condenser, water condenses and the stream gradually becomes richer in air. By the time the mixture reaches the opposite end of the condenser, its temperature may be well below the original condensation temperature, especially in countercurrent configurations. When entering the vacuum pump at this point, the concentration of air in the saturated mixture may be expected to be higher than the optimal fraction calculated under homogeneous conditions, thus lowering the mass flow through and power of the vacuum pump (e.g., if the pure water vapor condensation temperature is 35 °C, a temperature of 32 °C at the vacuum pump inlet already corresponds to an air

fraction of at least 15 % by mole, which is much higher than the optimum homogeneous air fractions at this temperature). Measurement of the total pressure and the inlet temperature of the vacuum pump (from which the partial pressure of water can be determined) allows an easy determination of the composition of the saturated vapor so that control of the pumping speed is possible. (The homogeneous point model would have required a very accurate relative humidity sensor.)

In desalination plants the air removal system sometimes appears to be double staged: a booster compressor (e.g., of the lobe type) performs a first moderate compression, thus significantly reducing the specific volume of the flow, whereafter the stream is intercooled (with further water condensation) and finally enters the forepump (e.g., of the rotary piston type) to be discharged at ambient pressure (Snyder (1966)). Ophir and Paul (1991) use the same configuration in their entirely water-based ice maker. In these instances too, an optimal air flow rate through each of the stages can be expected to exist. An alternative air removal system used in desalination is a liquid ejector (Lucas et al. (1985)).

Although the model used in this section is very crude and believed to overestimate the parasitic power consumption, it nevertheless indicates that under normal operating conditions the penalty for applying direct contact heat exchange on the load side is limited and inexistent for direct contact heat exchange in the condenser. It also illustrates that an optimal volume flow through the vacuum pump exists that minimizes the total energy consumption. The optimal volume flow value is variable and depends on such parameters as condenser total pressure, vacuum pump inlet temperature, isentropic efficiencies, whether or not precooling is applied, etc.

4.5. Other phase change materials.

Cool storage by means of the heat of fusion of ice features higher storage densities, and thus smaller installations, than cool storage by means of the sensible heat of water. For air conditioning applications, however, the melting temperature is lower than what is needed, resulting in a performance penalty. Cho et al. (1991) proposed to use a mixture of hydrocarbons and water as a heat transfer fluid in district cooling systems. This would reduce both the piping diameter and the pumping power. Tetradecane and pentadecane have the right fusion temperatures (5.8 °C and 9.9 °C respectively). It is possible to use these substances also for thermal storage. No modification needs to be made to the configuration of fig. 2.6. Evaporation of the water in the vacuum freeze evaporator now

causes the phase change materials to solidify. Since the evaporation temperature is higher, both the head and volume flow requirements of the compressor reduced. Table 4.2 summarizes some values.

T evaporation (°C)	w (isentropic) (kJ/kg)	adiabatic head (m)	specific flow (m^3/kJr)
-0.5	569	58002	93.61*10^{-3}
5.3	474	48318	62.63*10^{-3}
9.4	414	42202	47.84*10^{-3}

Table 4.2 Specific flow and required adiabatic head
for different evaporation temperatures.

As for ice production, a driving force of 0.5 °C is assumed for the cases of tetra- and pentadecane. All values are for a maximum condensation temperature of 50 °C and for simple isentropic compression. For an identical cooling capacity the volume flow is reduced by about one third and half, and the adiabatic head by 17 % or 27 %, for tetra- and pentadecane respectively. The temperature of fusion of hexadecane (18.1 °C) is considered too high by Cho et al. (1991) for use as phase change material, although it may function in a mixture with tetradecane. Such mixtures with variable fusion temperatures can in principle be cooled reversibly in a batchwise manner in the same way as the sensible cooling of water (cf. section 2.3). However, since the temperature difference between initial and final conditions is much lower than for water cooling, no significant improvement can be expected. This possibility has therefore not been further explored in this work.

Fig. 4.16 compares the COP for different thermal storage systems. The ice storage systems with ammonia and water refrigerant cycles correspond to those of fig. 2.9. If the low temperature of the ice storage systems is not needed for the application, there definitely is a clear energetic advantage in using phase change materials with a higher fusion temperature. The vacuum freeze evaporator avoids problems with clogging of heat exchanger surfaces. The favorable characteristic of pumpability is indeed maintained for these mixtures.
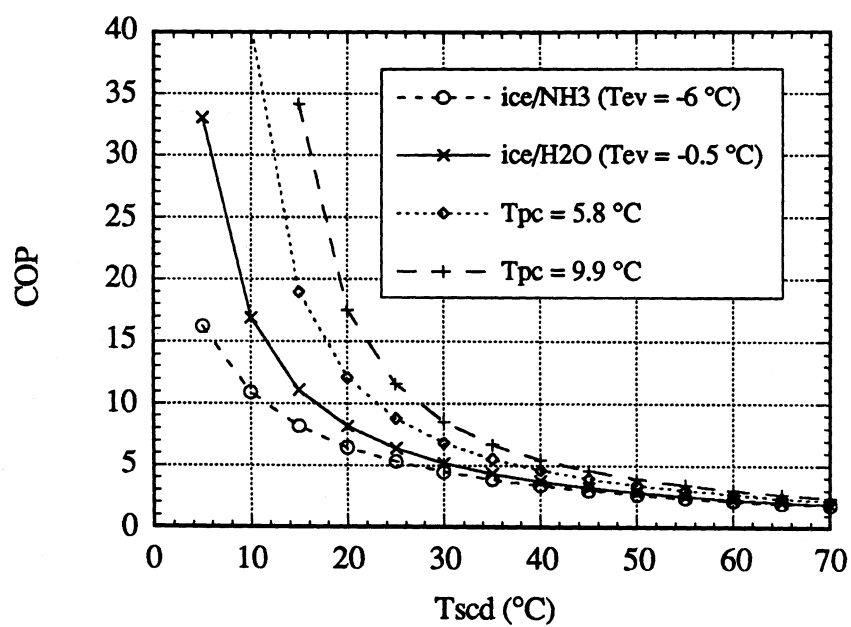
Fig. 4.16 COP for different thermal storage materials.

Chapter 5
Conclusion and recommendations.

Water has long proven to be an excellent working fluid for power cycles in electricity generation. In recent years mechanical vapor compression has been at the basis of open cycle heat pumps in the process industry. These cycles usually operate around 100 °C. Extending the domain of mechanical vapor compression towards temperatures at or below ambient offers the opportunity to use water as a working fluid in refrigeration cycles or heat pumps with the environment as a heat source. The compression of low temperature water vapor poses a great technological challenge, but the ecological soundness of water and the potential for significant energy savings in many applications warrant further research and development efforts.

5.1. Conclusion.

McLinden and Didion (1987) summarize the different requirements that a substance must satisfy to function as a refrigerant. An obviously absolute necessary condition is that of chemical stability over the entire range of operating conditions of the refrigeration cycle. Water certainly satisfies this requirement. Three further fundamental requirements are related to health, safety and the environment: the refrigerant should be non-toxic, non-flammable and environmentally benign. Water also excellently fulfills each and every of these demands, distinguishing it from almost all other refrigerants. The other desirable features given by McLinden are of a technological nature and are not as strict. They concern physical properties (vapor pressure, heat capacity, viscosity, ...) that influence the actual design and performance of the refrigeration equipment. Water differs substantially from other refrigerants with respect to these thermophysical characteristics.

Physically, it is possible to use pure water as refrigerant down to its triple point temperature of 0.01 °C. At this temperature the vapor pressure is very low -less than 1 % of the atmospheric pressure-, resulting in a very large specific volume. The ratio of the condenser pressure to the evaporator pressure is higher for water than for classical refrigerants. As a consequence, also the compression work per unit mass, or equivalently head, is larger. The simultaneous occurrence of a huge volume flow and large adiabatic

head poses unique requirements on the compressor. Compressors with these characteristics are not readily available on the market.

The simple molecular structure of water (consisting of 3 atoms only) gives it a low specific heat, causing, in combination with the large compression work, high compressor outlet temperatures in a simple cycle configuration. These high superheat temperatures constitute an important irreversibility. Although the throttling of water is relatively reversible -due to the small vapor fraction that is generated-, this does not fully compensate for the high desuperheating irreversibility so that, overall, water has a somewhat lower efficiency than most traditional refrigerants in a simple refrigeration cycle.

Energy savings can nevertheless be achieved in those situations where water also functions as heat transfer or thermal storage medium. In these instances the heat transfer surface in the evaporator can be eliminated, and with it the heat transfer temperature drop. The COP improvement is especially important for the case of ice making. In addition, the ice produced in a vacuum freeze evaporator is in the form of a fine slurry which is readily pumpable. In theory it is also possible to realize large energy savings in the case of sensible water cooling by operating in a batchwise manner. The practicality of this concept is less certain, however. In water cooled condensers the heat rejection surface can be eliminated too, further improving the COP.

A still further reduction of the energy consumption is obtainable through modifications to the simple refrigeration cycle that reduce the desuperheating irreversibility. Due to the high head requirements, multistaging is an absolute necessity for centrifugal compressors. This unfavorable feature per se may be turned into an advantage by intercooling the vapor between successive stages and by multistage flashing. These changes mitigate the desuperheating irreversibility and thus lessen the compression work. Theoretically, the same effect can be obtained by means of two phase compression.

The flow processing capacity of positive displacement compressors is very limited compared to the demands of low pressure vapor compression. Even with considerable design changes, their use appears restricted to installations with a small cooling power. Dynamic compressors have a much larger flow handling capacity, but require multistaging to achieve the necessary head. Simply using standard compressors would make a water-based system prohibitively expensive compared to classical refrigerant systems which can do with a much compacter compressor. In order for water to be competitive, special vacuum compressors must therefore be developed that exploit the fact that the aerodynamic forces at low pressure are very small. Very light construction and possibly unconventional

materials may hold the cost down. Ophir and Paul (1991) present a large diameter centrifugal compressor with very thin, flexible blades as the basis of their vacuum ice maker which they claim to be economically feasible. This vacuum ice maker design may well be the first ever to accomplish a mechanical vapor compression refrigeration cycle with only water as refrigerant.

In summary, it can thus be concluded that water theoretically can function as refrigerant for operating temperatures above its freezing point. The combined use of water as refrigerant and thermal storage medium or heat carrier results in reduced energy consumption, despite the somewhat unfavorable intrinsic thermodynamic properties of water. This disadvantage is further mitigated by cycle modifications. The realization of this potential depends on the successful development of a totally new generation of vacuum compressors. Using water as refrigerant thus implies a trade-off between excellent safety, health and environmental features, and the ease of technological implementation.

5.2. Recommendations.

The primary objective of further research must indeed be the vacuum compressor. The large volume flow associated with the vacuum operating conditions and the high adiabatic head pose an extreme technological challenge, but the low operating pressure also opens the opportunity for light construction materials. These conditions, so fundamentally different from those at which almost all compressors normally operate, call for a radically new design philosophy. The development during the 80's of high pressure steam compressors for open cycle heat pumps was realized through minor modifications to existing compressors in order to accommodate for water instead of for example air (e.g., buffer fluids between the seals). Such an approach cannot be successful for low pressure water vapor compression: it is not only a matter of a different fluid but above all of totally different operating conditions. Only completely new designs can at the same time meet the extreme requirements and use to good advantage the low pressure difference, resulting in both efficient and economically viable systems. Open-mindedness and critical review of all limitations of classical compressors are a prerequisite for success.

Unconventional materials, such as synthetic composites, may possibly be well suited for vacuum compressors. Interdisciplinary cooperation between the fields of material science and fluid dynamics is therefore recommended. Research institutions and

public utilities such as the Gas Research Institute, Electricité de France and Electricity Council Research Centre (England) have played a leading role in coordinating, sponsoring and executing the development of high pressure steam compressors, as can be witnessed from the papers on three International Symposia on Heat Pumps. Given the many times greater challenge of developing a vacuum steam compressor, an equally active stand by these and similar institutions is therefore highly desirable. Although success is not guaranteed, the need for an environmental benign refrigerant warrants further research funding. The benefit of the development of efficient, large flow vacuum compressors does not need to be restricted to water-based refrigeration systems, but may extend to other industrial vacuum processes and open up new applications that are thus far not technically feasible. If the expectations concerning the compressor development are redeemed, a further area of research and experiments must be the technology of pumpable ice slurries. It offers many new opportunities but also requires further investigation.

Appendix A
Analysis of the lobe compressor.

Fig. A.1 shows a schematic cross section of a lobe compressor (also called rotary blower or Roots compressor). In order to assess the usability of the lobe compressor for vacuum steam compression, some modelling of this machine was done. Table A.1 gives an excerpt of the performance 'data' sheet for two blowers from the manufacturer Curtis (undated). The CRB-80 and CRB-90 are the largest frame sizes. The pressure data are based on inlet air conditions of 14.7 psia (i.e. atmospheric pressure) and 70 °F. The vacuum data have the same inlet temperature and discharge at 29.92 "Hg (i.e. also atmospheric pressure). Based on these data, the isentropic efficiency (i.e. ratio of the adiabatic, isentropic power to the brake horse power) is calculated as tabulated in table 3.2. As can be seen, the efficiency is rather low, especially when the pressure difference (or rather the pressure ratio as will be illustrated hereunder) becomes large. So as to allow extrapolation of these data to the operating conditions of vacuum steam compression, the following modelling attempt is made.
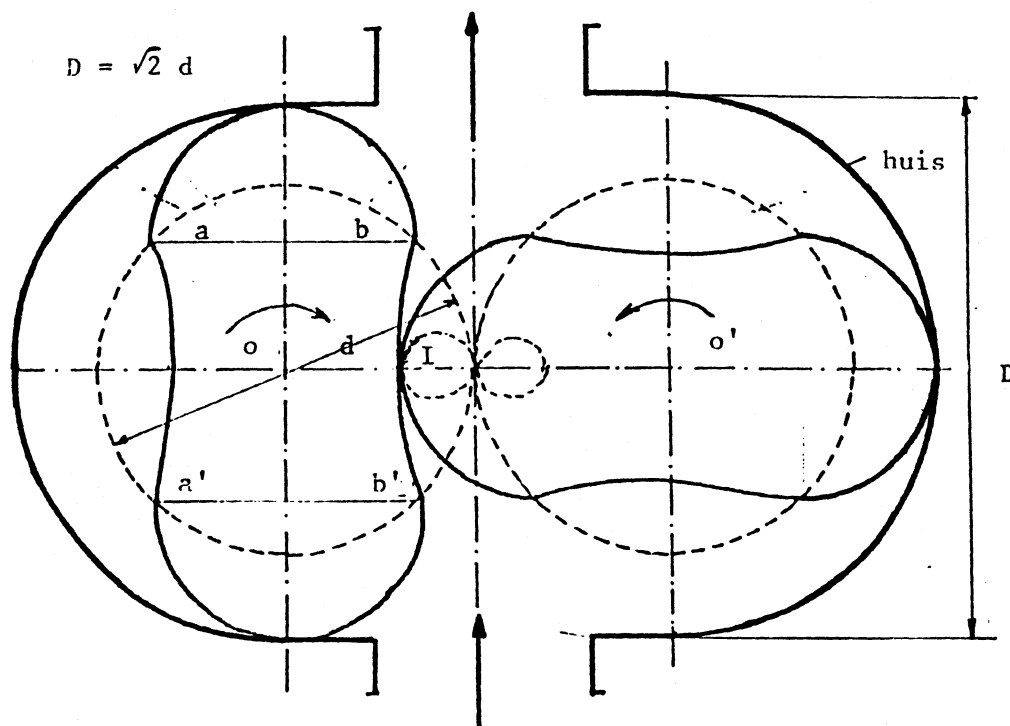
Fig. A.1 Schematic cross section of a lobe compressor (from Berghmans, 1988).

Table: pressure (psi)

model	speed (rpm)	cfm	BHP	cfm	BHP	cfm	BHP	cfm	BHP	cfm	BHP	cfm	BHP	cfm	BHP
pressure (psi)		2	2	4	4	6	6	8	8	10	10	12	12	15	15
CRB-80	500	3723	55.5	3408	94.6	3166	133	2962	172	2783	212	2620	251		
	800	6414	88.9	6099	151	5857	214	5653	276	5474	339	5311	401	5091	495
	1000	8208	111	7893	189	7651	267	7447	345	7268	424	7105	502	6885	619
	1200	10002	133	9687	227	9445	321	9241	⁻415	9062	508	8899	602	8679	743
CRB-90	500	5871	75.1	5516	133	5244	192	5014	251	4812	309	4630	368	4382	456
	800	9907	120	9553	214	9280	307	9051	401	8849	495	8666	589	8419	730
	1000	12598	150	12244	267	11971	384	11742	502	11540	619	11357	736	11110	912
	1200	15289	180	14935	321	14662	461	14433	602	14231	743	14048	884	13801	1095

Table: vacuum ("Hg)

model	speed (rpm)	cfm	BHP	cfm	BHP	cfm	BHP	cfm	BHP	cfm	BHP	cfm	BHP	cfm	BHP
vacuum ("Hg)		2	2	6	6	8	8	10	10	12	12	14	14	15	15
CRB-80	500	3932	35.6	3451	74	3238	93.2	3023	112	2796	131	2550	151		
	800	6623	57	6142	118	5929	149	5714	180	5487	210	5241	241	4964	272
	1000	8417	71.3	7936	148	7723	186	7508	225	7281	263	7035	301	6758	340
	1200	10211	85.5	9730	177	9517	223	9302	270	9075	316	8829	362	8552	408
CRB-90	500	6106	45.2	5565	102	5325	131	5082	160	4828	189	4550	218		
	800	10142	72.4	9601	164	9361	210	9119	256	8864	303	8587	349	8275	395
	1000	12833	90.5	12292	205	12052	263	11810	321	11555	378	11278	436	10966	494
	1200	15524	108	14983	247	14743	316	14501	385	14246	454	13969	523	13657	592

Table A.2 Performance data sheet of Curtis CRB-80 and CRB-90 lobe compressors.

Two major contributions to the non-ideal compression are the leakage flow and the the sudden opening of the trapped volume to the high pressure plenum. Between the rotors themselves and the rotors and the casing, small clearances exist. This causes a flow back of air from the high to the low pressure side. The net processed volume flow is therefore smaller than the gross flow determined by the swept volume per unit time. The ratio of both is the volumetric efficiency, η_{vol}. The sudden pressure rise, together with mechanical friction and other factors causes an additional power consumption. The ratio of the real work input to the isentropic work input (after eliminating the leakage flow) is here called the internal isentropic efficiency, $\eta_{int\ is}$. The overall isentropic efficiency η_{is} is the product of the volumetric and internal isentropic efficiency:

$$\eta_{is} = \eta_{vol} * \eta_{int\ is} \tag{A.1}$$

Both factors are now analyzed in more detail.

model	speed (rpm)	eta is	eta is	eta is	eta is	eta is	eta is	eta is
pressure (psi)		2	4	6	8	10	12	15
CRB-80	500	0.559	0.3	0.198	0.143	0.109	0.087	
	800	0.601	0.336	0.228	0.171	0.135	0.11	
	1000	0.616	0.348	0.239	0.18	0.143	0.118	
	1200	0.626	0.355	0.245	0.185	0.149	0.123	
CRB-90	500	0.651	0.345	0.228	0.167	0.13	0.105	0.08
	800	0.688	0.372	0.252	0.188	0.149	0.123	0.096
	1000	0.7	0.382	0.26	0.195	0.155	0.129	0.101
	1200	0.708	0.388	0.265	0.2	0.16	0.132	0.105
vacuum ("Hg)		2	6	8	10	12	14	16
CRB-80	500	0.462	0.195	0.145	0.113	0.0892	0.0706	
	800	0.486	0.218	0.166	0.133	0.109	0.0909	0.0763
	1000	0.493	0.224	0.174	0.139	0.116	0.0977	0.0831
	1200	0.499	0.23	0.178	0.144	0.12	0.102	0.0876
CRB-90	500	0.565	0.228	0.17	0.133	0.107	0.0872	
	800	0.585	0.245	0.186	0.149	0.122	0.103	0.0876
	1000	0.593	0.251	0.192	0.154	0.128	0.108	0.0928
	1200	0.601	0.254	0.195	0.157	0.131	0.112	0.0964

Table A.2 Overall isentropic efficiency.

a. Volumetric efficiency.

The volumetric efficiency can be determined from the flow data only. Let $\dot{V}_{real}$ be the volume flow at inlet conditions (as given in table 3.1), $\dot{V}_{theor}$ the swept volume per unit time and $\dot{V}_{leak}$ the volumetric leakage flow (reduced to inlet conditions). They are related by

$$\dot{V}_{real} = \dot{V}_{theor} - \dot{V}_{leak} \tag{A.2}$$

The volumetric efficiency is defined as the ratio of the net flow to the swept volume per unit time, thus

$$\eta_{vol} = \frac{\dot{V}_{real}}{\dot{V}_{theor}} = 1 - \frac{\dot{V}_{leak}}{\dot{V}_{theor}} \tag{A.3}$$
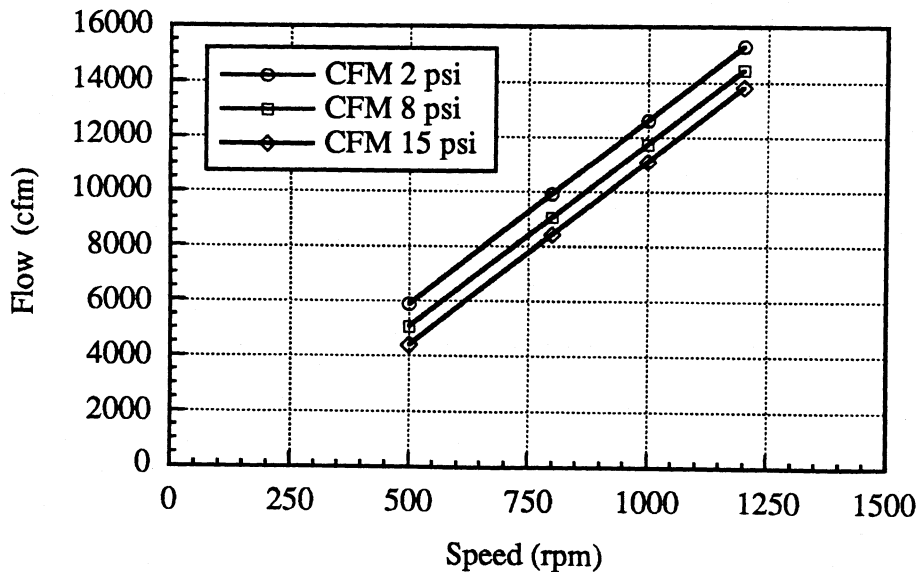
Fig. A.2 Volume flow as a function of rotational speed (pressure data).

Fig. A.2 shows the volume flows as a function of the rotational speed for different pressure rises. It is seen that the flow increases linearly with the speed and that the slope is independent of the pressure increase. The intersection of the (extended) straight lines with the abscissa (flow zero) gives what will here be called the "leakage speed", n_{leak}. This is

the speed at which the displaced volume equals the leakage flow for the given inlet and outlet pressures, so that no net flow occurs. The curves for the discharge pressures other than those graphed and for vacuum operation are also straight lines, parallel to those in the graph. The volume flow thus follows the law

$$\dot{V}_{real} = G * (n - n_{leak})$$

(A.4)

with G a geometrical constant solely determined by the size and shape of the lobes. Its value is found to be 13.455 cf/r (cubic foot per rotation) for the CRB-90. (Note: $\dot{V}_{leak} = G * n_{leak}$, independent of the speed in this model). As is obvious from fig. A.2, the leakage speed depends on the operating pressures.

Fig. A.3 Leakage speed (both pressure and vacuum data).

Further analysis of both the pressure and vacuum data yields that the leakage flow is solely determined by the ratio of the discharge pressure (P_d) to the inlet pressure (P_i) in the following way:

$$n_{leak} = n_{leak, two} \sqrt{\left(\frac{P_d}{P_i}\right) - 1}$$

(A.5)

with $n_{leak, two}$ a constant giving the leakage speed for a pressure ratio of 2. For the CRB-90 its value turns out to be 172.554 rpm. Fig. A.3 illustrates how well the curve fit matches the data.
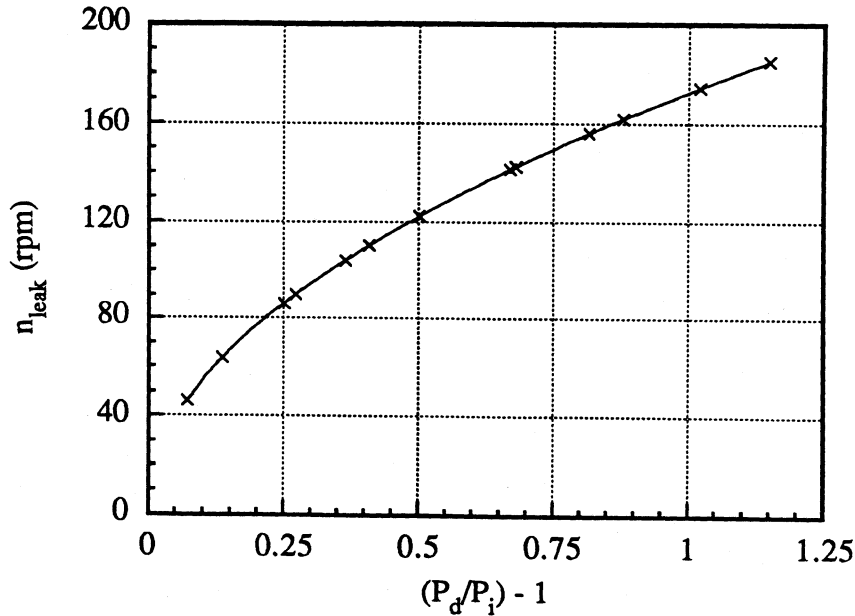
A posteriori, the formula for the leakage speed can be rationalized as follows. Applying the first law of thermodynamics to a small control volume upstream of any clearance, leads to (neglecting the work performed by the rotor):

$$h_2 - h_1 + \frac{v_2^2 - v_1^2}{2} = 0$$

(A.6)

with state 2 exactly at the meshing point and state 1 sufficiently far away in the high pressure zone (h: enthalpy; v: speed). v_1 is then approximately zero. If, in addition, the fluid is supposed to behave as incompressible (which is indeed only valid for small pressure ratios), one obtains (isentropic flow):

$$h_2 - h_1 = \int_{P_d}^{P_i} v \, dP = v_i * (P_i - P_d)$$

(A.7)

with v_i the specific volume at the inlet side, which can be calculated from the ideal gas law. Let A_c be the total clearance area, then:

$$\dot{V}_{leak} = A_c * v_2 = A_c \sqrt{\frac{2*R*T_i}{P_i}*(P_d-P_i)} \propto \sqrt{\left(\frac{P_d}{P_i}\right) - 1}$$

(A.8)

which confirms formula A.5.

Combining equations A.3 and A.4 leads to:

$$\eta_{vol} = 1 - \frac{n_{leak}}{n}$$

(A.9)

with n_{leak} as given by A.5. This simple two parameter model thus totally determines the flow characteristics of a given machine as function of three variables: the inlet pressure P_i, the discharge pressure P_d and the rotational speed n. Two test runs under different conditions allow in principle to obtain the two parameters. Application of the model to other frame sizes has confirmed the results.

b. Internal isentropic efficiency.

The overall isentropic efficiency depends both on the speed and the inlet and outlet pressures, as can be observed in table A.2. From this overall efficiency and from the volumetric efficiency as determined above, the internal isentropic efficiency can be calculated by means of equation A.1. The results for the pressure case are plotted in fig. A.4, showing that the internal isentropic efficiency is independent of the rotational speed. The same holds true for vacuum operation. Attempts to accurately curve fit both cases into one single formula have been unsuccessful.
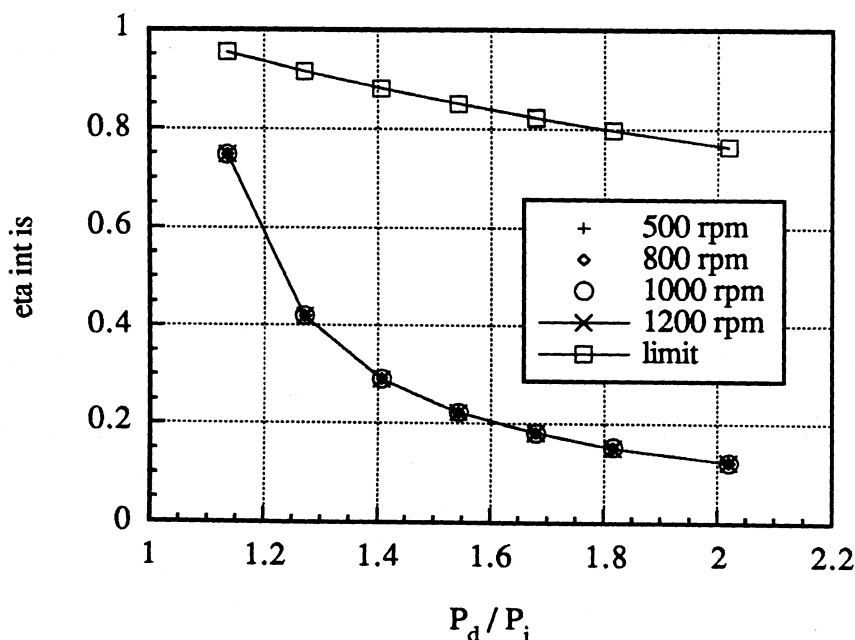
Fig. A.4 Internal isentropic efficiency as a function of the pressure ratio.

It is possible, however, to derive an upper limit for the internal isentropic efficiency. Fig. A.5 depicts the evolution of pressure and volume with time in a normal positive displacement compressor (states 1-2-3n-4) and a lobe compressor (states 1-2-3l-4). In both instances a volume is created that fills with low pressure gas (1-2). In a normal positive displacement compressor this volume is then gradually reduced, causing the pressure to rise according to approximately an isentropic law. Once the discharge pressure is reached, contact with the high pressure plenum is established and the remaining volume is annihilated while expelling the gas at constant pressure. The area enclosed by the curves

between 1-2-3n-4 is a measure for the required work input. In lobe compressors the volume with low pressure gas is not being squeezed before contact is made with the discharge side: the gas simply travels at constant volume along the periphery of the casing and then suddenly opens up to the high pressure plenum. At this point in time the high pressure gas flows back into the volume, causing a momentary rise in pressure from point 2 to 31. It is only when the second rotor enters the volume swept by the first one (90° later) that the expulsion of the gas starts. The area circumscribed by the state points of a lobe compressor (1-2-31-4) is clearly much larger than in the case of a normal positive compressor (for an identical swept volume 1-2).

Fig. A.5 (P,v)-diagram for lobe compressor and common positive displacement compressor.

The work input per unit mass for the isentropic compression is (ideal gas):

$$w_{is} = r * T_i * \left(\frac{k}{k-1}\right) * \left[\left(\frac{P_d}{P_i}\right)^{\frac{k-1}{k}} - 1\right]$$

(A.10)

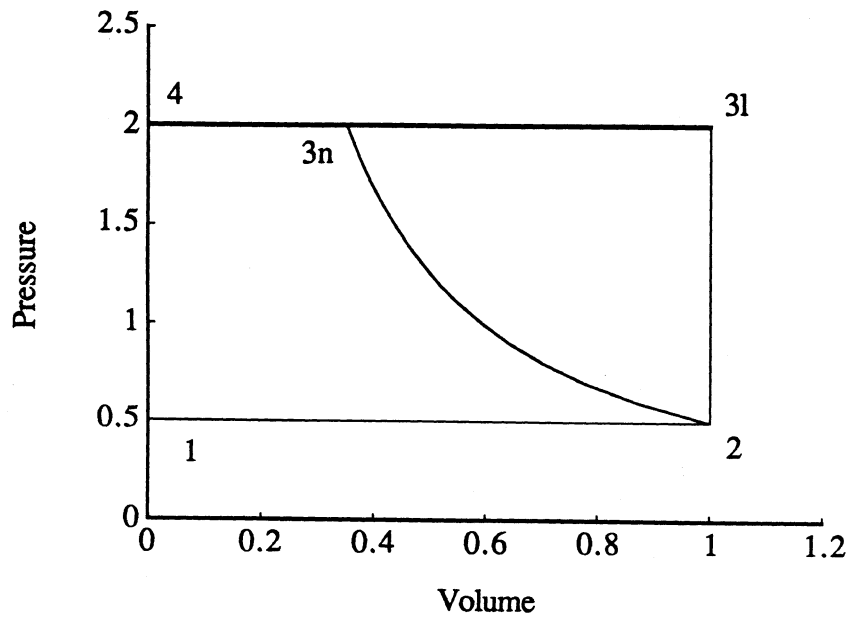with r the specific gas constant, T_i the inlet temperature and k the ratio of the specific heat at constant pressure to the specific heat at constant volume. For the lobe compressor the work input becomes:

$$w_l = v_i*(P_d-P_i) = r * T_i * \left(\frac{P_d}{P_i} - 1\right)$$

(A.11)

with v_i the specific volume at inlet conditions. The ratio of the isentropic work to the work of the lobe compressor (which is also the ratio of the two areas in fig. A.5) gives a limit for the internal isentropic efficiency of the lobe compressor:

$$\eta_{int\ is,\ lim} = \frac{w_{is}}{w_l} = \frac{\left(\frac{k}{k-1}\right) * \left[\left(\frac{P_d}{P_i}\right)^{\frac{k-1}{k}} - 1\right]}{\left(\frac{P_d}{P_i}\right) - 1}$$

(A.12)

This limiting efficiency is also plotted in fig. A.5. The real efficiencies are clearly much lower.

The fact that the isentropic efficiency of the lobe compressor is so low, inherently due to its operating principle, is not generally acknowledged in most textbooks. Indeed, the simple two parameter curve fit used here for modelling the the volume flow retrieves the equations that have been used to generate the manufacturer's data, rather than that it captures the complex behavior of a real machine, which certainly depends on much more parameters. A much more sophisticated model has been presented by Patterson and Ritchie (1969).

With respect to vacuum steam compression, it is important to note that the internal isentropic efficiency is determined by the pressure ratio and not the pressure difference. Although the pressure difference is very small for vacuum compression of water, the pressure ratio may easily attain a value of 10 (condensation temperature of about 36 °C for vacuum ice making), which certainly precludes the common lobe compressor from being applied in refrigeration systems with water as refrigerant -even when only the limiting isentropic efficiency is considered (which has a value of 34.6 % for water at a pressure ratio of 10).

Appendix B
Sample programs.

B.1. Engineering Equation Solver-worksheet for an ideal refrigeration cycle for the refrigerant R502 (cf. section 2.1)

```
{Ideal refrigeration cycle}
Tev=273.16
Pev=Pressure(R502,T=Tev,x=1)
{inlet conditions compressor}
Tci=Tev
hci=Enthalpy(R502,T=Tci,x=1)
sci=Entropy(R502,T=Tci,x=1)

TscdK=273.15+TscdC
Pcd=Pressure(R502,T=TscdK,x=1)
{outlet conditions compressor}
sco=sci
hco=Enthalpy(R502,P=Pcd,s=sco)
TKco=Temperature(R502,P=Pcd,s=sco)
TCco=TKco-273.15
{work compressor}
wc=hco-hci

{in- and outlet conditions expansion valve}
hei=Enthalpy(R502,T=TscdK,x=0)
heo=hei

{heat transfer evaporator and condenser}
qev=hci-heo
qcd=hco-hei

{coefficient of performance}
COP=qev/wc

{specific volume flow}
vci=Volume(R502,T=Tci,x=1)
specfl=vci*1000/qev

deltaP=Pcd-Pev
Pratio=Pcd/Pev

{power/powerCarnot}
COPCarnot=Tev/(TscdK-Tev)
eff2nd=COP/COPCarnot
pow\powCar=1/eff2nd
```

B.2. Engineering Equation Solver-worksheet for a water-based refrigeration cycle with 7 stage compression and expansion, and refrigerant intercooling (cf. section 4.3).

For an explanation of the functions HaWaY for water properties, see B.3.
The condensation temperature and the interstage pressures are set in the table.

```
{in-and outlet conditions}
TCci=-0.5
TKci=273.15+TCci
Pci=HaWaY(15,TKci,1,2)
vci=HaWaY(15,TKci,1,6)
hci=HaWaY(15,TKci,1,3)
sci=HaWaY(15,TKci,1,4)

TKscd=273.15+TCscd
Pco=HaWaY(15,TKscd,1,2)

{7 stage compression}
ns=7
etas=0.7

Pc1o=P12
Pc2o=P23
Pc3o=P34
Pc4o=P45
Pc5o=P56
Pc6o=P67
Pc7o=Pco

{interstage saturation pressures and enthalpies}
P12=HaWaY(15,TKs12,1,2)
hl12=HaWaY(15,TKs12,0,3)
vv12=HaWaY(15,TKs12,1,6)
hv12=HaWaY(15,TKs12,1,3)
sv12=HaWaY(15,TKs12,1,4)
P23=HaWaY(15,TKs23,1,2)
hl23=HaWaY(15,TKs23,0,3)
vv23=HaWaY(15,TKs23,1,6)
hv23=HaWaY(15,TKs23,1,3)
sv23=HaWaY(15,TKs23,1,4)
P34=HaWaY(15,TKs34,1,2)
hl34=HaWaY(15,TKs34,0,3)
vv34=HaWaY(15,TKs34,1,6)
hv34=HaWaY(15,TKs34,1,3)
sv34=HaWaY(15,TKs34,1,4)
P45=HaWaY(15,TKs45,1,2)
hl45=HaWaY(15,TKs45,0,3)
vv45=HaWaY(15,TKs45,1,6)
```

```
hv45=HaWaY(15,TKs45,1,3)
sv45=HaWaY(15,TKs45,1,4)
P56=HaWaY(15,TKs56,1,2)
hl56=HaWaY(15,TKs56,0,3)
vv56=HaWaY(15,TKs56,1,6)
hv56=HaWaY(15,TKs56,1,3)
sv56=HaWaY(15,TKs56,1,4)
P67=HaWaY(15,TKs67,1,2)
hl67=HaWaY(15,TKs67,0,3)
vv67=HaWaY(15,TKs67,1,6)
hv67=HaWaY(15,TKs67,1,3)
sv67=HaWaY(15,TKs67,1,4)

{expansion valve in- and outlet conditions}
he7i=HaWaY(15,TKscd,0,3)
he7o=he7i
he6i=hl67
he6o=he6i
he5i=hl56
he5o=he5i
he4i=hl45
he4o=he4i
he3i=hl34
he3o=he3i
he2i=hl23
he2o=he2i
he1i=hl12
he1o=he1i

{1st stage}
vc1i=vci
hc1i=hci
sc1i=sci
qev=hc1i-he1o
mflis1=1000/qev          {g/kJevap}
mflnis1=1000/qev         {g/kJevap}
vfliscli=mflis1*vc1i     {dm3/kJevap}
vflniscli=mflnis1*vc1i   {dm3/kJevap}
{isen}
sisclo=sc1i
hisclo=HaWaY(248,P12,sisclo,TKs12,3)
TKisclo=HaWaY(248,P12,sisclo,TKs12,1)
TCisclo=TKisclo-273.15
wisc1=hisclo-hc1i
{non-isen}
wnisc1=wisc1/etas
hnisclo=hc1i+wnisc1
snicslo=HaWaY(238,P12,hnisclo,TKs12,4)
TKnisclo=HaWaY(238,P12,hnisclo,TKs12,1)
TCnisclo=TKnisclo-273.15

{2nd stage}
```

vc2i=vv12
hc2i=hv12
sc2i=sv12
{isen}
mflis2=mflis1*(hisc1o-he1i)/(hc2i-he2o)
vflisc2i=vc2i*mflis2
mflis12=mflis2-mflis1
sisc2o=sc2i
hisc2o=HaWaY(248,P23,sisc2o,TKs23,3)
TKisc2o=HaWaY(248,P23,sisc2o,TKs23,1)
TCisc2o=TKisc2o-273.15
wisc2=hisc2o-hc2i
{non-isen}
mflnis2=mflnis1*(hnisc1o-he1i)/(hc2i-he2o)
vflnisc2i=vc2i*mflnis2
mflnis12=mflnis2-mflnis1
wnisc2=wisc2/etas
hnisc2o=hc2i+wnisc2
TKnisc2o=HaWaY(238,P23,hnisc2o,TKs23,1)
TCnisc2o=TKnisc2o-273.15

{3rd stage}
vc3i=vv23
hc3i=hv23
sc3i=sv23
{isen}
mflis3=mflis2*(hisc2o-he2i)/(hc3i-he3o)
vflisc3i=vc3i*mflis3
mflis23=mflis3-mflis2
sisc3o=sc3i
hisc3o=HaWaY(248,P34,sisc3o,TKs34,3)
TKisc3o=HaWaY(248,P34,sisc3o,TKs34,1)
TCisc3o=TKisc3o-273.15
wisc3=hisc3o-hc3i
{non-isen}
mflnis3=mflnis2*(hnisc2o-he2i)/(hc3i-he3o)
vflnisc3i=vc3i*mflnis3
mflnis23=mflnis3-mflnis2
wnisc3=wisc3/etas
hnisc3o=hc3i+wnisc3
TKnisc3o=HaWaY(238,P34,hnisc3o,TKs34,1)
TCnisc3o=TKnisc3o-273.15

{4th stage}
vc4i=vv34
hc4i=hv34
sc4i=sv34
{isen}
mflis4=mflis3*(hisc3o-he3i)/(hc4i-he4o)
vflisc4i=vc4i*mflis4
mflis34=mflis4-mflis3
sisc4o=sc4i

hisc4o=HaWaY(248,P45,sisc4o,TKs45,3)
TKisc4o=HaWaY(248,P45,sisc4o,TKs45,1)
TCisc4o=TKisc4o-273.15
wisc4=hisc4o-hc4i
{non-isen}
mflnis4=mflnis3*(hnisc3o-he3i)/(hc4i-he4o)
vflnisc4i=vc4i*mflnis4
mflnis34=mflnis4-mflnis3
wnisc4=wisc4/etas
hnisc4o=hc4i+wnisc4
TKnisc4o=HaWaY(238,P45,hnisc4o,TKs45,1)
TCnisc4o=TKnisc4o-273.15

{5th stage}
vc5i=vv45
hc5i=hv45
sc5i=sv45
{isen}
mflis5=mflis4*(hisc4o-he4i)/(hc5i-he5o)
vflisc5i=vc5i*mflis5
mflis45=mflis5-mflis4
sisc5o=sc5i
hisc5o=HaWaY(248,P56,sisc5o,TKs56,3)
TKisc5o=HaWaY(248,P56,sisc5o,TKs56,1)
TCisc5o=TKisc5o-273.15
wisc5=hisc5o-hc5i
{non-isen}
mflnis5=mflnis4*(hnisc4o-he4i)/(hc5i-he5o)
vflnisc5i=vc5i*mflnis5
mflnis45=mflnis5-mflnis4
wnisc5=wisc5/etas
hnisc5o=hc5i+wnisc5
TKnisc5o=HaWaY(238,P56,hnisc5o,TKs56,1)
TCnisc5o=TKnisc5o-273.15

{6th stage}
vc6i=vv56
hc6i=hv56
sc6i=sv56
{isen}
mflis6=mflis5*(hisc5o-he5i)/(hc6i-he6o)
vflisc6i=vc6i*mflis6
mflis56=mflis6-mflis5
sisc6o=sc6i
hisc6o=HaWaY(248,P67,sisc6o,TKs67,3)
TKisc6o=HaWaY(248,P67,sisc6o,TKs67,1)
TCisc6o=TKisc6o-273.15
wisc6=hisc6o-hc6i
{non-isen}
mflnis6=mflnis5*(hnisc5o-he5i)/(hc6i-he6o)
vflnisc6i=vc6i*mflnis6
mflnis56=mflnis6-mflnis5

wnisc6=wisc6/etas
hnisc6o=hc6i+wnisc6
TKnisc6o=HaWaY(238,P67,hnisc6o,TKs67,1)
TCnisc6o=TKnisc6o-273.15

{7th stage}
vc7i=vv67
hc7i=hv67
sc7i=sv67
{isen}
mflis7=mflis6*(hisc6o-he6i)/(hc7i-he7o)
vflisc7i=vc7i*mflis7
mflis67=mflis7-mflis6
sisc7o=sc7i
hisc7o=HaWaY(248,Pco,sisc7o,TKscd,3)
TKisc7o=HaWaY(248,Pco,sisc7o,TKscd,1)
TCisc7o=TKisc7o-273.15
wisc7=hisc7o-hc7i
{non-isen}
mflnis7=mflnis6*(hnisc6o-he6i)/(hc7i-he7o)
vflnisc7i=vc7i*mflnis7
mflnis67=mflnis7-mflnis6
wnisc7=wisc7/etas
hnisc7o=hc7i+wnisc7
TKnisc7o=HaWaY(238,Pco,hnisc7o,TKscd,1)
TCnisc7o=TKnisc7o-273.15

{total work}
term1=mflis1*wisc1+mflis2*wisc2+mflis3*wisc3+mflis4*wisc4
term2=mflis5*wisc5+mflis6*wisc6+mflis7*wisc7
wistot=(term1+term2)*1e-3
COPis=1/wistot
term3=mflnis1*wnisc1+mflnis2*wnisc2+mflnis3*wnisc3+mflnis4*wnisc4
term4=mflnis5*wnisc5+mflnis6*wnisc6+mflnis7*wnisc7
wnistot=(term3+term4)*1e-3

COPnis=1/wnistot

B.3. External function (Think Pascal code) for the Engineering Equation Solver for the calculation of the thermodynamic properties of water (cf. section 1.2).

The code contains no checking for the number of arguments passed. Nor does it check whether the value of the parameters is within the boundaries of validity of the equations. It returns no error messages. Great care must be taken in its use. Infinite loops may occur if inappropriate values are entered. Many numerical improvements are possible.

Three different function can be called up:

1. Two phase domain.

    function call: HaWaY(15,TK,x,output#)

    The number 15 identifies the function, TK is the temperature in Kelvin (between 173.15 K and 473.15 K), x the vapor fraction (between 0 and 1) and the output number determines the thermodynamic property whose value is desired (see below).

2. Superheated domain.

    function call: HaWaY(238,PkPa,h,TKsat,output#)

    This function determines all state variables for a given pressure (in kPa), specific enthalpy (in kJ/kg) and the saturation temperature (in Kelvin) corresponding to the given pressure. Validity: see paper by Young.

3. Superheated domain.

    function call: HaWaY(248,PkPa,s,TKsat,output#)

    This function determines all state variables for a given pressure (in kPa), specific entropy (in kJ/(K*kg)) and the saturation temperature (in Kelvin) corresponding to

the given pressure. Validity: see paper by Young.

Output numbers:

1: TK : temperature in Kelvin

2: PkPa : pressure in kPa

3: h : specific enthalpy in kJ/kg

4: s : specific entropy in kJ/(K*kg)

6: v : specific volume in m^3/kg

7 : u : internal energy in kJ/kg

```pascal
unit EESX1417;

interface

type
 ParamRecPtr = ^ParamRec;
 ParamRec = record
   Value: extended;
   next: ParamRecPtr;
  end;

function Main (var PString: str255; Mode: integer; ParamPtr: ParamRecPtr): extended;

implementation

function Main (var PString: str255; Mode: integer; ParamPtr: ParamRecPtr): extended;
 var
 P: ParamRecPtr;
 TK, x, PkPa, h, s, v, u, TKsat, res: extended;
 outp: integer;

 function ipow (a: extended; i: integer): extended;
{integer power: returns a to the power i (a^i)}
  var
  t: integer;
  resul: real;
 begin
 if i = 0 then
  resul := 1;
 if i > 0 then
  begin
  resul := 1;
  for t := 1 to i do
   resul := resul * a;
```

```
    end;
  if i < 0 then
    resul := 1 / ipow(a, -i);
  IPOW := resul;
  end;


function pow (a, b: extended): extended;
{power: returns a to the power b (a^b)}
  begin
  if a > 0 then
    POW := exp(b * ln(a))
  else { 1/b must be an odd integer}
    POW := -exp(b * ln(-a));
  end;


function Psatice (TK: extended): extended;
{eqn. 18 HaW Ashrae 1983}
{TK must be in K, P is returned in kPa}
  var
    m: array[0..6] of extended;
    term1, term2, pTK: extended;
    i: integer;
  begin
  m[0] := -0.56745359E4;
  m[1] := 0.63925247E1;
  m[2] := -0.96778430E-2;
  m[3] := 0.62215701E-6;
  m[4] := 0.20747825E-8;
  m[5] := -0.94840240E-12;
  m[6] := 0.41635019E1;
  term1 := m[0] / TK;
  pTK := 1;
  for i := 1 to 5 do
    begin
    term1 := term1 + m[i] * pTK;
    pTK := pTK * TK;
    end;
  term2 := m[6] * ln(TK);
  Psatice := 1E-3 * exp(term1 + term2);
  end;


function vsatice (TK: extended): extended;
{eqn. 2 HaW Ashrae 1983}
{TK must be in K, v is returned in m3/kg}
  var
    A: array[0..2] of extended;
  begin
  A[0] := 0.1070003E-2;
  A[1] := -0.249936E-7;
  A[2] := 0.371611E-9;
  vsatice := A[0] + A[1] * TK + A[2] * TK * TK;
  end;
```

```pascal
function hsatice (TK, PkPa: extended): extended;
{eqn. 3 HaW Ashrae 1983}
{TK must be in K and PkPa in kPa, h is returned in kJ/kg}
  var
  D: array[0..4] of extended;
  res, pTK: extended;
  i: integer;
  begin
  D[0] := -0.647595E3;
  D[1] := 0.274292;
  D[2] := 0.2910583E-2;
  D[3] := 0.1083437E-5;
  D[4] := 0.107E-5;
  res := D[0];
  pTK := TK;
  for i := 1 to 3 do
    begin
    res := res + D[i] * pTK;
    pTK := pTK * TK;
    end;
  res := res + D[4] * PkPa; {dimensions of P remain to be checked !}
  hsatice := res;
  end;


function ssatice (TK, PkPa: extended): extended;
{eqn. 4 HaW Ashrae 1983}
{TK must be in K and PkPa in kPa, s is returned in kJ/(K*kg)}
  var
  E: array[0..5] of extended;
  term1, term2: extended;
  begin
  E[0] := -0.4470727E1;
  E[1] := 0.582109E-2;
  E[2] := 0.1625155E-5;
  E[3] := 0.274292E0;
  E[4] := -0.249936E-7;
  E[5] := 0.743288E-9;
  term1 := E[0] + E[1] * TK + E[2] * TK * TK + E[3] * ln(TK);
  term2 := (E[4] + E[5] * TK) * (101.325 - PkPa);
  ssatice := term1 + term2;
  end;


function Psatliq (TK: extended): extended;
{eqn. 17 HaW Ashrae 1983}
{TK must be in K, P is returned in kPa}
  var
  g: array[-1..4] of extended;
  term1, term2, pTK: extended;
  i: integer;
  begin
  g[-1] := -0.58002206E4;
```

```
g[0] := 0.13914993E1;
g[1] := -0.48640239E-1;
g[2] := 0.41764768E-4;
g[3] := -0.14452093E-7;
g[4] := 0.65459673E1;
term1 := g[-1] / TK;
pTK := 1;
for i := 0 to 3 do
  begin
   term1 := term1 + g[i] * pTK;
   pTK := pTK * TK;
  end;
  term2 := g[4] * ln(TK);
  Psatliq := 1E-3 * exp(term1 + term2);
 end;


 function dPsatliqdT (TK, PkPa: extended): extended;
{derivative of eqn. 17 HaW Ashrae 1983}
{TK must be in K and PkPa in kPa, dPsatliq/dT is returned in kPa/K}
 var
  dg: array[-1..4] of extended;
  fact1, TK2: extended;
 begin
  dg[-1] := -0.58002206E4;
  dg[1] := -0.48640239E-1;
  dg[2] := 0.83529536E-4;
  dg[3] := -0.43356279E-7;
  dg[4] := 0.65459673E1;
  TK2 := TK * TK;
  fact1 := -dg[-1] / TK2 + dg[4] / TK + dg[1] + dg[2] * TK + dg[3] * TK2;
  dPsatliqdT := fact1 * PkPa;
 end;


 function vsatliq (TK: extended): extended;
{eqn. 5 HaW Ashrae 1983}
{TK must be in K, v is returned in m3/kg}
 var
  F: array[0..7] of extended;
  denom, num, pTK: extended;
  i: integer;
 begin
  F[0] := -0.2403360201E4;
  F[1] := -0.140758895E1;
  F[2] := 0.1068287657;
  F[3] := -0.2914492351E-3;
  F[4] := 0.373497936E-6;
  F[5] := -0.21203787E-9;
  F[6] := -0.3424442728E1;
  F[7] := 0.1619785E-1;
 denom := F[0];
 pTK := TK;
 for i := 1 to 5 do
```

```
  begin
    denom := denom + F[i] * pTK;
    pTK := pTK * TK;
  end;
  num := F[6] + F[7] * TK;
  vsatliq := num / denom;
end;

function hsatliq (TK, vsatliq, dPsatkPadT: extended): extended;
{eqn. 11 HaW Ashrae 1983}
{TK must be in K, vsatliq in m3/kg and dPsatkPadT in kPa/K, h is returned in kJ/kg}
  var
    L: array[0..6] of extended;
    M: array[0..5] of extended;
    term1, term2, term3, alpha, pTK: extended;
    i: integer;
  begin
    if TK <= 373.125 then {273.15<=TK<=373.125}
    begin
      L[0] := -0.11411380E4;
      L[1] := 0.41930463E1;
      L[2] := -0.8134865E-4;
      L[3] := 0.1451133E-6;
      L[4] := -0.1005230E-9;
      L[5] := -0.563473;
      L[6] := -0.082893063; {=-0.036*2.302585093(=-0.036*ln10)}
      term1 := L[0];
      pTK := TK;
      for i := 1 to 4 do
        begin
          term1 := term1 + L[i] * pTK;
          pTK := pTK * TK;
        end;
      term2 := L[5] * exp(L[6] * (TK - 273.15));
      alpha := term1 + term2;
    end
    else
    begin
      M[0] := -0.1141837121E4;
      M[1] := 0.4194325677E1;
      M[2] := -0.6908894163E-4;
      M[3] := 0.105555302E-6;
      M[4] := -0.7111382234E-10;
      M[5] := 0.6059E-6;
      term1 := M[0];
      pTK := TK;
      for i := 1 to 4 do
        begin
          term1 := term1 + M[i] * pTK;
          pTK := pTK * TK;
        end;
      if TK <= 403.128 then {373.125<=TK<=403.128}
```

```
    alpha := term1
    else {403.128<=TK<=473.15}
    begin
     term2 := -M[5] * exp(3.1 * ln(TK - 403.128));
     alpha := term1 + term2;
    end;
  end;
 hsatliq := alpha - 0.01214 + TK * vsatliq * dPsatkPadT;
 end;


function ssatliq (TK, vsatliq, dPsatkPadT: extended): extended;
{eqn. 5 HaW Ashrae 1983}
{TK must be in K, vsatliq in m3/kg and dPsatliqdT in kPa/K, s is returned in kJ/(K*kg)}
{273.15<=TK<=373.125}
 var
 Q: array[0..6] of extended;
 w: array[0..5] of extended;
 term1, term2, term3, pTK: extended;
 i: integer;
begin
 if TK <= 373.125 then
  begin
  Q[0] := -0.234707325E2;
  Q[1] := -0.1177858E-3;
  Q[2] := 0.1501808E-6;
  Q[3] := -0.8946646E-10;
  Q[4] := 0.4188095E1;
  Q[5] := -0.1976361E-2;
  Q[6] := -0.865209E-1;
  term1 := Q[0];
  pTK := TK;
  for i := 1 to 3 do
   begin
    term1 := term1 + Q[i] * pTK;
    pTK := pTK * TK;
   end;
   term2 := Q[4] * ln(TK) + Q[5] * exp(Q[6] * (TK - 273.15));
   term3 := vsatliq * dPsatkPadT * 1E-3;
   ssatliq := term1 + term2 + term3;
  end
 else {373.125<=TK<=473.15}
  begin
  w[0] := -0.23500869E2;
  w[1] := -0.13817789E-3;
  w[2] := 0.1583330E-6;
  w[3] := -0.9481843E-10;
  w[4] := 0.41943257E1;
  w[5] := -0.202367E-8;
  term1 := w[0];
  pTK := TK;
  for i := 1 to 3 do
   begin
```

```
      term1 := term1 + w[i] * pTK;
      pTK := pTK * TK;
    end;
    if TK <= 403.125 then {373.125<=TK<=403.128}
      term2 := w[4] * ln(TK)
    else {403.128<=TK<=473.15}
      term2 := w[4] * ln(TK) + w[5] * exp(3 * ln(TK - 403.128));
    term3 := vsatliq * dPsatkPadT;
    ssatliq := term1 + term2 + term3;
    end;
  end;


function Bvir (TK: extended): extended;
{eqn. 24 Young ASME '88}
{TK must be in K, Bvir is returned in m^3/kg}
  var
    a: array[1..3] of extended;
    alpha, denom, tau, etau, term: extended;
  begin
    a[1] := 0.0015;
    a[2] := -0.000942;
    a[3] := -0.0004882;
    alpha := 10000;
    denom := 1 + TK / alpha;
    tau := 1500 / TK;
    etau := exp(tau);
    term := a[2] * etau * pow(1 - 1 / etau, 2.5) * pow(tau, -0.5);
    Bvir := a[1] / denom + term + a[3] * tau;
  end;

function dBvirdT (TK: extended): extended;
{derivative of eqn. 24 Young ASME '88}
{TK must be in K, dBdTvir is returned in m^3/(kg*K)}
  var
    a: array[1..3] of extended;
    alpha, denom, tau, etau, term1, term2: extended;
  begin
    a[1] := 0.0015;
    a[2] := -0.000942;
    a[3] := -0.0004882;
    alpha := 10000;
    denom := 1 + TK / alpha;
    tau := 1500 / TK;
    etau := exp(tau);
    term1 := etau * pow(1 - 1 / etau, 2.5) * pow(tau, -0.5) * (1 - 0.5 / tau);
    term2 := 2.5 * pow(tau, -0.5) * pow(1 - 1 / etau, 1.5);
    dBvirdT := -a[1] / (alpha * ipow(denom, 2)) - tau / TK * (a[2] * (term1 + term2) + a[3]);
  end;

function Cvir (TK: extended): extended;
{eqn. 25 Young ASME '88}
{TK must be in K, Cvir is returned in m^6/kg^2}
```

```
var
  a, b, c, alpha, tau0, tau, etau: extended;
begin
  a := 1.772;
  b := 1.5E-6;
  c := 647.286;
  alpha := 11.16;
  tau0 := 0.8978;
  tau := TK / c;
  etau := exp(-alpha * tau);
  Cvir := a * (tau - tau0) * etau + b;
end;


function dCvirdT (TK: extended): extended;
{derivative of eqn. 25 Young ASME '88}
{TK must be in K, dCdTvir is returned in m^6/(kg^2*K)}
  var
  a, c, alpha, tau0, tau, etau: extended;
begin
  a := 1.772;
  c := 647.286;
  alpha := 11.16;
  tau0 := 0.8978;
  tau := TK / c;
  etau := exp(-alpha * tau);
  dCvirdT := a * etau * (1 - alpha * (tau - tau0)) / c;
end;


function vvap (TK, PkPa, B, C: extended): extended;
{Young ASME '88}
{TK must be in K, PkPa in kPa, B in m^3/kg, C in m^6/kg^2}
{v is returned in  m^3/kg}
  var
  R, pi, i, d, e, m, a, disc, srtdisc, res, res1, res2, res3, supp, theta, delta, eps: extended;
begin
  R := 0.46151;
  pi := 3.141592654;
  i := R * TK / PkPa;
  d := -i * (3 * B + i) / 9;
  e := -i * (2 * ipow(i, 2) + 9 * B * i + 27 * C) / 54;
  disc := ipow(e, 2) + ipow(d, 3);
  if disc > 0 then
   begin
    srtdisc := pow(disc, 0.5);
    delta := pow(-e + srtdisc, 1 / 3);
    eps := pow(-e - srtdisc, 1 / 3);
    res := i / 3 + delta + eps;
   end
  else if disc = 0 then
   begin
    a := pow(e, 1 / 3);
    if a > 0 then
```

```
    res := i / 3 + a
    else
     res := i / 3 - 2 * a;
    end
   else
    begin
     m := 2 * pow(-d, 0.5);
     supp := -ipow(d, 3) / ipow(e, 2) - 1;
     theta := arctan(pow(supp, 0.5)) / 3;
     if theta < pi / 3 then
      res := i / 3 + m * cos(theta)
     else
      res := i / 3 + m * cos(theta + 4 * pi / 3);
    end;
   vvap := res;
  end;


 function hvap (TK, v, B, C, dBdT, dCdT: extended): extended;
 {Young ASME '88}
 {TK must be in K,v in m^3/kg, B in m^3/kg, C in m^6/kg^2, dBdT in m^3/(kg*K),
 dCdT in m^6/(kg^2*K)}
 {hvap is returned in kJ / kg}
  var
   cp: array[1..6] of extended;
   hig, hc, R: extended;
   i: integer;
  begin
   R := 0.46151;
   cp[1] := 46.0;
   cp[2] := 1.47276;
   cp[3] := 8.3893E-4;
   cp[4] := -2.19989E-7;
   cp[5] := 2.46619E-10;
   cp[6] := -9.70466E-14;
   hc := 1811.06;
   hig := 0;
   for i := 6 downto 2 do
    hig := (hig + cp[i] / (i - 1)) * TK;
   hig := hig + cp[1] * ln(TK) + hc;
   hvap := hig + R * TK * ((B - TK * dBdT) / v + (C - TK * dCdT / 2) / pow(v, 2));
  end;


 function svap (TK, v, B, C, dBdT, dCdT: extended): extended;
 {Young ASME '88}
 {TK must be in K, v in m^3/kg, B in m^3/kg, C in m^6/kg^2, dBdT in m^3/(kg*K),
 dCdT in m^6/(kg^2*K)}
 {svap is returned in kJ / ( K * kg ) }
  var
   cp: array[1..6] of extended;
   sig, sc, R: extended;
   i: integer;
```

```pascal
begin
  R := 0.46151;
  cp[1] := 46.0;
  cp[2] := 1.47276;
  cp[3] := 8.3893E-4;
  cp[4] := -2.19989E-7;
  cp[5] := 2.46619E-10;
  cp[6] := -9.70466E-14;
  sc := 0.97042;
  sig := 0;
  for i := 6 downto 3 do
    sig := (sig + cp[i] / (i - 2)) * TK;
  sig := sig + (cp[2] - R) * ln(TK) - cp[1] / TK + sc;
  svap := sig + R * (ln(v) - (B + TK * dBdT) / v - (C + TK * dCdT) / (2 * pow(v, 2)));
end;


function enth (TK, PkPa: extended): extended;
var
  B, C, dBdT, dCdT, v: extended;
begin
  B := Bvir(TK);
  C := Cvir(TK);
  dBdT := dBvirdT(TK);
  dCdT := dCvirdT(TK);
  v := vvap(TK, PkPa, B, C);
  enth := hvap(TK, v, B, C, dBdT, dCdT);
end;


function entr (TK, PkPa: extended): extended;
var
  B, C, dBdT, dCdT, v: extended;
begin
  B := Bvir(TK);
  C := Cvir(TK);
  dBdT := dBvirdT(TK);
  dCdT := dCvirdT(TK);
  v := vvap(TK, PkPa, B, C);
  entr := svap(TK, v, B, C, dBdT, dCdT);
end;


procedure comb15 (TK, x: extended; var PkPa, h, s, v, u: extended);
var
  B, C, dBdT, dCdT, vv, hv, uv, sv, vc, hc, uc, sc, y, dPsatkPadT: extended;
begin
  if TK < 273.16 then {condensed phase is ice}
  begin
    PkPa := Psatice(TK);
    if x > 0 then {there is vapor present}
    begin
      B := Bvir(TK);
      C := Cvir(TK);
      dBdT := dBvirdT(TK);
```

```
  dCdT := dCvirdT(TK);
  vv := vvap(TK, PkPa, B, C);
  hv := hvap(TK, vv, B, C, dBdT, dCdT);
  uv := hv - PkPa * vv;
  sv := svap(TK, vv, B, C, dBdT, dCdT);
 end;
if x < 1 then{there is ice present}
 begin
  vc := vsatice(TK);
  hc := hsatice(TK, PkPa);
  uc := hc - PkPa * vc;
  sc := ssatice(TK, PkPa);
 end;
if x = 0 then{pure ice}
 begin
  v := vc;
  u := uc;
  h := hc;
  s := sc;
 end
 else if x = 1 then{pure vapor}
 begin
  v := vv;
  u := uv;
  h := hv;
  s := sv;
 end
 else{both ice and vapor present}
 begin
  y := 1 - x;
  v := x * vv + y * vc;
  u := x * uv + y * uc;
  h := x * hv + y * hc;
  s := x * sv + y * sc;
 end;
end
else{condensed phase is liquid}
begin
 PkPa := Psatliq(TK);
 if x > 0 then{there is vapor present}
 begin
  B := Bvir(TK);
  C := Cvir(TK);
  dBdT := dBvirdT(TK);
  dCdT := dCvirdT(TK);
  vv := vvap(TK, PkPa, B, C);
  hv := hvap(TK, vv, B, C, dBdT, dCdT);
  uv := hv - PkPa * vv;
  sv := svap(TK, vv, B, C, dBdT, dCdT);
 end;
if x < 1 then{there is liquid present}
 begin
```

```
    vc := vsatliq(TK);
    dPsatkPadT := dPsatliqdT(TK, PkPa);
    hc := hsatliq(TK, vc, dPsatkPadT);
    uc := hc - PkPa * vc;
    sc := ssatliq(TK, vc, dPsatkPadT);
  end;
if x = 0 then{pure liquid}
  begin
    v := vc;
    u := uc;
    h := hc;
    s := sc;
  end
else if x = 1 then{pure vapor}
  begin
    v := vv;
    u := uv;
    h := hv;
    s := sv;
  end
else{both liquid and vapor present}
  begin
    y := 1 - x;
    v := x * vv + y * vc;
    u := x * uv + y * uc;
    h := x * hv + y * hc;
    s := x * sv + y * sc;
  end;
 end;
end;


procedure comb238 (PkPa, h, TKsat: extended; var TK, s, v, u: extended);
 var
  TKp, TKpp, TKcppp, TKcpp, TKcp, hpp, hp, deltaTK, Li: extended;
  B, C, dBdT, dCdT: extended;
  i: integer;
begin
{initialization}
  TKpp := TKsat;
  TKp := 1073.15;
  TKcppp := TKsat - 10;
  TKcpp := TKcppp;
  TKcp := TKsat;
  hpp := enth(TKpp, PkPa);
  hp := enth(TKp, PkPa);
  Li := TKp - TKcp;
{iterative determination of the TK}
{Dekker-Brent method: p18 Bultheel}
  repeat
    begin
    if Tkcp <> TKcppp then
      begin
```

```
        deltaTK := (TKpp - TKp) * (h - hp) / (hpp - hp);{straight line approximation}
        if (deltaTK * Li > 0) or (abs(deltaTK) >= abs(Li)) then {bisection}
        deltaTK := -Li / 10 {"bisection" but only small step}
        end
      else
        deltaTK := -Li / 10;{"bisection" but only small step}

      TKpp := TKp;
      hpp := hp;
      TKp := TKp + deltaTK;
      hp := enth(TKp, PkPa);
      TKcppp := TKcpp;
      TKcpp := TKcp;
      if (h - hpp) * (h - hp) <= 0 then
        TKcp := TKpp;
      Li := TKp - TKcp;
     end;
   until abs(Li) < 1e-3;
   TK := (TKp + TKcp) / 2;
{calculation of the other thermodynamic properties}
   B := Bvir(TK);
   C := Cvir(TK);
   dBdT := dBvirdT(TK);
   dCdT := dCvirdT(TK);
   v := vvap(TK, PkPa, B, C);
   s := svap(TK, v, B, C, dBdT, dCdT);
   u := h - PkPa * v;
  end;


  procedure comb248 (PkPa, s, TKsat: extended; var TK, h, v, u: extended);
  var
   TKp, TKpp, TKcppp, TKcpp, TKcp, spp, sp, deltaTK, Li: extended;
   B, C, dBdT, dCdT: extended;
   i: integer;
  begin
{initialization}
   TKpp := TKsat;
   TKp := 1073.15;
   TKcppp := TKsat - 10;
   TKcpp := TKcppp;
   TKcp := TKsat;
   spp := entr(TKpp, PkPa);
   sp := entr(TKp, PkPa);
   Li := TKp - TKcp;
{iterative determination of the TK}
{Dekker-Brent method: p18 Bultheel}
   repeat
    begin
    if Tkcp <> TKcppp then
      begin
        deltaTK := (TKpp - TKp) * (s - sp) / (spp - sp);{straight line approximation}
        if (deltaTK * Li > 0) or (abs(deltaTK) >= abs(Li)) then {bisection}
```

```pascal
    deltaTK := -Li / 2 {bisection}
    end
  else
    deltaTK := -Li / 2;{bisection}

    TKpp := TKp;
    spp := sp;
    TKp := TKp + deltaTK;
    sp := entr(TKp, PkPa);
    TKcppp := TKcpp;
    TKcpp := TKcp;
    if (s - spp) * (s - sp) < 0 then
      TKcp := TKpp;
    Li := TKp - TKcp;
    end;
  until abs(Li) < 1e-3;
  TK := (TKp + TKcp) / 2;
{calculation of the other thermodynamic properties}
  B := Bvir(TK);
  C := Cvir(TK);
  dBdT := dBvirdT(TK);
  dCdT := dCvirdT(TK);
  v := vvap(TK, PkPa, B, C);
  h := hvap(TK, v, B, C, dBdT, dCdT);
  u := h - PkPa * v;
  end;

begin
 P := ParamPtr;
 if P^.Value = 15 then {combination 15}
  begin
  P := P^.next;
  TK := P^.Value;
  P := P^.next;
  x := P^.Value;
  P := P^.next;
  outp := round(P^.Value);
  comb15(TK, x, PkPa, h, s, v, u);
  if outp = 2 then
   res := PkPa;
  if outp = 3 then
   res := h;
  if outp = 4 then
   res := s;
  if outp = 6 then
   res := v;
  if outp = 7 then
   res := u;
 end;

 if P^.Value = 248 then {combination 248}
  begin
```

```
    P := P^.next;
    PkPa := P^.Value;
    P := P^.next;
    s := P^.Value;
    P := P^.next;
    TKsat := P^.Value;
    P := P^.next;
    outp := round(P^.Value);
    comb248(PkPa, s, TKsat, TK, h, v, u);
    if outp = 1 then
     res := TK;
    if outp = 3 then
     res := h;
    if outp = 6 then
     res := v;
    if outp = 7 then
     res := u;
   end;

 if P^.Value = 238 then {combination 238}
  begin
   P := P^.next;
   PkPa := P^.Value;
   P := P^.next;
   h := P^.Value;
   P := P^.next;
   TKsat := P^.Value;
   P := P^.next;
   outp := round(P^.Value);
   comb238(PkPa, h, TKsat, TK, s, v, u);
   if outp = 1 then
    res := TK;
   if outp = 4 then
    res := s;
   if outp = 6 then
    res := v;
   if outp = 7 then
    res := u;
  end;

 Main := res;
end;


end.
```

B.4. Think Pascal program for the determination of the COP of batchwise water cooling (cf. section 2.4).

```
program batch;
uses
 waterpropHaWaY, combinationsY;
var
 TCin, TCout, deltaTC, TCscd: extended;

procedure batch (TCin, TCout, TCscd, deltaTK: extended);

var
  TKin, Pin, hin, sin, vin, uin, TKout, Pout, hout, sout, vout, uout, TKscd, etaC, etaP,
Patm: extended;
  m, min, mout, mstart, Ustart, mcd, x, sco, hco, TKco, vco, uco, wtotc, wisc, wnisc,
wisp, wnisp, wtot: extended;
  TK, PkPa, hl, sl, vl, ul, hv, sv, vv, uv, TKhs, PkPahs, hlhs, slhs, vlhs, ulhs, TKstart:
extended;
  PkPacd, hlcd, slcd, vlcd, ulcd, qev, COP: extended;
  n: integer;

begin
 etaC := 0.7;
 etaP := 0.6;
 Patm := 101.325;

 TKin := 273.15 + TCin;
 comb15(TKin, 0, Pin, hin, sin, vin, uin);
 TKout := 273.15 + TCout;
 comb15(TKout, 0, Pout, hout, sout, vout, uout);
 TKscd := 273.15 + TCscd;
 comb15(TKscd, 0, PkPacd, hlcd, slcd, vlcd, ulcd);

 {initialization of loop}
 TK := TKout;
 TKhs := TK + deltaTK;
 wtotc := 0;
 min := 1;
 mout := min;
 m := mout;

 {loop: temperature increases till initial conditions are reached (from energy balance for
filling process)}
 n := 1;
 repeat

       {saturated td properties at TK and TKhs}
   comb15(TK, 0, PkPa, hl, sl, vl, ul);
   comb15(TK, 1, PkPa, hv, sv, vv, uv);
```

```
      comb15(TKhs, 0, PkPahs, hlhs, slhs, vlhs, ulhs);

            {separation}
      x := (hlhs - hl) / (hv - hl);
      m := m / (1 - x);
      mstart := m;
      Ustart := mstart * ulhs;
      mcd := mstart - min;

            {compression of vapor}
      sco := sv;
      comb248(PkPacd, sco, TKscd, TKco, hco, vco, uco);
      wisc := hco - hv;
      wnisc := wisc / etaC;
      wtotc := wtotc + m * x * wnisc;

            {step up temperatures}
      TK := TKhs;
      TKhs := TK + deltaTK;

      writeln(TK : 6 : 2, n);
      n := n + 1

      until Ustart >= hin + mcd * hlcd;
      TKstart := TK;

{pump work}
   wisp := vout * (Patm - Pout);
   wnisp := wisp / etaP;

{total performance}
   qev := uin - uout;
   wtot := wtotc + wnisp;
   COP := qev / wtotc;

   writeln('mstart = ', mstart * 1E3 : 7 : 3, '   mcd = ', mcd * 1E3 : 7 : 3, '  wtotc = ', wtotc
: 7 : 3, '  wnisp = ', wnisp : 7 : 3);
   writeln('qev = ', qev : 9 : 3, '   wtot = ', wtot : 9 : 3, '  COP = ', COP : 9 : 3, '  Tstart =
', TKstart - 273.15 : 6 : 2);
   end;

begin

   TCin := 9;
   TCout := 4;
   TCscd := 35;
   deltaTC := 0.01;
   batch(TCin, TCout, TCscd, deltaTC);

end.
```

Bibliography.

Andersen, K. , F. V. Boldvig "Large capacity heat pump using vacuum ice production as heat source" 3rd International Symposium on the Large Scale Applications of Heat Pumps, Oxford, England : 25-27 March 1987

Ashrae Guide and Data Book. Equipment. "Chapter 13: steam jet refrigeration" (1969)

Ashrae Handbook "Equipment" , Atlanta, GA (1988)

Ashrae Handbook "Fundamentals" , Atlanta, GA (1989)

Ashrae Handbook "HVAC, Systems and applications", Atlanta, GA (1987)

Ashrae Handbook "Refrigeration, Systems and Applications", Atlanta, GA (1990)

Austmeyer, K.E. , M. Bruhns, A. Dickopp, F. Hoyer, K. Kleinhenz, R. Wimmerstedt "Mechanische Brüdenkompression" Brennstoff-Wärme-Kraft Vol. 39, No. 7-8, Jul-Aug 1987 (in German). Summary of "Mechanische Brüdenkompression" Vereinigung der Deutsche Ingenieure - Gesellschaft Energietechnik

Banquet, F. , J.M. Merigoux "Development and test of a high speed centrifugal compressor for mechanical vapour compression" 3rd International Symposium on the Large Scale Applications of Heat Pumps, Oxford, England : 25-27 March 1987

Berghmans, J. "Compressoren en koelmachines" course notes, Vlaamse Technische Kring, 1988 (in Dutch)

Bultheel, A., L. Buyst "Inleiding tot de numerieke wiskunde--Tweede deel" Katholieke Universiteit Leuven, Fakulteit Toegepast Wetenschappen, 1986 (in Dutch)

Cheng, C.Y. , W.C. Cheng, M.C. Yang "The vacuum freezing multiple phase transformation process" Desalination, Elsevier Science Publishers B.V., Amsterdam, Vol. 67 (1987)

Chlumsky, Vladimir "Reciprocating and rotary compressors" E&FN Spon Ltd. London 1965

Cho, Y.I. , E. Choi, H.G. Lorsch "A novel concept for heat transfer fluids used in district cooling systems" ASHRAE Transactions 1991, Vol. 97, Part 2

Collet, P.J. , J.W. Wormgoor, W.C. van Dorp "A vacuum-freeze installation for large heatpump installations" I.I.F.-I.I.R. Commission E2 - Trondheim (Norway) -1985-6

Collet, P.J. "Perspektieven voor korte termijn koude-opslag" 90-334/R.25/PBA (MT-TNO) the Netherlands (in Dutch) (1990?)

Collet , P.J. "Een vacuümvriesverdamper voor grote warmtepompinstallaties" in Koeltechniek (1987) nr 10 (oktober) (in Dutch)

Cummings, M. "Modeling, design, and control of partial ice-storage systems" Master of Science thesis, Solar Energy Laboratory, University of Wisconsin-Madison, 1989

Curtis, Commercial brochure on rotary air blowers, St. Louis, MO

Degueurce, Bernard, Marie-Thérèse Pascal, Bernard Zimmern "Problems encountered and results obtained in direct steam compression utilizing an oil injection free single screw compressor" Proceedings of the 1980 Purdue Compressor Technology Conference, Edited by Werner Soedel

Degueurce, B. , C. Tersiguel "Problems encountered and results obtained in the application of compressors in industrial processes for energy saving" International Symposium on the Industrial Application of Heat Pumps, held at the University of Warwick, U.K.: 24-26 March,1982

Degueurce, B. , F. Banquet, J-P Denisart , D. Favrat "Use of twin screw compressor for steam compression" 2nd International Symposium on the Large Scale Applications of Heat Pumps, York, England : 25-27 September 1984

EPRI reports
  Heist Engineering Corporation "Industrial applications of freeze concentration technology" EM-5232 Research Project 2662-1, Final report, June 1987
  Dairy Research, Inc. "Freeze concentration of dairy products, phase 1" CU-6292, Research Project 2782-1, Final report, March 1989

Fisher, U. "Compressor and system matching in vapour compression distillation unit" Isreal journal of technology, Vol.15, 1977

Gas Research Institute reports on trochoidal compressors
  Roche, R. H. and Stielstra, P.B. "Positive displacement rotary compressor for vapor compression" Annual Report Gas Research Institute Report, GRI-80/0134
  Roche, R. H. and Robbins, L.L. "Positive displacement rotary compressor for vapor compression" Final Report Gas Research Institute Report, GRI-80/0134
  Hoffmann, R. M. "Volumetric trochoidal gas compressor for use as a heat pump" Gas Research Institute Report, GRI-85/0026
  Hoffmann, R. M. "Advanced positive displacement rotary compressor for freon compression" Gas Research Institute Report, GRI-86/0212
  Wurm, J. and Czachorski, M. and Kountz, K.J."Evaluation and testing of trochoid refrigerating compressor" Gas Research Institute Report, GRI-87/0046
  Stewart, M.G. and Kaminski, H.L. and Heitsch, R.F. "Manufacturing cost and design analysis for trochoid power corporation rotary recuperative steam pump" Gas Research Institute Report, GRI-86/0284
  Hoffmann, R. M. "High speed volumetric trochoidal gas compressor for use as a heat pump" Gas Research Institute Report, GRI-86/0282

Gas Research Institute reports on centrifugal compressors
  Iles, T.L. and Burgmeier, L.R. and Stanko, J.E. "Open-cycle centrifugal vapor-compression heat pump" Annual Report Gas Research Institute Report, GRI-83/0085
  Iles, T.L. and Burgmeier, L.R. and Liu, A.Y. "Open-cycle centrifugal vapor-compression heat pump" Annual Report Gas Research Institute Report, GRI-85/0118
  Burgmeier, L.R. and Horner, J.E. "Open-cycle centrifugal vapor-compression heat pump" Final Report Gas Research Institute Report, GRI-87/0345

Gromoll, B. "High temperature heat pump with liquid-ring compressor using water as a refrigerant" 3rd International Symposium on the Large Scale Applications of Heat Pumps, Oxford, England : 25-27 March 1987

Hakim Faragallah, W. "Liquid ring vacuum pumps and compressors--Applications and principles of operation" Gulf Publishing Company, 1988

Heaton, A.V. , R. Benstead "Steam recompression drying" 2nd International Symposium on the Large Scale Applications of Heat Pumps, York, England : 25-27 September 1984

Heist, James A. "Freeze crystallization" Chemical Engineering May 7, 1979

Hoffman, Daniel "Second generation low temperature vapor compression plants" Desalination, Elsevier Science Publishers B.V., Amsterdam, Vol. 23 (1977)

Hyland, R.W. , A. Wexler "Formulations for the thermodynamic properties of the saturated phases of H_2O from 173.15 K to 473.15 K" Ashrae Transactions 1983 Part 2A

Hyland, R.W. , A. Wexler "Formulations for the thermodynamic properties of dry air from 173.15 K to 473.15 K, and of saturated moist air from 173.15 K to 372.15 K, at pressures up to 5 MPa" Ashrae Transactions 1983 Part 2A

International Symposium on the Industrial Application of Heat Pumps, held at the University of Warwick, U.K.: 24-26 March,1982

2nd International Symposium on the Large Scale Applications of Heat Pumps, York, England : 25-27 September 1984

3rd International Symposium on the Large Scale Applications of Heat Pumps, Oxford, England : 25-27 March 1987

Klein, S.A. , F.L. Alvarado "Engineering Equation Solver" F-Chart Software, 1990

Kornhauser, Alan A. "The use of an ejector as a refrigerant expander" Proceedings of the 1990 USNC/IIR-Purdue Refrigeration Conference ASHRAE-Purdue CFC Conference, July 17-20, 1990

Lazare, Leon "Absorption refrigeration process" US Patent 4,475,352, Oct. 9, 1984 and "Serial absorption refrigeration process" US Patent 4,475,353, Oct. 9, 1984

Lucas, M. , B. Tabourier "The mechanical vapour compression process applied to sea water desalination: a 1500 ton/day unit installed in the nuclear power plant of Flamandville, France" Desalination, Elsevier Science Publishers B.V., Amsterdam, Vol. 52 (1985)

McDermott, John "Desalination by freeze concentration" Noyes Data Corporation, 1971

McLinden, Mark O. , David A. Didion "Quest for alternatives" ASHRAE JOURNAL December 1987

Neerken, Richard F. "Keys to compressor selection" in "Fluid movers--pumps, compressors, fans and blowers" Edited by Jay Matley Chemical Engineering McGraw-Hill Publications Co., New York, NY

Ophir, A. , J. Paul "The Ecochiller - a mechanical vapour compression cycle using water vapour as refrigerant" to be published in the proceedings of the 18th International Congress of Refrigeration IIF-IIR-Montréal-1991 (expected Dec. 1991)

Patterson, J. , J.B. Richie "Roots blower performamce" Int. J. mech. Sci. Pergamon Press, 1969, Vol. 11.

Peled, Abraham "Operation of the freeze desalination plant at Eilat, Israel" Proceedings of the First International Symposium on Water Desalination, Washington DC, Oct.3-9, 1965 U.S. Department of the Interior Office of Saline Water

Pirani, M. , J. Yarwood "Principles of vacuum engineering" Reinhold publishing corporation, New York (1961)

Power, B.D. "High vacuum pumping equipment" Reinhold publishing corporation, New York (1966)

Rice, Warren "Calculated characteristics of a hydraulic refrigeration system" Journal of Energy Vol. 5, No. 6, Nov.-Dec. 1981 American Institute of Aeronautics and Astronautics, Inc.

Ryans, James L. , Daniel L. Roper "Process vacuum system design & operation" McGraw-Hill Book Company, 1986

Severson, D.S. "Integration of natural gas engine driven vapor recompression heat pumps into industrial processes" International Symposium on the Industrial Application of Heat Pumps, held at the University of Warwick, U.K.: 24-26 March,1982

Snyder, A.E. "Freezing methods" in "Principles of desalination" edited by K.S. Spiegler, 1966.

Spencer, E. "Estimating the Size and Cost of Steam Vacuum Refrigeration" Hydrocarbon processing June 1967, Vol. 46, No. 6

Tabb, E.S. , D.W. Kearney "An overview of the industrial heat pump applications assessment and technology development programs of the gas research institute, U.S.A." International Symposium on the Industrial Application of Heat Pumps, held at the University of Warwick, U.K.: 24-26 March,1982

Tuzson, J.J. "High pressure ratio centrifugal compressor development and a vapor compression application in the dairy industry" 2nd International Symposium on the Large Scale Applications of Heat Pumps, York, England : 25-27 September 1984

Young, J.B. "An equation of state for steam for turbomachinery and other flow calculations" Journal of Engineering for Gas Turbines and Power, January 1988, Vol.110

Zhu, Ruiqi, Han Baoqi, Meizhen Lin, Yongzhang Yu "Experimental investigation on an adsorption system for producing chill water" Proceedings of the 1990 USNC/IIR-Purdue Refrigeration Conderence ASHRAE-Purdue CFC Conference, July 17-20, 1990